ANALYSIS OF CHRNA5 EXPRESSION IN BREAST CANCER CELL LINES IN RESPONSE TO SERUM STARVATION AND ESTROGEN TREATMENT

A THESIS SUBMITTED TO
THE DEPARTMENT OF MOLECULAR BIOLOGY AND GENETICS
AND GRADUATE SCHOOL OF ENGINEERING AND SCIENCE
OF BILKENT UNIVERSITY
IN PARTIAL FULFILLMENT OF THE REQUIREMENTS
FOR THE DEGREE OF
MASTER OF SCIENCE

By Azer Aylin AÇIKGÖZ

August 2013

To my mother Esin, and to my brother Alihan..
Thank you for everything..

I certify that I have read this thesis and that, in my opinion, it is fully adequate in scope and in quality as a thesis for the degree of Master of Science

---

Assst. Prof. Özlen KONU (Advisor)

I certify that I have read this thesis and that, in my opinion, it is fully adequate in scope and in quality as a thesis for the degree of Master of Science

---

Asst. Prof. Ali O. GÜRE

I certify that I have read this thesis and that, in my opinion, it is fully adequate in scope and in quality as a thesis for the degree of Master of Science

---

Asst. Prof. Öznur TAŞTAN

Approved for the Graduate School of Engineering and Science

Prof. Dr. Levent ONURAL

Director of Graduate School of Engineering and Science

ABSTRACT

ANALYSIS OF CHRNA5 ISOFORMS IN BREAST CANCER CELL LINES IN RESPONSE TO SERUM STARVATION AND ESTROGEN TREATMENT

Azer Aylin Açıkgöz

MSc. in Molecular Biology and Genetics

Supervisor: Asst. Prof. Dr. Özlen Konu

August 2013

Breast cancer is a complex disease that can be classified into distinct molecular subtypes including Basal, Luminal A, Luminal B and HER2 positive. These molecular subtypes mainly differ in their hormone receptor expression and response to treatment. This makes the discovery of new molecular markers for further classification important. Cholinergic nicotinic acetylcholine receptors are ion channels involved in smoking behavior, neurodegenerative diseases and cancer. Cholinergic nicotinic receptor alpha 5 (CHRNA5) has been associated with nicotine addiction and recently with lung cancer yet its importance in breast cancer remains relatively unexplored. In the present study, a panel of 10 breast cancer cell lines were used for quantification of isoform-specific CHRNA5 expression using qPCR. Changes in CHRNA5 expression in response to serum starvation and estrogen treatment were assessed. qPCR showed that CHRNA5 was alternatively spliced, with at least five different isoforms in breast cancer cell lines. qPCR analysis for CHRNA5 expression in serum treated and serum starved cells were analyzed after outlier detection and exclusion; and statistical tests included ANCOVA using geometric mean of TPT1 and SDHA, as reference genes. Our results demonstrated that, CHRNA5 expression differed between different subtypes of breast cancer cell lines. CHRNA5 expression significantly responded to serum starvation in ZR75-1 and MDA-MB-157 cell lines, isoform specifically. Isoform expression of CHRNA5 exhibited significant alterations upon estrogen treatment in a dose and time-dependent manner. Expression of 1000bp variant, isoform2 and isoform3 of CHRNA5 significantly increased upon E2

treatment and total CHRNA5 and isoform2 CHRNA5 increased in expression at 24 hours when compared with 12 hours of treatment. Our findings show that CHRNA5 has multiple isoforms in breast cancer, with potential to be modulated by serum starvation and estrogen treatment in a cell-specific manner.

Keywords: Breast cancer, CHRNA5, estrogen, serum starvation, molecular subtype.

ÖZ

CHRNA5 İFADESİNİN MEME KANSERİ HÜCRE HATLARINDA ANALİZİ VE SERUM AÇLIĞI İLE ÖSTROJENE CEVABI

Azer Aylin Açıkgöz
Moleküler Biyoloji ve Genetik Yüksek Lisansı Tez Danışmanı:
Yrd. Doç. Dr. Özlen Konu
Ağustos 2013

Meme kanseri karmaşık bir hastalık olup, moleküler olarak bazal, luminal A, luminal B, HER2+ ve normal tipler olarak sınıflandırılabilir. Bu tipler arasındaki ana fark hormon reseprörlerinin ifadeleri açısındandır. Farklı tiplerin tedaviye cevapları da farklıdır. Bu nedenle, meme kanserini daha iyi sınıflandırabılmek için yeni moleküler markörler bulmanın önemi artmaktadır. Kolinerjik nikotinik asetilkolin reseptörleri , sigara içme alışkanlığında, nörodejeneretiv hastalıklarda ve kanserde rolü olduğu düşülünen iyon kanallarıdır. Kolinerjik reseptör nikotinik alfa 5 (CHRNA5) nikotin bağımlılığı ve akciğer kanseri ile ilişkilendirilmiştir ancak meme kanserindeki önemi henüz bilinmemektedir. Bu çalışmada, 10 adet meme kanseri hücre hattından oluşan bir panel kullanılarak, CHRNA5 varyantlarının ifadesi qPCR ile ölçülmüştür. CHRNA5 ifasesinin serum açlığı ve östrojen tedavisine bağlı değişimi incelenmiştir. qPCR sonuçları CHRNA5in meme kanseri hücre hatlarında alternatif kırpıldığını ve en az beş izoforma sahip olduğunu göstermiştir. Serum varlığında ve serum açlığında CHRNA5 ifadesini ölçen qPCR verilerinin analizleri aykırı verilerin bulunup çıkartılmasından sonra, TPT1 ve SDHA referans genlerinin geometrik ortalaması alınarak ANCOVA istatistiksel analizi ile yapılmıştır. Sonuçlarımız gösteriyor ki, CHRNA5 ifadesi farklı tip meme kanseri hücre hatları arasında farklılık göstermektedir. Serum yokluğunda ZR-75-1 ve MDA MB 157 hücre hatlarında CHRNA5 ifadesi izoformlara özgü olarak anlamli bir değişime uğramıştır. Östrojen tedavisi sonucunda, CHRNA5 izoformlarının ifadeleri doz ve zamana bağlı olarak değişmektedir. Toplam CHRNA5 ifadesi ve izoform 2 CHRNA5 ifadesi 24

saatte, 12 saate göre artış göstermiştir. Bulgularımız CHRNA5in meme kanserinde birden fazla izoformu olduğunu ve bu izoformların serum açlığı ve östrojen tedavisi sonucunda, hücre hattına bağlı olarak değişme potansiyelinin olduğunu göstermiştir.

Anahtar sözcükler: meme kanseri, CHRNA5, alternatif kırpılma, östrojen, serum açlığı, moleküler tip.

ACKNOWLEDGEMENTS

First of all, I would like to thank my thesis advisor Asst. Prof. Özlen Konu for her guidance throughout my thesis work.

I would like to thank Asst. Prof. Ali O. Güre and Asst. Prof. Öznur Taştan for their scientific assistance and advice for my thesis. I would also like to express my gratitude to Assoc. Prof. İhsan Gürsel for helping me both in my scientific and personal life whenever I needed.

I would especially like to mention Sıla, Nilüfer and Gurbet who have always been there for me, both scientifically and as dearest friends throughout these two years.

I would like to thank Ermira Jahja for cloning, sequencing and providing primer sequences and Gizem Ölmezer for assistance in cell culture experiments.

I'm grateful to the MBG family, especially to Damla and to the members of IG Group for a friendly and understanding working environment.

I would like to express my heartfelt gratitude to İhsan, for always being there for me in these past two years, for being with me, helping and supporting me both in the best and worst of the times.

I would like to convey my deepest love and gratitude towards my family: my grandparents Şaziye and Celal; my best friend and brother Alihan; and foremost, my beautiful super-mom Esin. Without you I would not be where I'm today. I appreciate everything you have done for me and I'm eternally grateful.

The research presented in this thesis has been funded by TUBITAK (TBAG-111T316). I was supported by Bilkent University Molecular Biology and Genetics Department, and TUBITAK for my graduate studies.

Contents

List of Figures

List of Tables

Abbreviations

AC	Adenocarcinoma
ACh	Acetylcholine
AF	Ascites Fluid
ANLN	Anilin
ATCC	American Type Culture Collection
bp	base pairs
BRCA	Breast Cancer Susceptibility Gene
CDC	Cell Division Cycle
cDNA	complementary Deoxyribonucleic Acid
CHEK2	Checkpoint Kinase2
CHRN	Cholinergic Receptor Nicotinic
CHRNA	Cholinergic Receptor Nicotinic Alpha
CHRNB	Cholinergic Receptor Nicotinic Beta
DC	Ductal Carcinoma
ddH2O	double-distilled water
DMEM	Dulbecco's Modified Eagle's Medium
DMSO	Dimethyl sulfoxide
DNA	Deoxyribonucleic Acid
dNTPs	deoxyribonucleotide triphosphates
E2	β-Estradiol
EDTA	Ethylenediaminetetraacetic Acid
ER	Estrogen Receptor
ERB-B2	Erythroblastic Leukemia Viral Oncogene Homolog 2
ERE	Estrogen Response Elements
ESE	Exonic Splicing Enhancer

ESS	Exonic Splicing Silencer
EST	Expressed Sequence Tag
EtOH	Ethanol
FBS	Fetal Bovine Serum
GABA	Gamma Amino Butyric Acid
glyR	Glycine Receptor
GWA	Genome Wide Association
HER2	Human Epidermal Growth Factor Receptor 2
IDC	Invasive Ductal Carcinoma
IGFBP4	Insulin-like Growth Factor Binding Protein 4
ISE	Intronic Splicing Enhancer
ISS	Intronic Splicing Silencer
MC	Metaplastic Carcinoma
MCM2	Minichromosome Maintenance Complex Component 2
MYC	myelocytomatosis
nAChR	Nicotinic Acetylcholine Receptor
PB	Primary Breast
PBS	Phosphate Buffered Saline
PCR	Polymerase Chain Reaction
PF	Pleural Effusion
PR	Progesterone Receptor
PTEN	Phosphatase and Tensin Homolog
qPCR	Quantitative Real Time Polymerase Chain Reaction
RNA	Ribonucleic Acid
rpm	rounds per minute
RPMI	Roswell Park Memorial Institute

SDHA	Succinate Dehydrogenase Complex, Subunit A
SNP	Single Nucleotide Polymorphism
snRNPs	Small Nucleic Ribonucleoproteins
TAE	Tris-Acetate-EDTA
TFF1	Trefoil Factor 1
TP53	Tumor Protein 53
TPT1	Tumor Protein, Translationally-Controlled
WISP2	WNT1 Inducible Signaling Pathway Protein 2
XBP1	X-box Binding Protein 1

Chapter 1

INTRODUCTION

1.1 Breast Cancer

Breast cancer is the most common cancer among females. In the USA, breast cancer constitutes 28% of all new cancer cases and 26% of cancer-related deaths in women.[1]

1.1.1 Types and Progression

Breast cancer can either be hereditary or sporadic. In hereditary breast cancer, patients have susceptibility to breast cancer due to a germline mutation that they inherited. The major genes that result in susceptibility are BRCA1 and BRCA2 but mutations in PTEN and TP53 can also cause breast cancer.[2] The contributions of mutations of particular genes to susceptibility of hereditary breast cancer are shown in Figure 1.1. Sporadic breast cancer occurs as a result of the accumulation of mutations in somatic tissues.[2,3]

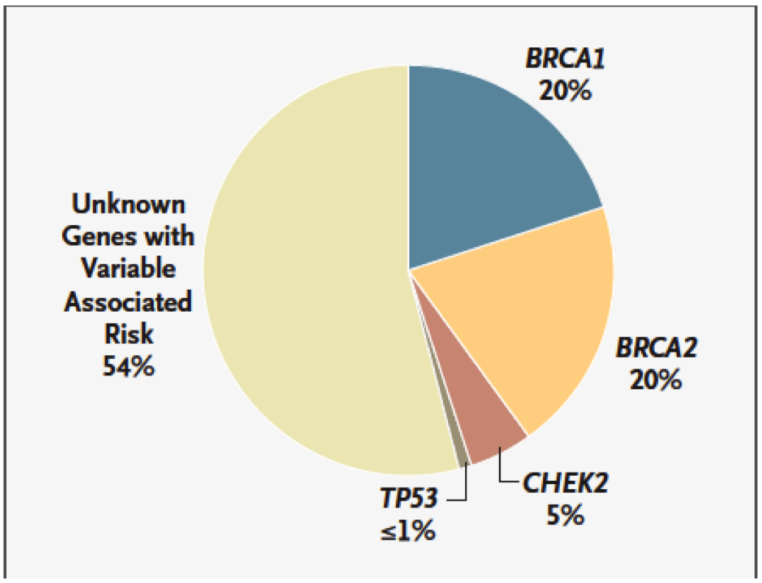

Figure 1.1: The genetics of breast cancer. *(Reproduced with permission from Wooster et al., 2003 Copyright Massachusetts Medical Society)*

The transformation from a normal cell to a malignant cell can be described in 3 steps. In step 1, which is named 'carcinoma in situ', a normal cell changes into an atypical cell type and, after successive divisions, becomes a lesion. Step 2 is where the lesion becomes malignant and step 3 is the formation of metastases.[3]

1.1.2 Genes Involved in Breast Cancer

The genes implicated in breast cancer tumorigenesis can be divided into 6 groups. Oncogenes (e.g. MYC, ERBB2), tumor suppressor genes (e.g. BRCA1, BRCA2, p53), apoptosis genes, steroid receptors (e.g. ERα, ERβ, PR) and genes involved in invasion/cell adhesion and angiogenesis.[3]

1.1.3 Risk Factors

The major breast cancer risk factors are gender and age. Although familial breast cancers constitute around 10% of all breast cancers, family history is also an important risk factor, with increasing susceptibility to breast cancer in women with one or more relatives with breast cancer.

Hormonal and reproductive risk factors include the main female hormone estrogen and lack of childbearing at an early age. Early menarche and late menopause are also thought to increase the risk of getting breast cancer in women.[4]

Other major and minor risk factors include usage of hormone replacement therapy or oral contraceptives, lack of physical activity during adolescence, weight gain after menopause, obesity, history of some non-malignant breast diseases, environmental factors such as diet, consumption of alcohol on a daily basis and exposure to radiation.[4]

1.1.4 Classification

Classification of breast cancer is done in several categories in order to decide on the best treatment approach. The most common ones among these categories are the histopathological type, tumor grade, tumor stage, receptor status and classifications that are based on DNA.

1.1.4.1 Histopathological Type

Histopathological type is defined based on the growth pattern of the breast cancer, with the most common type being invasive ductal carcinoma or IDC. There are, at least, 17 different histopathological types of breast cancer.[5]

1.1.4.2 Tumor Grade

The grading of the breast cancer tumors is based on the comparison of the appearance of the tumor tissue with the normal breast tissue under the microscope. Three different criteria are assessed and a score from 1 to 3 is given for each of them. The grade of the tumor is identified after the summation of the scores for each criteria. 3 to 5 points indicate that the tumor is well-differentiated (low grade), 6 to 7 points indicate that the tumor is moderately differentiated (intermediate grade) and 8 to 9 points indicate that the tumor is poorly differentiated (high grade). The histological grades are generally

correlated with the prognosis of breast cancer, with the poorly differentiated high grade tumors having the worst prognosis.[6]

1.1.4.3 Tumor Stage

Tumor staging is the procedure by which the location and the size of the cancer is determined. Staging is done after the assessment of mainly three properties which are tumor size (T), the involvement of lymph-nodes (N) and the presence of metastasis (M). This method, called the TNM staging system, is also used in the decision of the appropriate treatment for a patient and informs clinicians about the severity of the disease.[7,8] Stages differ from 0 to IV, with stage II and stage III having substages and stage IV being the most advanced stage, generally considered incurable. A larger tumor size, spreading to a number of nodes and metastasis tend to have a worse prognosis.[7,8]

1.1.5 Receptor Status and Molecular Subtype

Another category used to classify breast cancer is its receptor status. Expression, or lack thereof, of three most important ones, estrogen receptor (ER), progesterone receptor (PR) and HER2, helps in the determination of appropriate treatment type.

It was found out that breast tumors and breast cancer cell lines could be clustered into different subtypes according to the similarities and differences in their gene expression patterns. After microarray analysis, breast cancer was divided into four distinct molecular subtypes, namely luminal (ER+), basal (ER-, also called triple-negative breast cancer), ERB-B2+ (HER2+), and normal-like. Luminal type is further divided into luminal A and luminal B, with distinctive gene expression patterns.[9–12]

These molecular subtypes have different clinical outcomes and prognosis, with basal type having the worst prognosis and ERB-B2 having a considerably bad prognosis.[9–12]

1.1.6 Estrogen, Estrogen Receptor (ER) and Breast Cancer

Estrogens are the primary steroid hormones of females. Premenopausal women have high levels of serum estrogen, but this level decreases after menopause. Estrogen can be endogenous or exogenous. Exogenous sources include hormone-replacement therapies and oral contraceptive usage. Primary endogenous source of estrogen during the menstrual life are the ovaries. The small amount of estrogen present postmenopausally comes from extragonadal tissues like muscles, fat and liver.[13,14] Sources of estrogen and its target organs can be seen in Figure 1.2.

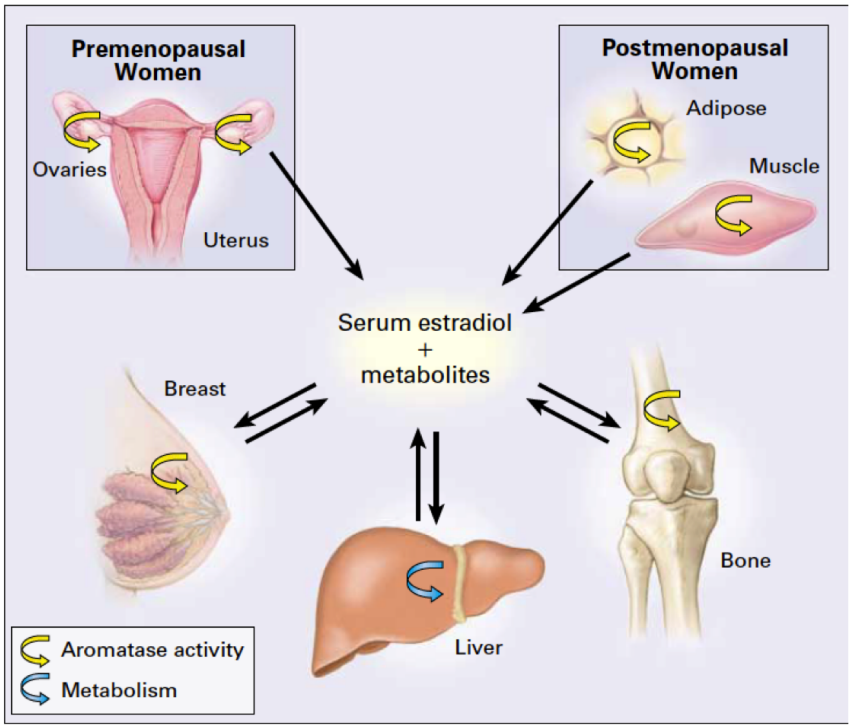

Figure 1.2: Sources of estrogen and its target organs. *(Reproduced with permission from Clemons et al., 2001 Copyright Massachusetts Medical Society)*

Estrogens go through the cell membrane via passive diffusion. In ER+ cells, estrogen forms a ligand-receptor complex with nuclear ER and the complex activates estrogen response elements (ERE). There are two types of estrogen

receptor, namely ER-α and ER-β. Although ER-α has a higher affinity for estrogen when compared to ER-β, a balanced ratio between the two types of receptors is important in determining the estrogen response of a tissue.[14,15] Pathways of ER signaling are summarized in Figure 1.3.

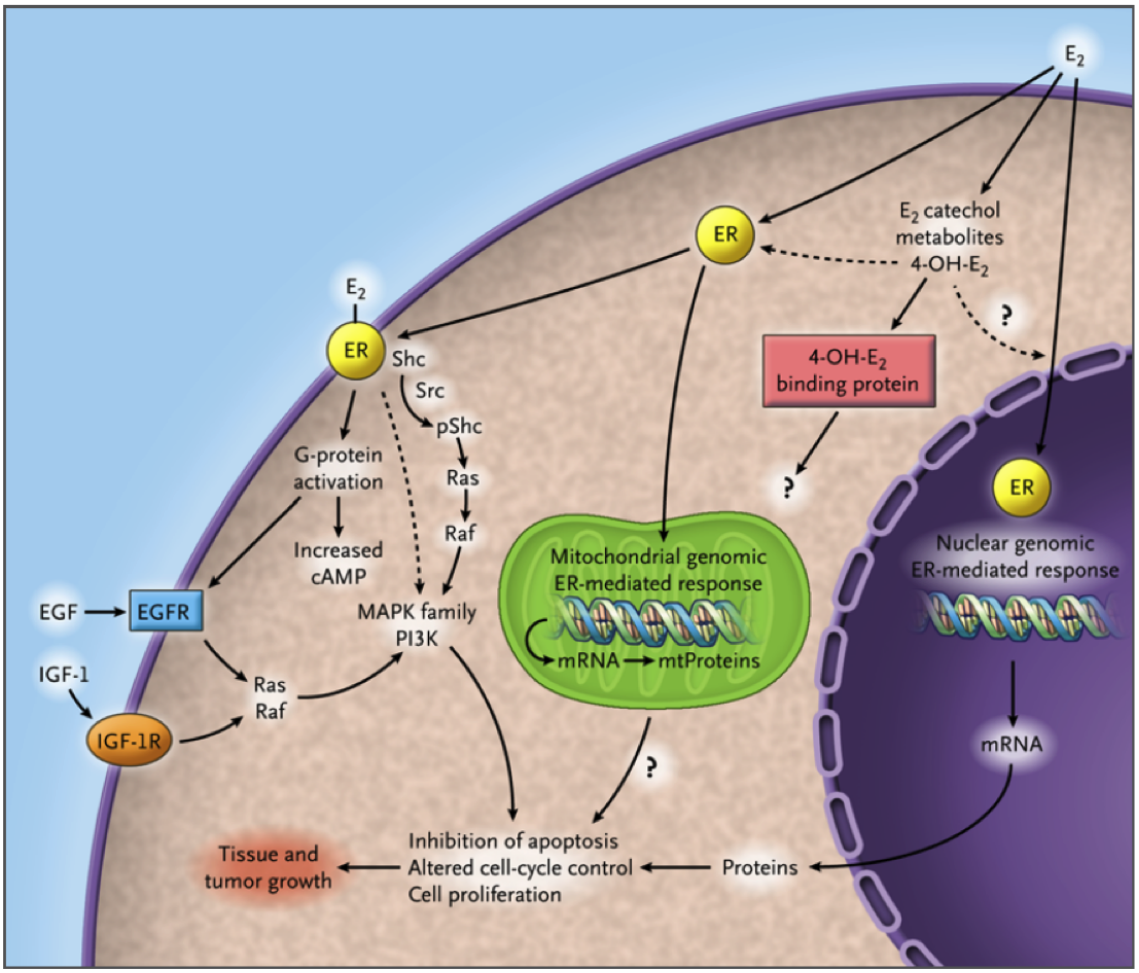

Figure 1.3: Estrogen receptor signaling pathways. *(Reproduced with permission from Yager et al., 2006 Copyright Massachusetts Medical Society)*

Estrogen is implicated in the carcinogenesis of the breast. In rodents, estrogen intake causes mammary tumors, excessive hormone stimulation may cause uncontrolled cell growth and division, resulting in malignancy.[14] The effects of estrogen are believed to be cumulative; when the exposure time lengthens, the risk increases. This is supported by the fact that women who

start their menstrual periods at an earlier age, or go through menopause at a later age tend to be at a higher risk of breast cancer.[13] Hormone replacement therapy also causes an increase in the breast cancer risk, but this increase can be reversed.[15] Estrogen has been associated both with the initiation and progression of breast cancer, but the mechanisms underlying this effect are complex.[13–15] Pathways that lead to estrogen carcinogenesis is summarized in Figure 1.4.

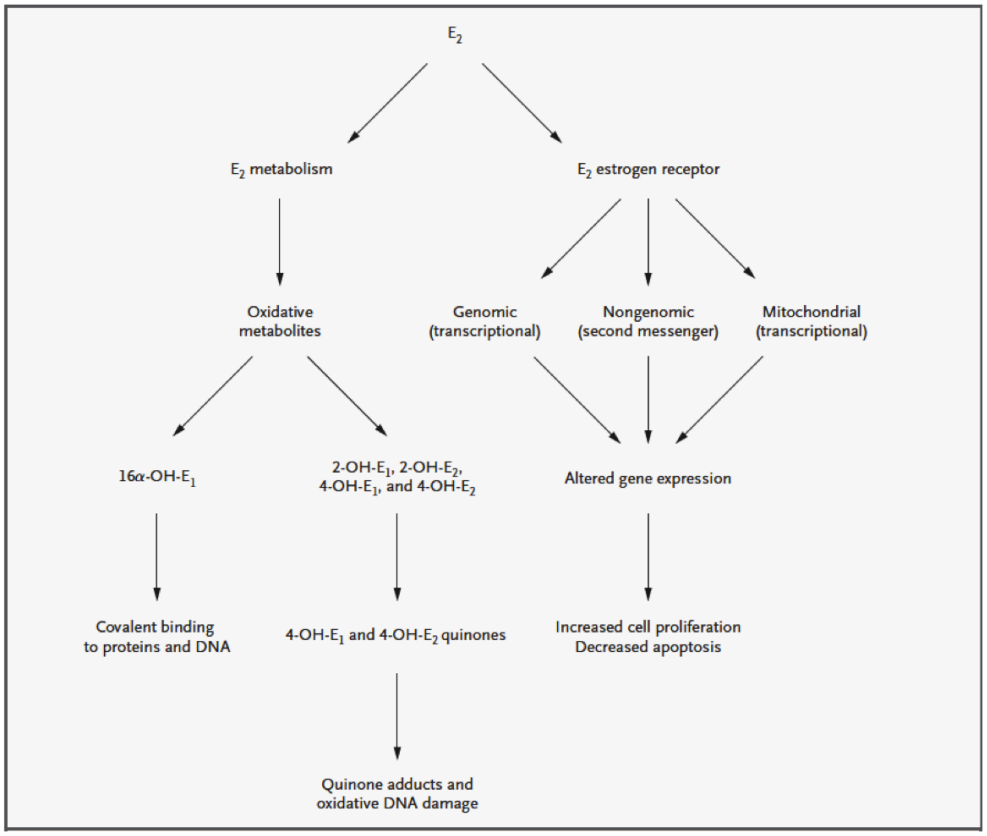

Figure 1.4: Pathways that lead to estrogen carcinogenesis. *(Reproduced with permission from Yager et al., 2006 Copyright Massachusetts Medical Society)*

Estrogens were shown to regulate a variety of target genes. There are three mechanisms with which estrogen exerts its effects on its target genes.[16] These are:

1. Direct interaction of ER with DNA through estrogen response elements

2. Recruitment of other transcription factors by ER

3. Indirect modulation

Effects of estrogen on gene expression is thought to be cell specific.[16] The effects of estrogen on proliferation, apoptosis and gene expression were investigated mainly in ER-responsive (ER+) breast cancer cell lines. In the ER+ breast cancer cell lines MCF7 and T47D, estrogen treatment resulted in increased proliferation[17,18] but this was not the case in an ER- breast cancer cell line MDA MB 436.[17] A variety of primary and secondary responses (either up- or down-regulation) to estrogen treatment were identified in ER+ cell lines. These include genes involved in cell cycle and apoptosis (Cyclin D1, CDC2, CDC6, MCM2), genes that code for growth factors and cytokines (IGFBP4, WISP2) and TFF1/PS2, XBP1, CCND1, FOS and E2F.[16,19–21]

1.1.7 Breast Cancer Cell Lines

A large part of the research on breast cancer relies on the use of breast cancer cell lines. Breast cancer cell lines are immortalized cell lines, generally isolated from metastatic breast tumors and they have varying phenotypic and molecular characteristics, resembling the diversity of breast tumors. The origins of the cell lines used in this study can be found in Table 1.1.

Table 1.1: The origins of breast cancer cell lines used in this study.[22]

	Cell Line	Source	Tumor	Age	Ethnicity
1	BT-20	PB	IDC	74	White
2	HCC 1937	PB	DC	24	White
3	MCF7	PE	IDC	69	White
4	MDA MB 157	PE	MC	44	Black
5	MDA MB 231	PE	AC	51	White
6	MDA MB 361	PB	AC	40	White
7	MDA MB 453	PE	AC	48	White
8	MDA MB 468	PE	AC	51	Black
9	T47D	PE	IDC	54	N/A
10	ZR-75-1	AF	IDC	63	White

AC, adenocarcinoma; AF, ascites fluid; DC, ductal carcinoma; IDC, invasive ductal carcinoma; MC, metaplastic carcinoma; PB, primary breast; PE, pleural effusion.

Breast cancer cell lines can, like breast cancer tumors, be divided into molecular subtypes, mainly characterized by their expression of hormone receptors ER, PR and HER2.[23] Table 1.2 shows which subtypes express which receptors.

Table 1.2: Hormone receptor characterization of molecular subtypes.[23]

Subtype	ER	PR	HER2
Basal	-	-	-
Luminal A	+	+ or -	-
Luminal B	+	+ or -	+
HER2	-	-	+

According to their expression of these receptors, the 10 breast cancer cell lines used in this study falls into the following molecular subtypes:[22,24,25]

Table 1.3: Molecular characterization of breast cancer cell lines.[22,24,25]

	Cell Line	ER	PR	HER2	Subtype
1	BT-20	-	-	-	Basal
2	HCC 1937	-	-	-	Basal
3	MCF7	+	+	-	Luminal
4	MDA MB 157	-	-	-	Basal
5	MDA MB 231	-	-	-	Basal
6	MDA MB 361	+	+	+	HER2
7	MDA MB 453	-	-	+	HER2
8	MDA MB 468	-	-	-	Basal
9	T47D	+	+	-	Luminal
10	ZR-75-1	+	+	-	Luminal

1.2 Cholinergic Receptor Nicotinic Alpha (CHRNA or nAChR)

Nicotinic acetylcholine receptors or cholinergic nicotinic receptors are excitatory, transmembrane ligand-gated ion channels that belong to a superfamily along with other transmembrane ligand-gated channels such as GABA and glyR. They can bind acetylcholine (ACh) and nicotine and are mainly found at the neuromuscular junction and in some neurons both in the central and the peripheral nervous system.[26–28]

nAChRs have 2 different types of subunits identified, namely α, β and are found in either homomeric (consisting of a single subunit) or heteromeric (consisting of multiple subunits) pentamers. Each of the subunits have 4 transmembrane domains and a long extracellular N-terminal domain. To date, 9 α subunits (α2-10) and 3 β subunits (β2-4) have been identified, making a total of 12 subunits.[27] Different combinations of these subunits in pentamers results in receptors with different electrophysiological properties.

Some of the nAChRs were found out to have mRNAs that can be alter-

natively spliced, which further increases the diversity, with different splice variants resulting in different receptor subtypes. These subtypes may explain the variable tolerance and addiction to nicotine or different release of neurotransmitters in different synapses.[26,28]

Schematic representation of nAChRs and an example of a heteromeric nAChR can be seen in Figure 1.5 and 1.6, respectively.

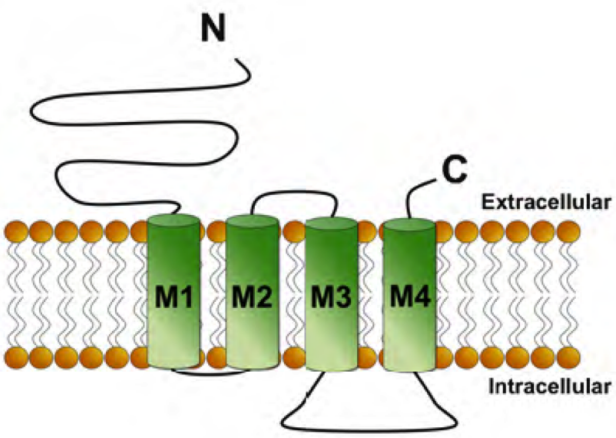

Figure 1.5: Schematic representation of a nAChR. *(Reprinted from Improgo et al., 2010, with permission from Elsevier)*

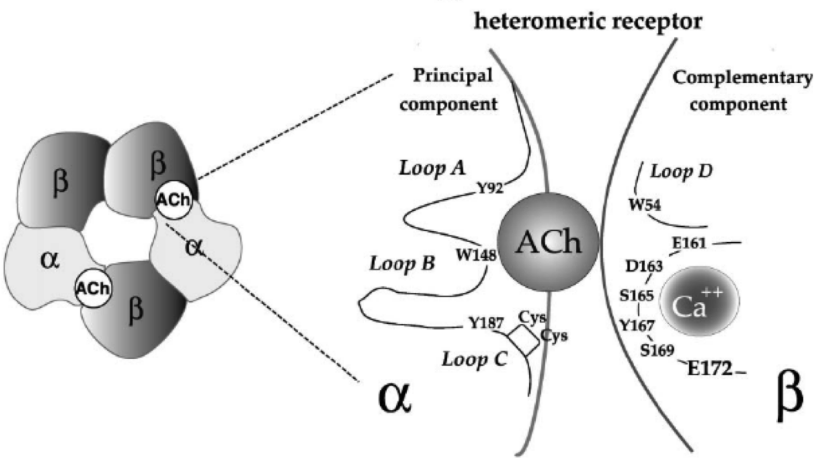

Figure 1.6: Schematic representation of a heteromeric nAChR and ACh binding site. *(Reprinted from Itier et al., 2001, with permission from Elsevier)*

nAChRs are implicated in a variety of diseases, disorders and behaviors, including nicotine addiction and smoking behavior, Alzheimer's Disease, Parkinson's Disease, schizophrenia, epilepsy, and cancer.[26–28]

1.3 CHRNA5

nAChR subunits $\alpha 3$, $\alpha 5$ and $\beta 4$ cluster together in the genome.[29,30] These were later mapped to chromosome 15 in humans (15q24-25) and chromosome 9 in mice.[31] Figure 1.7 shows the gene cluster and relative positions of these three subunits in the genome.

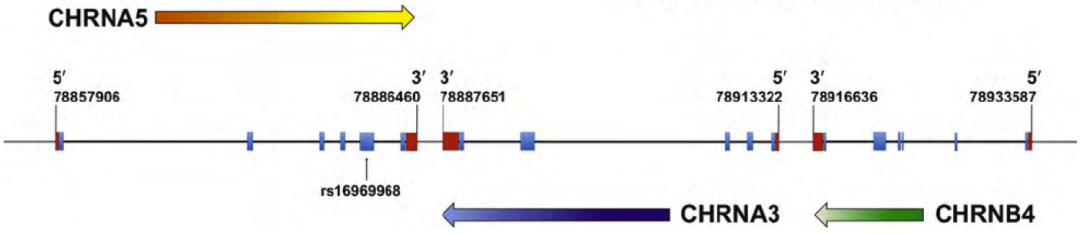

Figure 1.7: Schematic representation of CHRNA3-CHRNA5-CHRNB4 gene cluster. *(Reprinted from Improgo et al., 2010, with permission from Elsevier)*

When combined with $\alpha 3\beta 3$ subunits, $\alpha 5$ subunit has been shown to cause faster and a higher amount of desensitization of the receptor complex.[32,33]

CHRNA5 has 6 exons and is alternatively spliced, with at least three alternative transcripts identified.[34] It is implicated in smoking behavior with a single nucleotide polymorphism (SNP) and a common haplotype, resulting in high nicotine dependence and nicotine addiction.[35–37] CHRNA5 has also been associated with cognitive performance[38,39]

CHRNA5 is implicated in lung cancer[37] with at least three independent GWA studies[40–42] showing association between the chromosomal region of this gene cluster and lung cancer. CHRNA5 was found to be upregulated 30 times in lung adenocarcinoma, compared to normal lung tissue. 5 different transcripts of CHRNA5 was identified in normal lung tissue, due to alternative splicing

of the 5th exon. 1 of these isoforms is the full length CHRNA5 transcript and the others are shorter versions. All of these variants were expressed significantly higher in lung adenocarcinoma.[43] Splicing of these isoforms can be seen in 1.8.

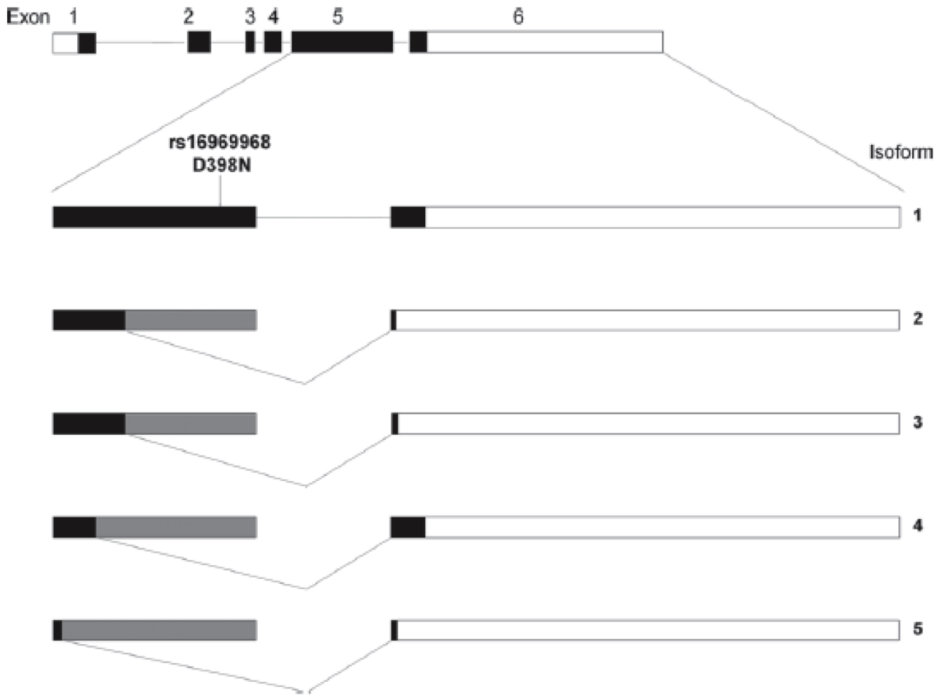

Figure 1.8: Alternative splicing of CHRNA5 in lung. *(Reprinted from Falvella et al., 2013, with permission from Oxford University Press)*

CHRNA5 was also shown to be expressed in breast tumors and breast cancer cell lines.[44]

1.4 Alternative Splicing

Alternative splicing is the process by which a single gene is allowed to produce a variety of protein isoforms. This event has a pivotal role in differential expression of genes. Since eukaryotic genes have introns, pre-mRNA splicing is necessary to remove intronic sequences and form the functional mRNA, consisting only of exons. Splicing of the pre-mRNA to the mature mRNA is

done by a complex called the spliceosome, which includes 5 small nuclear ribonucleoproteins (snRNPs) and a large number of other proteins.[45,46] Proper localization of the spliceosome is also dependent on *cis*-regulatory elements, named exonic and intronic splicing enhancers (ESE and ISE) and exonic and intronic splicing silencers (ESS and ISS), as well as *trans* regulatory splicing factors.[47]

Correct splicing is very important, as errors in parts of this mechanism lead to a variety of diseases. Especially in genes that are implicated in apoptosis, invasion, differentiation and metastasis, splicing occurs differently in tumors.[45,48,49]

At least five different alternative splicing patterns were identified.[45,49,50] They are shown in Figure 1.9. These include:

1. **Cassette Exon:** these exons are either skipped during splicing (spliced out) or included in the mature mRNA.

2. **Alternative 3' Splice Site:** an alternative to the normal 3' splice junction is used, resulting in an altered 5' end of the exon that is downstream. This can either lengthen or shorten the exon. Also called alternative acceptor site.

3. **Alternative 5' Splice Site:** an alternative to the normal 5' splice junction is used, resulting in an altered 3' end of the exon that is upstream. This can either lengthen or shorten the exon. Also called alternative donor site.

4. **Mutually Exclusive Exons:** one of these exons is included in the processed mRNA after splicing, but never both.

5. **Intron Retention:** in this pattern, an intron is not removed and included in the mature mRNA product.

Among these patterns, exon-skipping is the one that is most commonly observed in mammals, while intron retention is the least commonly observed.[51]

A combination of different alternative splicing patterns can be used in processing of a single pre-mRNA.[47] In addition to these main patterns, the presence of variants may be due to having multiple promoter sequences or multiple polyadenylation sites. Different isoforms of a gene can also be cell/tissue type or developmental stage-specific.[45,47–49] It was shown that the 5th exon of CHRNA5 is an exon with alternative splice sites, and there are at least 5 isoforms that either include or exclude parts of this exon.[43]

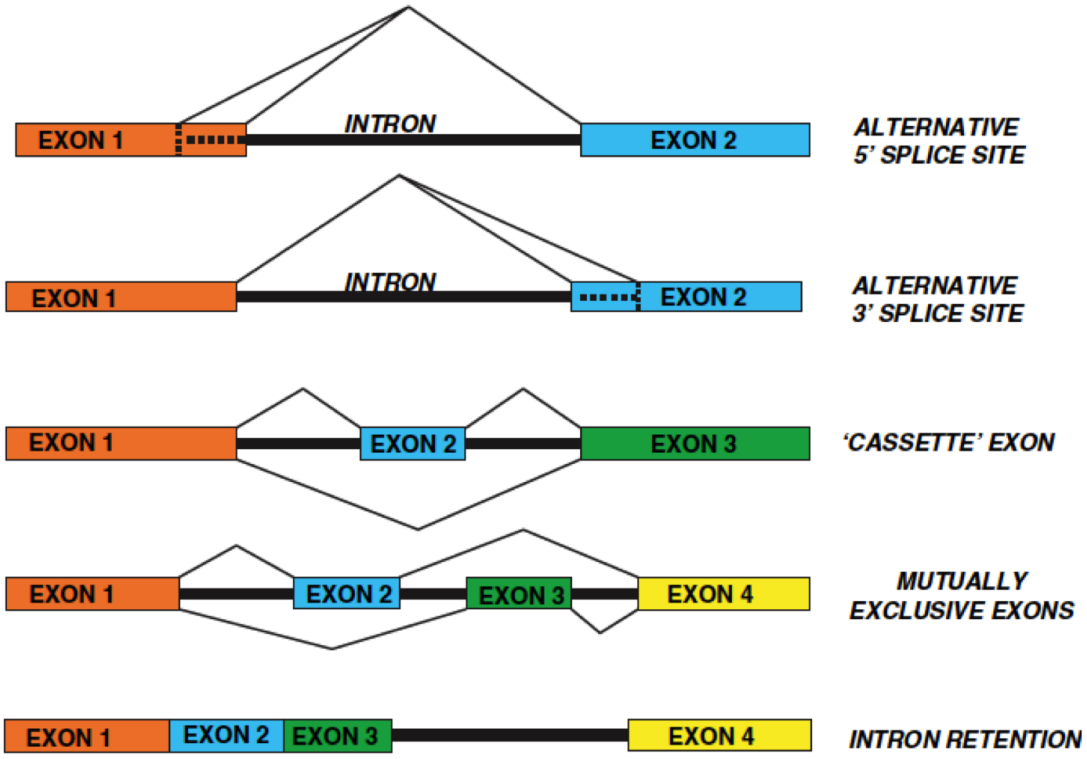

Figure 1.9: Different types of alternative splicing. *(Reprinted from Ladomery et al., 2006, with permission from Elsevier)*

Alterations in splicing patterns of particular genes have been observed or implicated in a number of diseases, including different types of cancer. These alterations may include mutations in *cis* or *trans* regulatory elements of splicing and result in changes in the selection of splice sites, leading to the formation of 'unnatural' mature mRNAs that are normally not present in a specific tissue or to changes in the ratios of natural splice variants in specific

tissues.[46,47] An illustration of how alterations in splicing can lead to malignancy is shown in Figure 1.10.

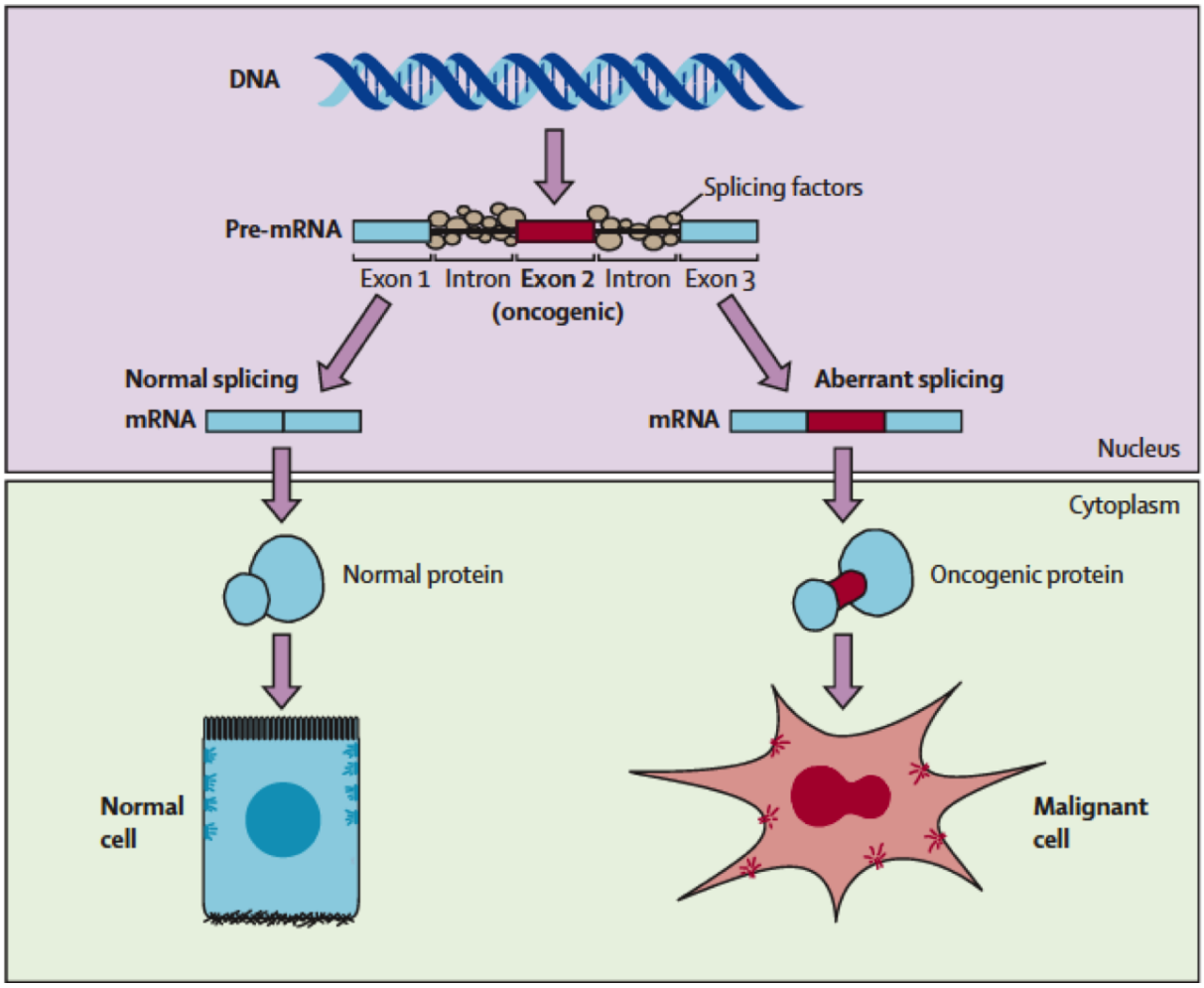

Figure 1.10: Abnormal pre-mRNA splicing can lead to malignancy. *(Reprinted from Pajares et al., 2007, with permission from Elsevier)*

In tumors, these so called 'abnormal' splicing variants, or aberrant transcripts are seen in genes that are involved in many processes in cancer susceptibility, initiation, development and progression. These include genes that are involved in apoptosis (*p53, Klf6, MDM4, Bcl-x, Caspase-2, Fas*), metabolism (*Pyruvate kinase M*), invasiveness and metastasis (*CD44, FGFs, Rac1, Ron,*

Crk), angiogenesis (*VEGFA*) and proto-oncogenes (*Cyclin D1, H-Ras*).[46,48,52]

Classical methods for identification of splice variants in cancer included cDNA sequencing and RT-PCR, but recently more global, genome-wide methods have been devised. These methods include EST alignment, splicing-specific exon-junction microarrays and bead-based fiber microarrays.[46,47,53]

1.5 Serum Starvation

For years, serum starvation has been widely used as an experimental procedure, mainly to obtain cells with synchronized cell cycles. Although some scientists oppose the utility of serum starvation as a method of cell synchronization,[54,55] a large number of researchers use this method in order to obtain cells with a G0/G1 phase arrest in the cell cycle. It is not exactly clear how serum starvation results in cell cycle arrest, but there has been a number of explanations. One of these associate the cell cycle arrest with inactivation of TOR and decreased Cyclin D1 levels, while another links it to increased p21 levels.[56,57]

Serum starvation has also been related to apoptosis. Prolonged exposure to serum-free media can cause apoptosis by itself, both in a p53-dependent[58] and p53-independent manner.[59] A number of caspases were also implicated in serum starvation induced apoptotic processes.[60,61]

Apart from being used as a method to synchronize cells, serum starvation has also been used as a method to investigate apoptosis, stress response of cells, autophagy and protein degradation, and regulation of gene expression. Microarrays were used to study molecular mechanisms of serum starvation/depletion (unpublished data from Konu Lab). It is important to note that, generally, serum starvation response differs between the cells and the cell culture protocols used.[62]

1.6 Quantitative Real Time Polymerase Chain Reaction (qPCR) Analysis

Quantitative real-time PCR (qPCR) has become the method of choice, both in research and in clinic, for quantification of gene expression. Among its many advantages are the fact that it is a high-throughput method, it is cost-effective, sensitive, specific and relatively easy to perform.[63,64] Still, interpreting and analyzing the data can be a challenge due to the complexity that having a number of variables brings.

Experimental design is very important, starting from the RNA to the analysis of the data obtained from qPCR. The things that need to be considered include, but are not limited to, RNA isolation and storage, preparation of the experimental setup, number of replicates (both biological and technical), normalization and statistical analysis methods.[63,64] In order to increase the statistical significance and meaning of the results, sample size must be increased and both biological and technical replicates must be present. Having biological replicates are thought to have more value than technical replicates, though technical replicates may help in the identification of outlier values.[65,66] There could be sample to sample or run to run variations between samples. Normalization is the method used to correct sample to sample variations that can arise from total RNA converted to cDNA, cDNA conversion efficiency, high individual variation or technical differences among runs and sampling errors.[63,65,67,68] Selecting a proper normalization method is of great importance since normalization affects the interpretation of the data. Normalization is generally done by using one or more reference genes. Using multiple reference genes for normalization is advised, with three being considered the optimal number.[63] When using multiple reference genes, normalization can be done by calculating the geometric mean of the reference genes. To aid with the selection of reference genes, a number of programs were devised, including GeNorm and BestKeeper.[63,64]

qPCR results can sometimes be variable, with the causes for this variabil-

ity being either biological, technical or due to an inappropriate experimental design.[65] This high number of possible causes for variability makes data analysis very important in interpreting the result of qPCR. Statistical analysis of the obtained data aims to identify differences in gene expression that are truly due to treatment, after minimizing the technical noise and identify the biological variability of the samples.[68] To this end, a proposed list of steps for data analysis includes the identification and exclusion of outliers (experimental errors), followed by averaging of technical and biological replicates and choosing a statistical test to perform.[69,70] The presence of three samples was said to be enough to be able to detect outliers with statistical significance.[70] Outliers can be identified as data points that do not obey the distribution of other data points in the data set. These are considered irregulars, distinct from the rest of the data set.[66] Identification and handling of these outliers is important to obtain statistically meaningful results and prevent wrong interpretations of the data.

It was proposed that a graphical representation of the distribution of the data may be of aid in the identification of outlier values.[66] To this end, an easy method was devised using box plots.[66] In these boxplots, the median value of the data points for a set is calculated and a box that represents the interquartile range is drawn around the median. The data points that fall outside of the whiskers are marked as potential outliers.[66] Statistical analyses, such as Grubb's test may be needed to assess the significance of the potential outliers.[66] The identified outlier values can later be removed from the data prior to analysis, increasing the statistical power.

Chapter 2

AIM

Breast cancer is the most common cancer and the secondary cause of cancer-related deaths in women in the Western world. This year, in the United States alone, more than 200000 women are expected to develop breast cancer, with an estimated death of around 40000.[71] Since breast cancer is a complex disease, classification has been important in prognosis. Histopathological type, tumor grading and staging were classically used to classify breast cancer and help with prognosis, but the observation that breast cancer is a more complex disease than previously thought lead to molecular classification of breast cancer and molecular subtypes.

Molecular subtype is described essentially by hormone receptor status, such as ER+, PR+, HER2+. According to this classification, breast cancers are now subdivided to 5 main molecular subtypes. These are basal or triple negative, luminal A, luminal B, HER2+ and normal-like. Even though this lead to a better classification, it was seen that there were significant differences in response to a particular therapy, clinical outcomes and prognosis, even in patients that are categorized under the same molecular subtype. This calls for a need for further molecular classification of breast cancer, and makes finding new molecular markers that can be used in novel categorization of great importance.

Cholinergic nicotinic receptors (CHRNs) are ion channels that have been associated with smoking behavior and nicotine addiction, neurodegenerative diseases and obesity. 9 alpha and 3 beta subunits have been identified in

humans. Recently, the $\alpha 5$ subunit has been associated with lung cancer. It was shown that CHRNA5 was expressed in breast cancers, but its transcriptional regulation was not extensively studied. In-silico analyses also suggest that CHRNA5 expression increases with estrogen treatment in ER+ breast cancer cell lines.[72]

Alternative splicing is an important way by which cells can increase their protein repertoire without the need for extra genes. Alternative splicing patterns of some genes were shown to be aberrant or abnormal in cancers, with either changes in the splice variants or changes in the ratios between specific variants.

In light of these information, in this study we asked whether CHRNA5 isoforms were alternatively spliced among different breast cancer cell lines under different serum regimes and whether an estrogen receptor positive cell line, MCF7, increased its CHRNA5 expression upon estrogen treatment.

In particular, the following were studied:

- Presence of alternative splicing of CHRNA5 in a breast cancer cell line panel and identification of different splice variants.
- Isoform-specific CHRNA5 expression in breast cancer cell lines with different molecular subtypes and identifying the relationship, if any, with ER status.
- The expression profile of CHRNA5 splice variants in breast cancer cell lines in response to serum starvation treatment.
- Isoform-specific CHRNA5 expression in response to estrogen treatment, and whether it changes according to dose and time of treatment in MCF7 cells.

Chapter 3

MATERIALS AND METHODS

3.1 Cell Culture Protocols

3.1.1 Cell Lines

10 different breast cancer cell lines (MCF7, T-47D, ZR-75-1, MDA-MB-361, MDA-MB-453, BT-20, HCC 1937, MDA-MB-468, MDA-MB-231, MDA-MB-157) were used in this study (ATCC; Manassas, USA). They have been cultured in Bilkent University MBG laboratories. Information about these cell lines are listed in Table 3.1

Table 3.1: Breast cancer cell lines and their properties.

Cell Line	Tissue	Derived from	Morphology	Disease	Age	Gender	Ethnicity	ATCC #
MCF7	mammary gland	pleural effusion	epithelial	adenocarcinoma	69 yo	female	Caucasian	HTB-22
T-47D	mammary gland	pleural effusion	epithelial	ductal carcinoma	54 yo	female	N/A	HTB-133
ZR-75-1	mammary gland	ascites	epithelial	ductal carcinoma	63 yo	female	Caucasion	CRL-1500
MDA-MB-361	mammary gland	brain	epithelial	adenocarcinoma	40 yo	female	Caucasian	HTB-27
MDA MB 453	mammary gland	pericardial effusion	epithelial	metastatic carcinoma	48 yo	female	Caucasion	HTB-131
BT-20	mammary gland	breast	epithelial	carcinoma	74 yo	female	Caucasian	HTB-19
HCC 1937	mammary gland	breast/duct	epithelial	ductal carcinoma	23 yo	female	Caucasian	CRL-2336
MDA MB 468	mammary gland	pleural effusion	epithelial	adenocarcinoma	51 yo	female	Black	HTB-132
MDA MB 231	mammary gland	pleural effusion	epithelial	adenocarcinoma	51 yo	female	Caucasian	HTB-26
MDA MB 157	mammary gland	breast/medulla	epithelial	medulallary carcinoma	44 yo	female	Black	HTB-24

3.1.2 Cell Growth Conditions

DMEM (SH30021.01), RPMI 1640 Medium (SH30255.01), FBS (SW30160.03), Penicillin/Streptomycin Solution (SV30010) and Trypsin/EDTA solution (SH30042.01) were from HyClone (Logan, USA). Non-essential amino acid solution (K0293) was from Biochrom AG (Berlin, Germany). PBS (17-516F) was from Lonza (Switzerland).

The growth medium of MCF7, MDA-MB-453, BT-20, MDA-MB-468 and MDA-MB-231 cells included DMEM with 10% Fetal Bovine Serum, 1% Penicillin/Streptomycin solution and 1% Non-essential amino acids.

The growth medium of ZR-75-1 cells included RPMI 1640 medium with 10% Fetal Bovine Serum, 1% Penicillin/Streptomycin solution, 1% Non-essential amino acids and 4,5 g/L D(+)-Glucose (Riedel-de-Haël, Hanover, Germany).

The growth medium of MDA-MB-361 and MDA-MB-157 cells included DMEM, with 10% Fetal Bovine Serum, 1% Penicillin/Streptomycin solution, 1% Non-essential amino acids and 1% Sodium Pyruvate (11360) (Gibco, USA).

3.1.3 Thawing Cells

One vial of frozen cells was taken from liquid nitrogen and were placed in the water bath at 37°C to melt. After melting, the cells were taken to a 15 ml, sterile tube with 10 ml complete medium and re-suspended. The cells were centrifuged at 1500 rpm for 5 minutes. After the supernatant was aspirated, the cells were re-suspended in complete growth medium and seeded in T25 flasks (Greiner Bio One, Frickenhausen, Germany) with 7-8 ml of complete medium.

3.1.4 Subculturing of Cells

All cell types were grown in T75 flasks (Grenier Bio One, Frickenhausen, Germany) with 13-14 ml of complete medium in a 37°C incubator with 5% CO_2. The cells were passaged to new flasks, on average, every 3 days, or when

they were around 80% confluent. For passaging, the growth medium was aspirated; flasks were washed with PBS. 0.5 - 1 ml Trypsin/EDTA solution was then added; flasks were kept in 37°C incubators for 5-8 minutes, until the cells detached from the surface. The cells were then collected with 7-8 ml complete growth medium and centrifuged at 1500 rpm for 5 minutes. The supernatant was aspirated; the cells were re-suspended in complete medium and were seeded to new flasks with the desired dilution.

3.1.5 Cryopreservation of Cells

For cryopreservation, freezing medium was prepared as 10% DMSO in FBS. The growth medium was aspirated; cells were washed with PBS, and trypsinized. After detachment, the cells were collected with complete medium and centrifuged at 1500 rpm for 5 minutes. Supernatant was aspirated and the cells were re-suspended in 2 ml PBS. They were centrifuged again at 1500 rpm for 3-5 minutes; supernatant was aspirated; and the cells were re-suspended in freezing medium. 1.5 ml of this was taken to 2 ml screw-capped cryotubes. The cryotubes were placed at - 20°C for 1-2 hours, and taken to - 80°C for 3-7 days after that. They were then placed and stored in liquid nitrogen.

3.1.6 Serum Starvation Treatment

Serum-deficient media were prepared, according to the cell type, as either DMEM or RPMI 1640 medium with 0.1% FBS instead of 10% FBS. The other additives in the media that were listed in Section 3.2 did not change. Serum starvation experiments were done for each of the 10 cell lines twice, at different times. (1st batch=set1-2, 2nd batch=set3-4).

For serum starvation experiments, 4 x T75 flasks were taken and 10 ml complete growth medium, specific to the particular cell type, was added to each. 3 x 10^6 cells were seeded to each T75 flask. The cells were incubated with complete medium for 24 hours. After 24 hours, the medium was aspirated and the cells were washed with PBS. 13 ml of 10% FBS medium was added to 2 of the T75 flasks, and 13 ml of 0.1% FBS medium was added to the

other 2 flasks. The cells were incubated for 48 hours.

3.1.7 β-Estradiol (E2) Treatment

For E2 treatment, the growth medium of the cells were changed to phenol red-free Dulbecco's MEM (F0475) (Biochrom AG, Berlin, Germany) with 5% charcoal/dextran-treated FBS (SH30068.02) (Hyclone, Logan, USA), 1% penicillin/streptomycin solution and 1% non-essential amino acids. To identify the effects of estrogen on breast cancer cell lines, β-Estradiol (E2758) (Sigma Aldrich, Missouri,USA) was used as estrogen substrate.

E2 stock solution was prepared by dissolving 27.238 mg E2 in 50 ml 100% EtOH (32221) (Sigma Aldrich, Missouri, USA) so that the final concentration of the stock solution was 2 mM. The stock solution was filtered and aliquoted to be stored in -20°C.

Final E2 treatment concentrations were 30 nM and 100 nM. For 30 mM final concentration, 0.75μl of 2 mM stock solution was added to 50 ml phenol red-free DMEM with 5% charcoal/dextran-treated FBS. For 100 mM final concentration, 2.5 μl of 2 mM stock solution was added to 50 ml phenol red-free DMEM with 5% charcoal/dextran-treated FBS.

The medium for 100nM E2 control group was prepared by adding 2.5 μl 100% EtOH to 50 ml phenol red-free DMEM with 5% charcoal/dextran-treated FBS.

MCF7 cells were counted and 12 x T75 flasks were seeded with 1 x 10^6 cells. They were incubated with regular 10% DMEM growth medium (with phenol red) for 24 hours. After 24 hours, the media of the cells were changed to phenol red-free DMEM with 5% charcoal dextran-treated FBS. The cells were incubated with this medium for 72 hours. 72 hours later, the media was changed to phenol red-free DMEM with 0.1% charcoal/dextran-treated FBS (the rest of the additives from the 5% medium were not changed) in order to synchronize the cell cycles of the cells to be able to properly assess the effect of E2 treatment.

After 24 hours, the 0.1% FBS medium was aspirated. 12 ml of media was added to each flask, with four of them being the control medium, 4 of them being 30 mM E2 treatment medium and 4 of them being 100 nM E2 treatment medium. After 12 hours, 2 of the controls, 2 of the 30 nM treatments and 2 of the 100 nM treatments were collected as pellets. The rest were collected after 24 hours.

3.1.8 MTT Assay

MTT assay was done for all of the cell lines, in order to assess the effect of serum starvation treatment on proliferation of breast cancer cell lines. Vybrant® MTT Cell Proliferation Assay Kit (V13154) (Molecular Probes, Oregon, USA).

12 mM MTT stock solution was prepared by dissolving 5 mg MTT in 1 ml sterile PBS and stored at +4°C. SDS solution was prepared by dissolving 1 g SDS in 10 ml, 0.01 M HCl.

For MTT assay, 96-well plates (Greiner Bio One, Frickenhausen, Germany) were used. 150 μl of 10% growth medium per well was added according to the cell type. 12 wells were filled for each cell line and 5000 cells per well were seeded. The cells were incubated at 37°C for 24 hours. After 24 hours, the media in the wells were discarded by using a micropippette rather than aspirating the medium with glass pasteurs. Then the plate was inverted to get rid of the remaining medium. The wells were washed with 80-100 μl PBS; PBS was, again, discarded by a micropippette; and the plate was inverted to get rid of the remaining PBS. For each cell line, 150 μl of 10% medium was added to 6 wells and 150 μl of 0.1% medium was added to 6 wells. The cells were incubated at 37°C for 48 hours. After 48 hours, the media in the wells were removed by a micropippette and the plate was inverted to get rid of the remaining media. 100 μl fresh medium was added to the wells (10% medium was used for the control groups and 0.1% medium was used for the serum starvation treatment groups). For negative control, 100 μl of 10% medium was added to 6 wells. 10 μl of the 12 mM MTT stock solution was added to

each well and carefully mixed. The plates were incubated at 37°C for 4 hours. After 4 hours, 100 μl of SDS-HCl solution was added to each well and the plates were incubated at 37°for 12-18 hours. After the final incubation, each sample was mixed again, and absorbance was read at 570 nm with μQuant spectrophotometer (BioTek Instruments, Vermont, USA).

3.2 Gene Expression Analyses

3.2.1 Total RNA Isolation

At the end of serum starvation and β-Estradiol treatments, pellets of cells were collected by aspirating the medium, washing the flasks with PBS and trypsinizing them. 7-8 ml of media was added to collect the trypsinized cells and the cells were centrifuged at 1500 rpm for 5 minutes. The supernatant was aspirated and the cells were re-suspended in 1-2 ml PBS. They were centrifuged at 1500 rpm for 5 minutes and the supernatant was aspirated. The pellets were stored at -80°C until RNA isolation.

Before total RNA isolation, the cell pellets were taken from -80°C and were thawed on ice. Then they were lysed completely with 1 ml TRIzol Reagent (15596-026) (Life Technologies, California, USA). The lysates were taken to 1.5 ml tubes and 200 μl of chloroform was added to each tube. The tubes were shaken vigorously for 10-15 seconds until they homogenized and they were left to incubate for 3-5 minutes at room temperature. The tubes were centrifuged at 13.200 rpm for 17 minutes at +4°C. After the centrifugation, a clear phase can be seen. 500 μl of the clear phase were taken to new 1.5 ml tubes and 500 μl isopropanol was added to each tube in order to precipitate total RNA pellet. The tubes were gently inverted for a couple of times and they were left to incubate at room temperature for 10 minutes. They were then centrifuged at 13.200 rpm for 12 minutes at +4°C. The supernatant was discarded, the pellet was washed with 1 ml 75% EtOH and centrifuged at 8000 rpm for 8 minutes at +4°C. The supernatant was discarded, 1 ml 100% EtOH was added and the tubes were centrifuged again at 8000 rpm for 8

minutes at +4°C. The supernatant was discarded and the pellets were left under laminar flow to air dry.

After the pellets dried, they were dissolved in 30-40 μl Hypure Molecular Biology Grade water (SH30538.03) (Hyclone, Logan, USA). The measurements of the samples were taken with NanoDrop® ND-1000 spectrophotometer (NanoDrop Technologies, USA). The RNA samples were stored at -80°C.

3.2.2 cDNA Synthesis

Isolated total RNA was used in cDNA synthesis. cDNA synthesis was done with RevertAid First Strand cDNA Synthesis Kit (K1621) (Thermo Fisher Scientific, Massachusetts, USA) according to the manufacturer's protocol. 1 μg (for serum starvation set3-4) - 1.5 μg (for serum starvation set1-2) total RNA was taken to 0.2 ml tubes. 1 μl oligo(dT) primer was added and the mixture was completed to 12 μl total volume by adding nuclease-free water. Other reagents were added (4 μl of 5x Reaction Buffer, 1 μl of RiboLock RNase Inhibitor, 2 μl of 10 mM dNTP Mix, 1 μl of RevertAid M-MuLV Reverse Transcriptase; in that order) to complete the total volume at 20 μl. The tubes were incubated at 42°C for 60 min, followed by 5 minutes at 70°C to terminate the reaction. They were stored at - 20°C.

3.2.3 Oligonucleotides

Primers that were used in this study are listed in Table 3.2.

Table 3.2: Primer sequences and their product sizes.

Gene		Sequence	Product Size
ANLN	Forward Reverse	5'-TAAAGCAGGTGATTGTTCGG-3' 5'-GTTCTTCATCAACACAGCAG-3'	180 bp
CHRNA5_W*	Forward Reverse	5'-TTAAGATGGAACCCTGATGACTATG-3' 5'-ATTGTTGGATCTCTTGGGCTTTTT-3'	Multiple
CHRNA5_All	Forward Reverse	5'-AGATGGAACCCTGATGACTATGGT-3' 5'-AAACGTCCATCTGCATTATCAAAC-3'	104 bp
CHRNA5_200	Forward Reverse	5'-CATCAGGTGTTGAAGATTGGAAAT-3' 5'-AAAAAGCCCAAGAGATCCAACAAT-3'	101 bp
CHRNA5_1000	Forward Reverse	5'-GGAAACTGAGAGTGGTAGTGGA-3' 5'-CTTCAACAACCTCACGGACA-3'	122 bp
CHRNA5_iso2†	Forward Reverse	5'-TGGAGAATGGGAGATTGTGAGTGCA-3' 5'-CCAATCTTCAACAACCAGCAACAGC-3'	78 bp
CHRNA5_iso3†	Forward Reverse	5'-TGGAGAATGGGAGATTGTGAGTGCA-3' 5'-CCAATCTTCAACAACGGATACCAGC-3'	78 bp
PS2‡	Forward Reverse	5'-CCATGGAGAACAAGGTGATCTGC-3' 5'-TTAGGATAGAAGCACCAGGGGAC-3'	208 bp
SDHA°	Forward Reverse	5'-TGGGAACAAGAGGGCATCTG-3' 5'-CCACCACTGCATCAAATTCATG-3'	86 bp
TPT1	Forward Reverse	5'-GATCGCGGACGGGTTGT-3' 5'-TTCAGCGGAGGCATTTCC-3'	100 bp

* Adapted from Warzecha et al., 2009[73]

† Adapted from Falvella et al., 2013[43]

‡Adapted from Alotaibi et al., 2006[74]

°Adapted from Gur-Dedeoglu et al., 2009[75]

3.2.4 Polymerase Chain Reaction

Polymerase Chain Reactions were done using OneTaq Quick-Load Master Mix (M0486L) (New England Biolabs, Massachusetts, USA) after optimizing manufacturer's protocol. The prepared PCRs and their reaction conditions are listed in Table 3.3 and Table 3.4, respectively.

Table 3.3: PCR reagents and their volumes.

PCR Reaction	**Volume**
2x OneTaq QuickLoad Master Mix	12.5 μl
Forward primer (10pmol)	0.5 μl
Reverse primer (10pmol)	0.5 μl
cDNA	1 μl
DNase/RNase-free water	9.5 μl
Total	**25 μl**

Table 3.4: PCR conditions for specific primers.

PCR Steps	**CHRNA5_W, CHRNA5_200**	**CHRNA5_All, CHRNA5_1000**	**SDHA, TPT1**
Initial Denaturation	95°C, 5'	94°C, 5'	94°C, 5'
Denaturation	95°C, 30"	95°C, 30"	95°C, 30"
Annealing	60°C, 90"	60°C, 30"	58°C, 30"
Extension	72°C, 90"	72°C, 30"	72°C, 30"
Number of cycles	35	40	40
Final Extension	68°C, 10'	72°C, 5'	72°C, 5'

' denotes minutes, " denotes seconds

3.2.5 Agarose Gel Electrophoresis

2% agarose gels were prepared by adding agarose to 1x TAE buffer. 1mg/ml ethidium bromide solution was added. After the gel polymerized, the wells were loaded with 10-12 μl PCR product. 4-5 μl GeneRuler 100bp DNA ladder (SM0241) (Thermo Scientific, Waltham, Massachusetts, USA) was used.

3.2.6 Quantitative Real Time-Polymerase Chain Reaction (qPCR)

qPCR was done using LightCycler® 480 SYBR Green I Master (04887352001) (Roche Applied Science, Germany) after optimizing the manufacturer's pro-

tocol. Every sample in the plates, including negative controls, were done in duplicates.
LightCycler® 480 PCR Instrument (Roche Applied Science, Germany) was used as the PCR machine and LightCycler® 480 Multiwell Plate 96 (04729692001) (Roche Applied Sciences, Germany) was used as plate in these reactions.
The prepared PCRs and their reaction conditions are listed in Table 3.5 and Table 3.6, respectively. Same conditions were used for each of the qPCR primers.

Table 3.5: qPCR reagents and their volumes.

PCR Reaction	**Volume**
LightCycler 480 SYBR Green I Master	5 μl
Forward primer (10pmol)	1 μl
Reverse primer (10pmol)	1 μl
cDNA	2 μl
DNase/RNase-free water	1 μl
Total	**10 μl**

Table 3.6: qPCR conditions.

PCR Steps	
Initial Denaturation	95°C, 5'
Denaturation	95°C, 10"
Annealing	58°C, 20"
Extension	72°C, 20"
Number of cycles	45
Acquisition	95°C, 5" 55°C, 1' 95°C, Continuous acquisition
Final Extension	40°C, 10"

' denotes minutes, " denotes seconds

3.3 Analyses of Serum-Starvation qPCR Results

The results of the qPCR experiments were taken as Cts (Cq) calculated by the 2nd derivative method.

3.3.1 Detection of qPCR Outliers with Matlab

Several outlier detection methods exist in the literature for analyzing microarray data and other datasets.[66,76] It is important that the outlier detection is done carefully, so that only the extreme outliers are removed.[77] If both of the technical duplicates of a sample as detected as outliers, they are not removed since this variation may pertain to the biological characteristics of the particular sample. Outliers that result from technical problems can occur because of inhibition of PCR reactions and these can be detected by using a PCR kinetics approach.[78] As well as using manual detection, researchers have also used existing softwares for the detection of unusually variable points in technical triplicates.[79,80] Standard deviations were also used as parameters within a study group with given restrictions (e.g. no more than a certain number of group members were excluded).[80] Visual inspection of boxplots of the data, followed by a statistical analysis was also suggested as a method for outlier detection.[66] According to this method, data points that fall outside the range of the box and whisker plots can be considered potential outliers.

Using Grubb's test has also been suggested for outlier detection and exclusion for qPCR data.[66] In this test, whether a data point belongs to the population is tested based on the difference between the mean and the most extreme value upon normalization with the standard deviation. This provides a statistical measure of how much suspected outlier deviates from normal distribution.[81]

In order to analyze a more uniform data and minimize experimental errors, in the present study, we used a method that is similar to that of Burns et al. (2005).[66] Existing functions for outlier detection based on IQR in Mat-

lab® (version: 2008b) were used to write a code (Appendix A Table 7.1) in order to detect the outlier Ct values of qPCRs. It was run for starvation set1-2 and starvation set3-4 separately. The boxplots themselves represent the 25% to 75% of the data, and the whiskers have a default length of 1.5. This corresponds to approximately 99.3 coverage, assuming the data is normally distributed. The working principle for the outlier detection code is as follows:

- It takes an xls file that contains both of the qPCR runs for a particular gene and a batch as input.
- It groups Ct values corresponding to each cell line and draws a boxplot (including both 10% and 0.1% values), separately for each cell line.
- The boxplot shows whether or not there are any outliers in Ct values for each cell line by marking it with a + sign.
- If there are any outliers, it detects the index of the outlier and replace that Ct value with 'NaN'.

After the replacement is done, the newly generated files are manually checked and if there are any samples in which both of the duplicates are flagged, these are replaced with their original Ct values.

3.3.2 Geometric Mean of Reference Genes

TPT1 and SDHA were chosen as reference genes and two runs of each was done for each set. Reference gene selection and the number of reference genes to be used are among important aspects of qPCR data normalization. It is assumed that RNA is converted to cDNA with equal efficiency and amount for each sample. A deviation from this expectation may result in sample variation attributable to either technical or biological issues and it is difficult to address which one is in effect. One solution to overcome the variations in RNA amounts in a qPCR run is the use of multiple reference genes for normalization.[63] Another issue with the use of reference genes is deciding which gene is appropriate for a given condition. Recent studies have shown

that there is no uniform reference gene that can be used in all studies.[79]

We addressed whether TPT1 and SDHA, two commonly used reference genes, can be used to assess the amounts of RNA preparation in our serum starvation experiments. For this, we looked for Affymetrix microarray experiments that were conducted on serum starved samples in the GEO database. For each dataset, TPT1 and SDHA probesets were analyzed using GEO2R utility of the GEO database. Table 3.7 shows the names of the GSE datasets analyzed for TPT1 and SDHA probesets. Figures 7.1 to 7.6 in Appendix B show the expression values of TPT1 and SDHA in the control (no starvation) and treatment (serum starved) groups.

Table 3.7: GSE datasets that were analyzed for TPT1 and SDHA probesets.

GEO Datasets*	SDHA probeset	TPT1 probeset	References
GSE21648	201093_x_at	212869_x_at	*Enoch S, Peake MA, Wall I, Davies L et* al. *'Young' oral fibroblasts are geno/phenotypically distinct. J Dent Res 2010 Dec;89(12):1407-13. PMID: 21098492*
GSE31040	201093_x_at	212869_x_at	*Matarrese P, Tinari A, Ascione B, Gambardella L et al. Survival features of EBV-stabilized cells from centenarians: morpho-functional and transcriptomic analyses. Age (Dordr) 2012 Dec;34(6):1341-59. PMID: 21904824*
GSE1692	201093_x_at	216520_s_at	*Cam H, Balciunaite E, Blais A, Spektor A et al. A common set of gene regulatory networks links metabolism and growth inhibition. Mol Cell 2004 Nov 5;16(3):399-411. PMID: 15525513*
GSE8597	201093_x_at	216520_s_at	*Bourdeau V, Deschênes J, Laperrière D, Aid M et al. Mechanisms of primary and secondary estrogen target gene regulation in breast cancer cells. Nucleic Acids Res 2008 Jan;36(1):76-93. PMID: 17986456*

** NCBI GEO: archive for functional genomics data sets. 10 years on. Tanya Barrett, Dennis B. Troup, Stephen E. Wilhite, Pierre Ledoux, Carlos Evangelista, Irene F. Kim, Maxim Tomashevsky, Kimberly A. Marshall, Katherine H. Phillippy, Patti M. Sherman, Rolf N. Muertter, Michelle Holko, Oluwabukunmi Ayanbule, Andrey Yefanov, Alexandra Soboleva. Nucleic Acids Res. 2011 January; 39(Database issue): D1005?D1010. Published online 2010 November 20. doi: 10.1093/nar/gkq1184.*

Based on these microarray analyses, TPT1 and SDHA seem to be relatively stable reference genes. A code was written in Matlab to get geometric averages of the Ct values in order to obtain a composite reference Ct value. The code takes the average Ct values of the duplicates in each run, then average Ct of the samples between runs. This was done separately for TPT1 and SDHA and for set1-2 and set3-4. After the generation of these two reference files for each set, geometric means of the Ct values for TPT1 and SDHA were calculated for each set and written on an xls file as an output. This newly generated file was used as reference in further analysis. The code used for this can be seen in Appendix A Table 7.2

A similar test was performed to see whether TPT1 and SDHA expressions change under β-estradiol stimulation, using a benchmark dataset from GEO (GSE8567). This also indicated that these two reference genes were stable between groups and did not exhibit large fold differences. The expression values of TPT1 and SDHA in control (no treatment) and treatment (β-estradiol treatment) groups can be seen in Figures 7.7 and 7.8 in Appendix B.

3.3.3 Statistical Analysis of qPCR Data

There are several methods for relative assessment of expression values obtained from qPCR data. Among these methods, $\Delta\Delta Ct$ or ΔCt method, with or without efficiency correction, is the most commonly used.[82] This requires the target gene expression to be subtracted from the reference gene expression for each of the samples. Then, if necessary, common reference samples are used to obtain a relative fold change value for each sample ($\Delta\Delta Ct$). Recent studies also advocate the use of log values rather than simple fold change for statistical accuracy purposes. Statistical analysis of qPCR data has been reviewed, focusing on comparisons of different statistical tests (multiple regression analysis, Analysis of Covariance (ANCOVA) and t-test).[83] They emphasized that equal amplification efficiencies were more important when using the $\Delta\Delta Ct$ method. Multiple regression analysis enables one to incorporate different effects, including treatment and gene effects, into the model, as well as any interactions between them. ANCOVA allows the usage of a

covariate, which makes it possible to test the difference between the control and the treatment groups after the effect of reference genes is taken away, thus standardizing the treatment effects from different batches. ANCOVA can be a very effective method to adjust for batch effects, especially when multiple qPCR runs of the same control and treatment groups are included in the analysis. It also permits detection of slope differences between treatment groups as well as provides a significance value for each group for testing the intercept. All of these methods, however, depends on the selection of true reference genes whose expressions are relatively stable among samples and experimental groups.

In our experimental design for serum starvation, two sets (set1-2 and set3-4) of control-treatment experiments were performed at different times with different batches of the same cell lines. In each set, a total of four replicates from two separate qPCR runs were included for each sample (n=4 per group, 2 groups). We have chosen an approach that sequentially incorporates:

- Detection of outliers that can be attributed to technical errors,
- Averaging of duplicates for a sample, followed by averaging the values of each sample from different runs,
- Geometric averaging of reference genes for each batch separately.

For a gene of interest (2 references and 2 target genes), duplicate values were averaged for each individual. For the reference genes this was done before obtaining a geometric average set-wise. The batches (set1-2 and set3-4) were then combined for ANCOVA, in which the geometric average of TPT1 and SDHA was used as the covariate to test for the differences in expression of CHRNA5 isoforms between cell lines for 10% FBS and 0.1% FBS treated cells separately and between serum starvation and control groups for each cell line separately.

3.3.3.1 Pearson Correlation Between 200bp and 1000bp CHRNA5 Isoforms

Scatter graphs for 200bp CHRNA5 and 1000bp CHRNA5 isoforms were plotted using Matlab®. To check for correlation between these two isoforms, Pearson correlation values were calculated, with r values and their associated p-values under serum and no serum conditions.

3.3.3.2 ANCOVA

a) For all cell lines

A Matlab code was written to analyze the expression differences of CHRNA5 isoforms between cell lines, normalized to the geometric mean of the two reference genes, using ANCOVA (aoctool). This was done separately for 10% FBS treated cell lines and 0.1% FBs treated cell lines.

The code written for ANCOVA for all cell lines can be seen in Appendix A Table 7.3.

b) For each cell line, for the effect of serum starvation

In order to test whether serum starvation affected the mean expression values of CHRNA5 isoforms between control and treatment groups, ANCOVA was used. This also allowed us to get rid of the batch effect that can result from using different batches of cell lines, since it standardizes over the geometric mean of TPT1 and SDHA across all sets at the same time. This model assumes that there is a linear relationship, if any, between the reference gene and target gene. The Matlab code written for ANCOVA for separate cell lines can be seen in Appendix A Table 7.4. In the code, a covariate description file, which includes the indices of cell lines, is used. Other files that are called from the code are ref12 or ref34 containing the geometric means of references for sets; and trg12 or trg34 containing the arithmetic means of targets (either 200bp variant of CHRNA5 or 1000bp variant of CHRNA5).

3.4 Analyses of β-Estradiol Treatment Results

For the analysis of β-Estradiol(E2) treatment, no outlier detection was performed since it is a smaller dataset and number of technical replicates is two. Geometric means of the two reference genes TPT1 and SDHA were, again, taken (after taking the averages of duplicates). The expressions of the reference genes TPT1 and SDHA were checked in GEO database using GSE8597 dataset, which includes β-estradiol treatment. Analysis indicated that these two genes were, again, relatively stable in the presence of estrogen as they were under starvation conditions. Two-way ANOVAs were performed in R (www.bioconductor.org) on logarithmically transformed fold changes ($\Delta\Delta Ct$ with reference genes) that were calculated using Microsoft Excel. $\Delta\Delta Ct$ values were calculated standardized to the average value of time specific control group for 12h and 24h, separately.

3.4.1 Two-way Anova analysis with R

Our experimental design involves two factors: a dose effect (0 and 100nM) and a time effect (12h and 24h). This calls for a statistical test in which all sources of variation, including the interaction between the two, could be accounted for at the same time to increase statistical power. In order to detect the effects of E2, a two-way ANOVA analysis was done for each primer that was used, using 'anova(lm())'function in R. csv files were generated for each primer, including information about the dose and time of E2 treatment and the fold changes observed, compared to the controls. Boxplots of changes in expression values were drawn, showing the differences between the means.

Table 3.8 shows an example of these csv files.

Table 3.8: An example of csv files used in two-way ANOVA analysis for E2-treatment data.

200bp	group	dose	time
0.815	0nm12	0	12
-0.815	0nm12	0	12
3.09	100nm12	100	12
0.22	100nm12	100	12
-0.65	0nm24	0	24
0.65	0nm24	0	24
2.765	100nm24	100	24
3.185	100nm24	100	24

3.4.2 ANCOVA of CHRNA5 expression

ANCOVA was done in Matlab in order to se if there is a difference in the trends of response to E2 between 12h and 24h. ANCOVA gives two p-values, one for the significance of dose and another for the significance of time.

3.4.3 Saturation Analysis of E2 Treatment

In order to identify the concentration of E2 that is required to reach a saturation level for the increase in CHRNA5 expressions, additional data points of 30nM E2 treated samples were used (both for 12h and 24h). These 30nM treated samples do not have their own controls but they will give us an idea about the E2 concentration needed for our future experiments. Logarithmically converted fold changes of CHRNA5 isoforms in response to 12h and 24h of 0nM, 30nM and 100nM E2 treatment were used to create scatter graphs with Microsoft Excel.

3.5 General Solutions

- **50x Tris-acetic-EDTA (TAE):** 242 g Tris base and 18.6 g EDTA were dissolved in ddH_2O. 57.1 ml glacial acetic acid was added and the volume was completed to 1 lt.

Chapter 4

RESULTS

4.1 Expression of CHRNA5 Isoforms in Cell Lines

To determine the presence of splice variants of CHRNA5 in breast cancer cell lines, primers that amplified all of the expected variants were used (CHRNA5_W in Table 3.2) for RT-PCR. TPT1 was used as a reference gene. Figure 4.1 shows that there are at least 4 isoforms of CHRNA5 using this primer pair in our breast cancer panel consisting of 10 cell lines and each of these isoforms are differentially expressed between different breast cancer cell lines. According to the results in Figure 4.1, we decided to focus on two of the splice variants of CHRNA5, namely the 200bp variant and the 1000bp variant. These isoforms have been cut from the gel, cloned and sequenced to verify that they belonged to CHRNA5 (data not shown). SDHA was used as the reference gene and expression of these two variants and another primer that amplifies all of the variant of CHRNA5 was determined in our panel. 2 sets for each cell line was used. Figure 4.2 shows that all the variants investigated can be amplified in all of the cell lines, using sequence specific primers (Table 3.2). Differences between cell lines could not be identified via regular RT-PCR, which made use of qPCR a necessity.

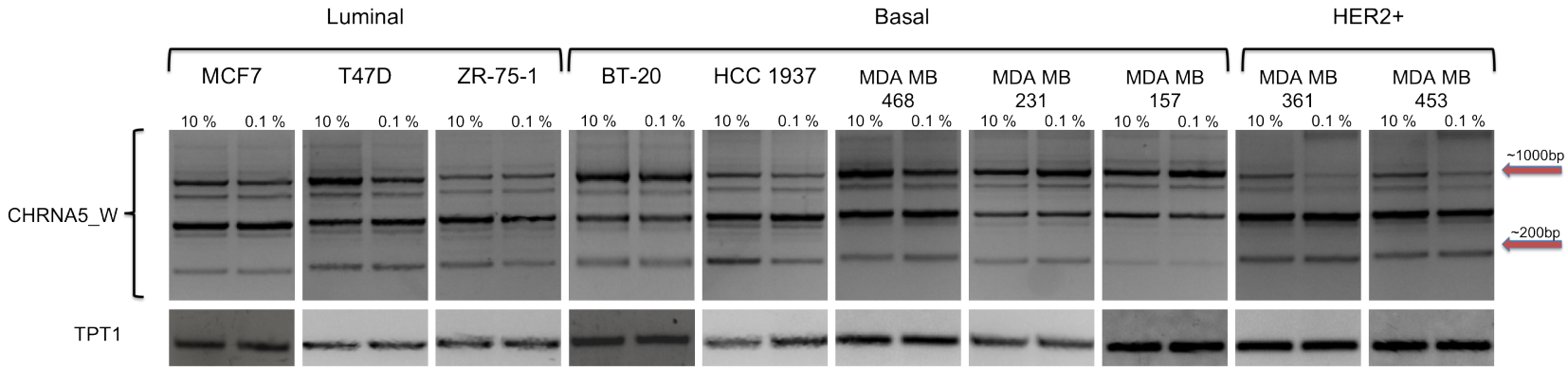

Figure 4.1: Representative expression of CHRNA5 alternative splicing products and TPT1 across breast cancer cell lines treated with 10% and 0.1% FBS. Arrows indicate the variants focused on this study.

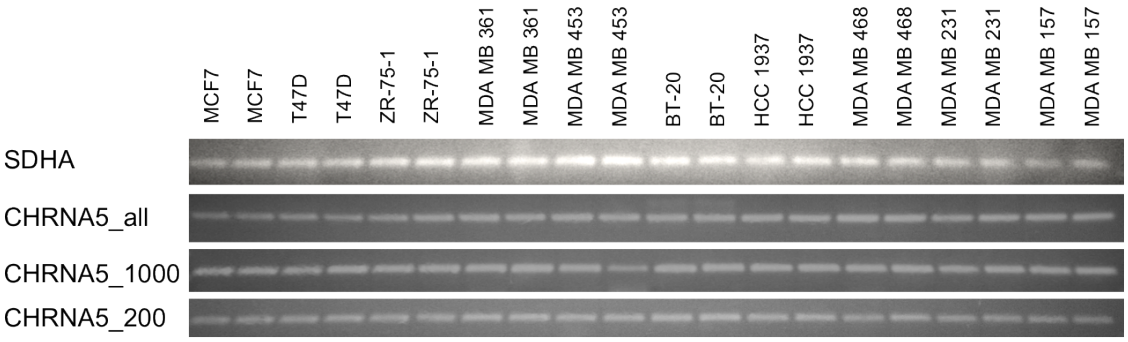

Figure 4.2: Expression of different CHRNA5 variants and SDHA across two sets of each of the 10 breast cancer cell lines.

4.2 Effects of Serum Starvation Treatment

4.2.1 Effects of Serum Starvation on Cell Proliferation and Viability

To investigate the effects of serum starvation treatment on cell viability and proliferation, MTT assay was done for each of the 10 cell lines. MTT assay is a colorimetric assay that measures the cell viability by the presence of enzymes in viable cells that are able to process MTT to formazan, giving a purple color. The absorbance value is proportional to cell viability. Figures 4.3 to 4.12 show the MTT assay results for the cell lines in Table 1.3. Data were analyzed using unpaired, equal variance t-tests for each cell line between the control and treatment groups using Microsoft Excel.

The results show a significant decrease in cell viability and proliferation for 7 of the 10 cell lines under study. For ZR-75-1, MDA MB 453, BT-20, MDA MB 468, MDA MB 231 cell lines; $p < 0.0001$, for MDA MB 361 cell line; $p < 0.005$, for MDA MB 157 cell line; $p < 0.05$ were observed. The remaining cell lines (MCF7, T47D, HCC 1937) did not exhibit a significant difference in their viability or proliferation rates in response to serum starvation treatment.

Table 4.1: MTT results for all cell lines.

Cell Line	Cnt. Abs.	Cnt. StD.	Strv. Abs.	Strv. StD.	p-value
MCF7	0.492	0.036	0.417	0.092	0.095851667
T47D	0.264	0.056	0.253	0.045	0.733955993
ZR-75-1	0.709	0.026	0.417	0.038	0.0000000280
MDA MB 361	0.182	0.046	0.101	0.025	0.003702561
MDA MB 453	0.390	0.047	0.130	0.025	0.0000002938
BT-20	0.838	0.091	0.383	0.035	0.0000004705
HCC 1937	0.188	0.035	0.182	0.040	0.788276551
MDA MB 468	0.645	0.052	0.292	0.047	0.0000002363
MDA MB 231	0.523	0.039	0.147	0.028	0.0000000030
MDA MB 157	0.217	0.060	0.141	0.026	0.016540839

Cnt. Abs.: absorbance values of control groups
Cnt. StD.: standard deviation of control groups
Strv. Abs.: absorbance values of starvation groups
Strv. StD.: standard deviation of starvation groups

Table 4.2: Fold changes of MTT absorbance values between 10% and 0.1% FBS treated breast cancer cell lines.

Cell Line	Fold Change	log.fc
ZR-75-1	0.588152327	-0.765738244
T47D	0.958333333	-0.061400545
HCC 1937	0.968085106	-0.046794211
MDA MB 231	0.281070746	-1.830994791
MCF7	0.847560976	-0.238610932
MDA MB 157	0.649769585	-0.62199988
MDA MB 453	0.333333333	-1.584962501
MDA MB 361	0.554945055	-0.849583157
MDA MB 468	0.452713178	-1.143330791
BT-20	0.457040573	-1.129605852

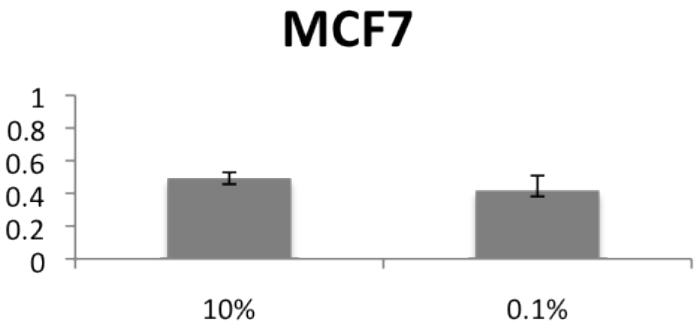

Figure 4.3: MTT assay results for MCF7 cells. Y axis shows cell viability and x axis shows treatment FBS.

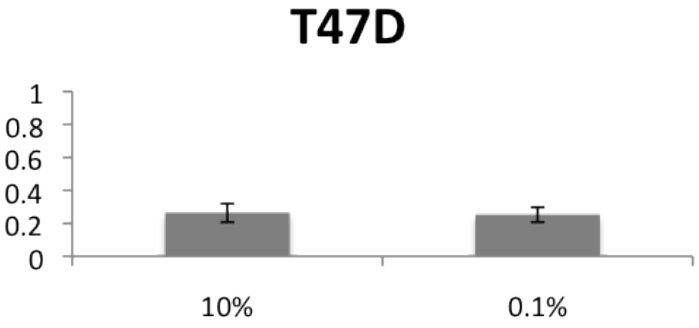

Figure 4.4: MTT assay results for T47D cells. Y axis shows cell viability and x axis shows treatment FBS.

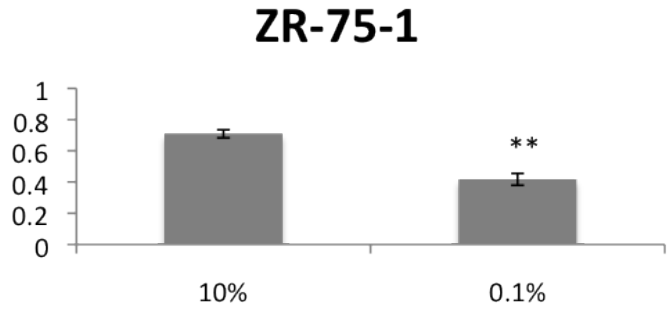

Figure 4.5: MTT assay results for ZR-75-1 cells. Y axis shows cell viability and x axis shows treatment FBS. **, $p<0.0001$

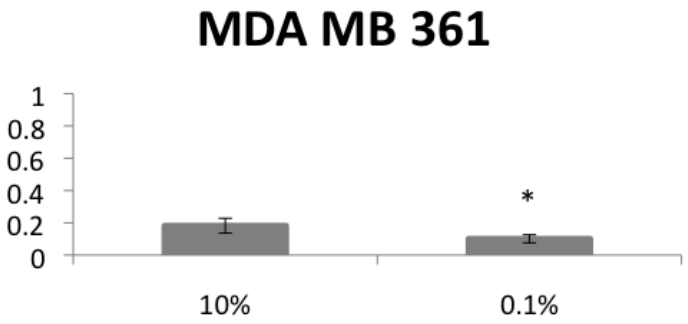

Figure 4.6: MTT assay results for MDA MB 361 cells. Y axis shows cell viability and x axis shows treatment FBS. *, $p<0.005$

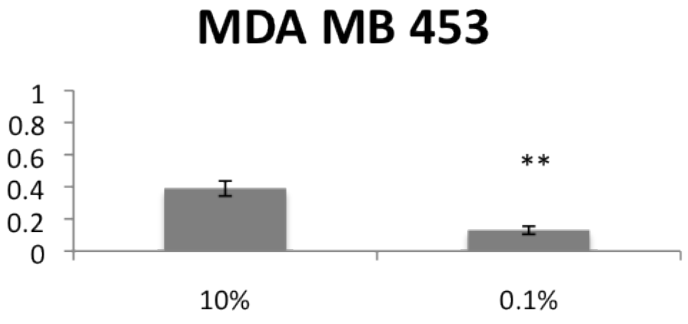

Figure 4.7: MTT assay results for MDA MB 453 cells. Y axis shows cell viability and x axis shows treatment FBS. **, $p<0.0001$

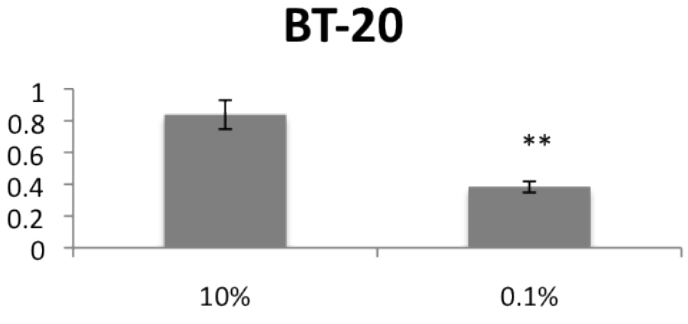

Figure 4.8: MTT assay results for BT-20 cells. Y axis shows cell viability and x axis shows treatment FBS. **, $p<0.0001$

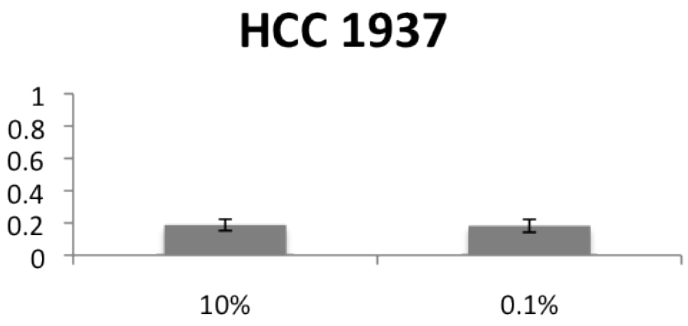

Figure 4.9: MTT assay results for HCC 1937 cells. Y axis shows cell viability and x axis shows treatment FBS.

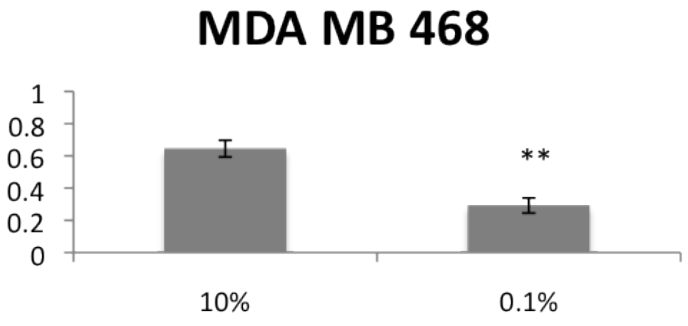

Figure 4.10: MTT assay results for MDA MB 468 cells. Y axis shows cell viability and x axis shows treatment FBS. **, p<0.0001

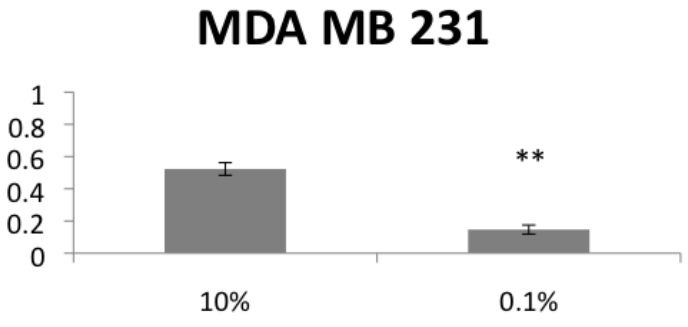

Figure 4.11: MTT assay results for MDA MB 231 cells. Y axis shows cell viability and x axis shows treatment FBS. **, p<0.0001

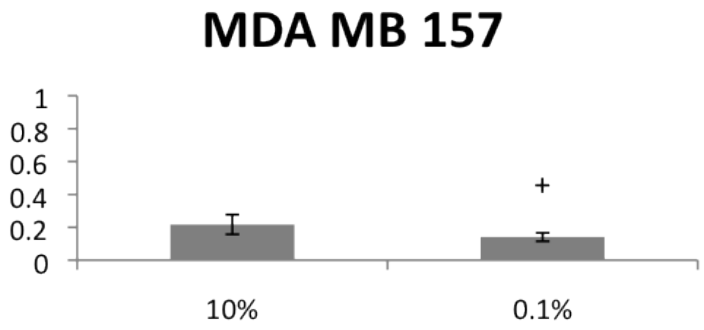

Figure 4.12: MTT assay results for MDA MB 157 cells. Y axis shows cell viability and x axis shows treatment FBS. +, $p<0.05$

4.2.2 Effects of Serum Starvation on CHRNA5 Variant Expression

4.2.2.1 Outlier Detection in qPCR data

In order to do a more accurate analysis of the qPCR data, potential outlier values due to possible experimental errors in single wells were identified and excluded from the analysis as explained in the Materials & Methods section. A Matlab code was used for the automation of this procedure (see Appendix A Table 7.1). Boxplots of Ct values for each cell line were drawn for each gene (Figures 4.13 to 4.16). Box plots identify the 52%-75% of the data distribution and whiskers cover about 99%. Potential outliers are marked with a '+' sign.

Figure 4.13 shows the outlier analysis for TPT1. In set1-2, two potential outlier values were detected (1 in MDA MB 231 cells and 1 in MDA MB 453 cells). In set3-4 five potential outlier values were detected (1 in MDA MB 231 cells, 1 in MDA MB 157 cells, 1 in MDA MB 453 cells and 2 in MDA MB 468 cells).

Figure 4.14 shows the outlier analysis for SDHA. In set1-2, two potential outlier values were detected (both in MDA MB 231 cells). In set3-4, eight potential outlier values were detected (4 in MDA MB 231 cells, 1 in MCF7

cells, 2 in MDA MB 157 cells and 1 in BT-20 cells).

Figure 4.15 shows the outlier analysis for 200bp variant of CHRNA5. In set1-2, eleven potential outlier values were detected (2 in ZR-75-1 cells, 1 in MCF7 cells, 3 in MDA MB 157 cells, 1 in MDA MB 453 cells, 2 in MDA MB 361 cells and 2 in BT-20 cells). In set3-4, 2 potential outlier values were detected (1 in MDA MB 453 cells, 1 in MDA MB 361 cells).

Figure 4.16 shows the outlier analysis for 1000bp variant of CHRNA5. In set1-2, seven potential outlier values were detected (3 in ZR-75-1 cells, 2 in MCF7 cells, 1 in MDA MB 361 cells and 1 in MDA MB 468 cells). In set3-4, eight potential outlier values were detected (1 in HCC 1938 cells, 1 in MDA MB 231 cells, 1 in MCF7 cells, 1 in MDA MB 453 cells, 1 in MDA MB 361 cells, 2 in MDA MB 468 cells and 1 in BT-20 cells).

All of the detected potential outliers were replaced with 'NaN'. After the replacements were done, the data was manually checked. If there were cases where both of the duplicates for a sample were replaced with 'NaN', both of these values were left unreplaced. There were two such cases, both in SDHA of set3-4, in which both of the duplicates in a sample from MDA MB 231 cells and a sample from MDA MB 157. Altogether, out of 1280 data points, 45 were detected as potential outliers using the boxplot method; and 41 of them were replaced with 'NaN', corresponding to 3.2% of the data.

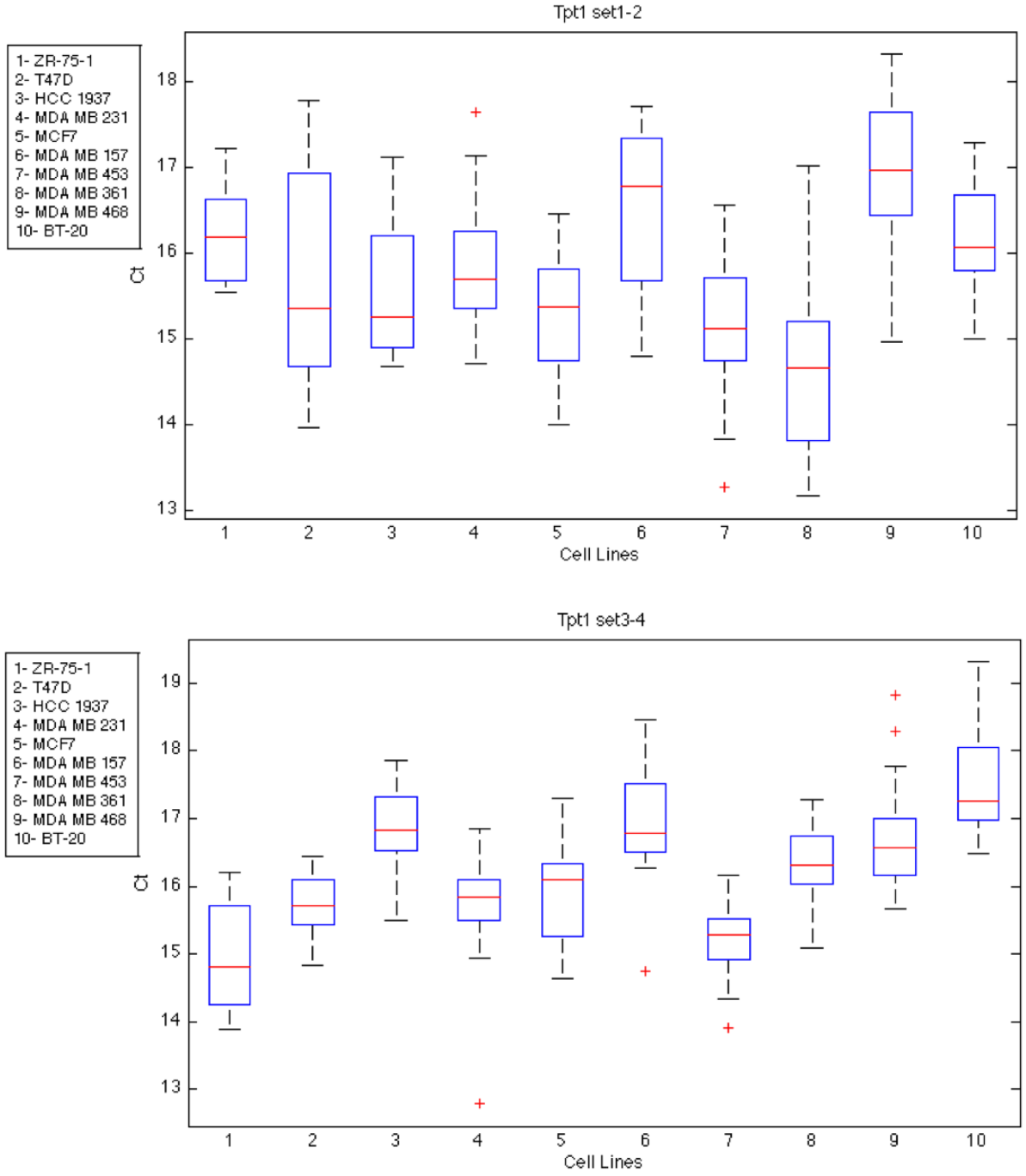

Figure 4.13: Outlier analysis for TPT1.

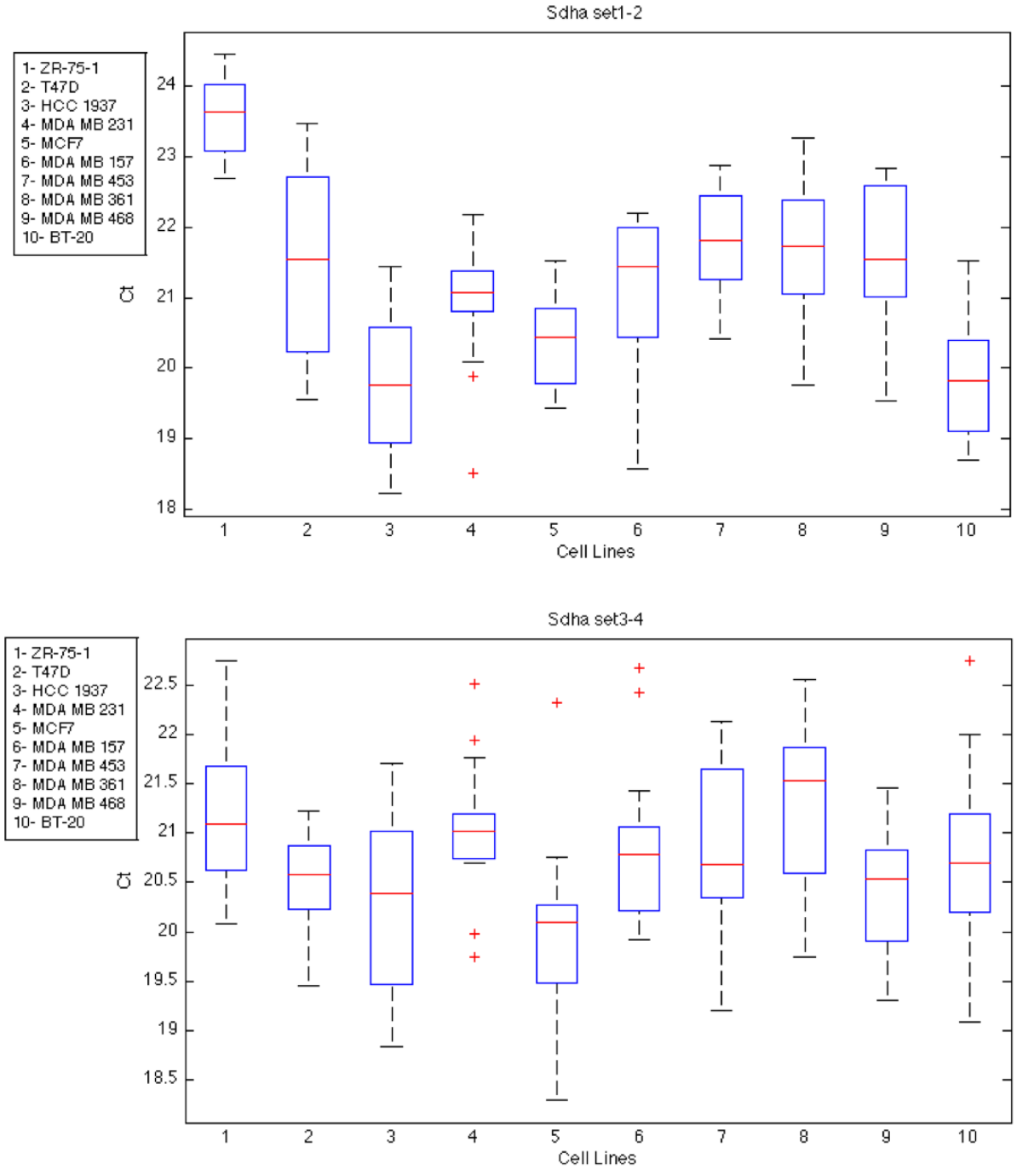

Figure 4.14: Outlier analysis for SDHA.

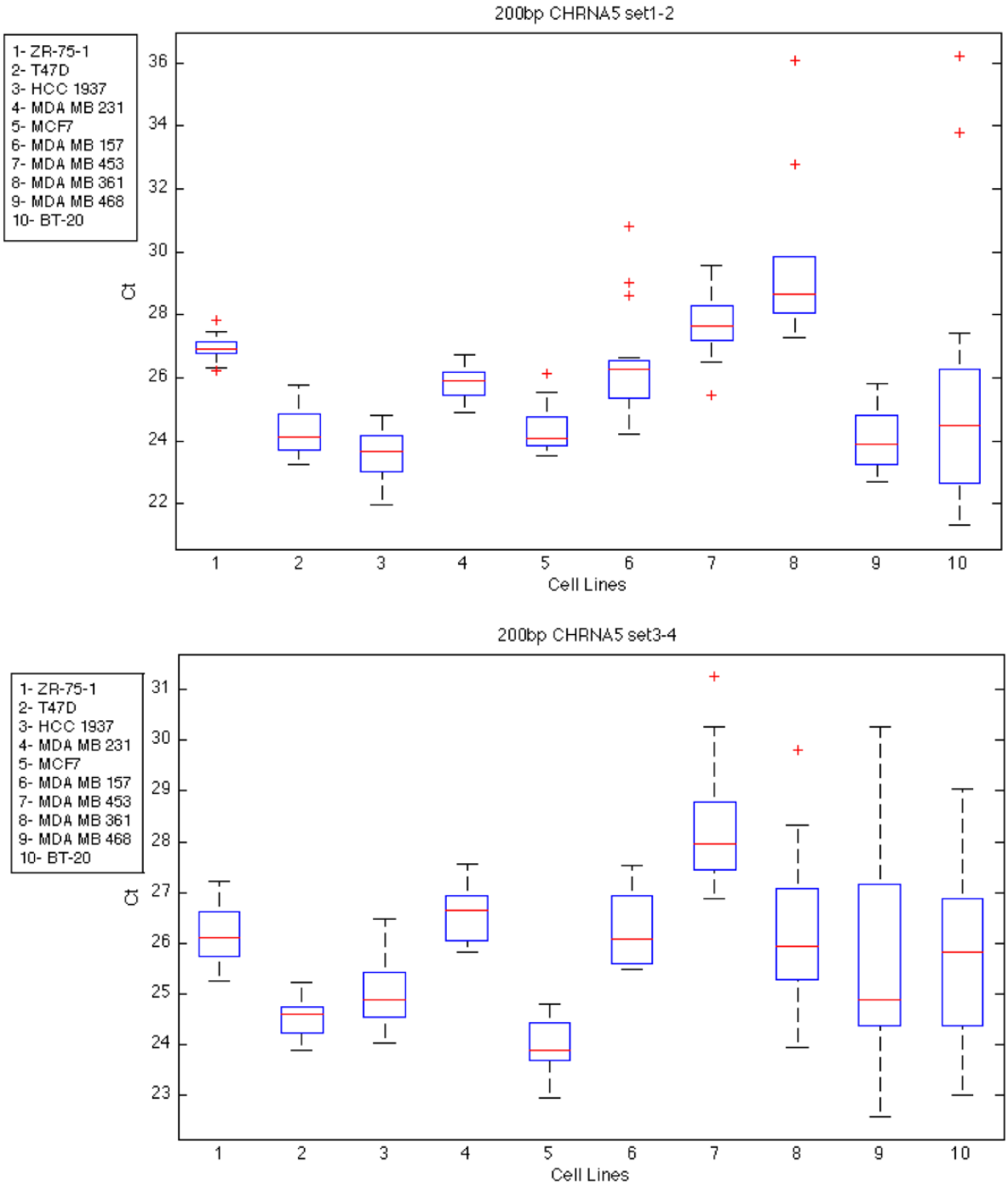

Figure 4.15: Outlier analysis for 200bp CHRNA5.

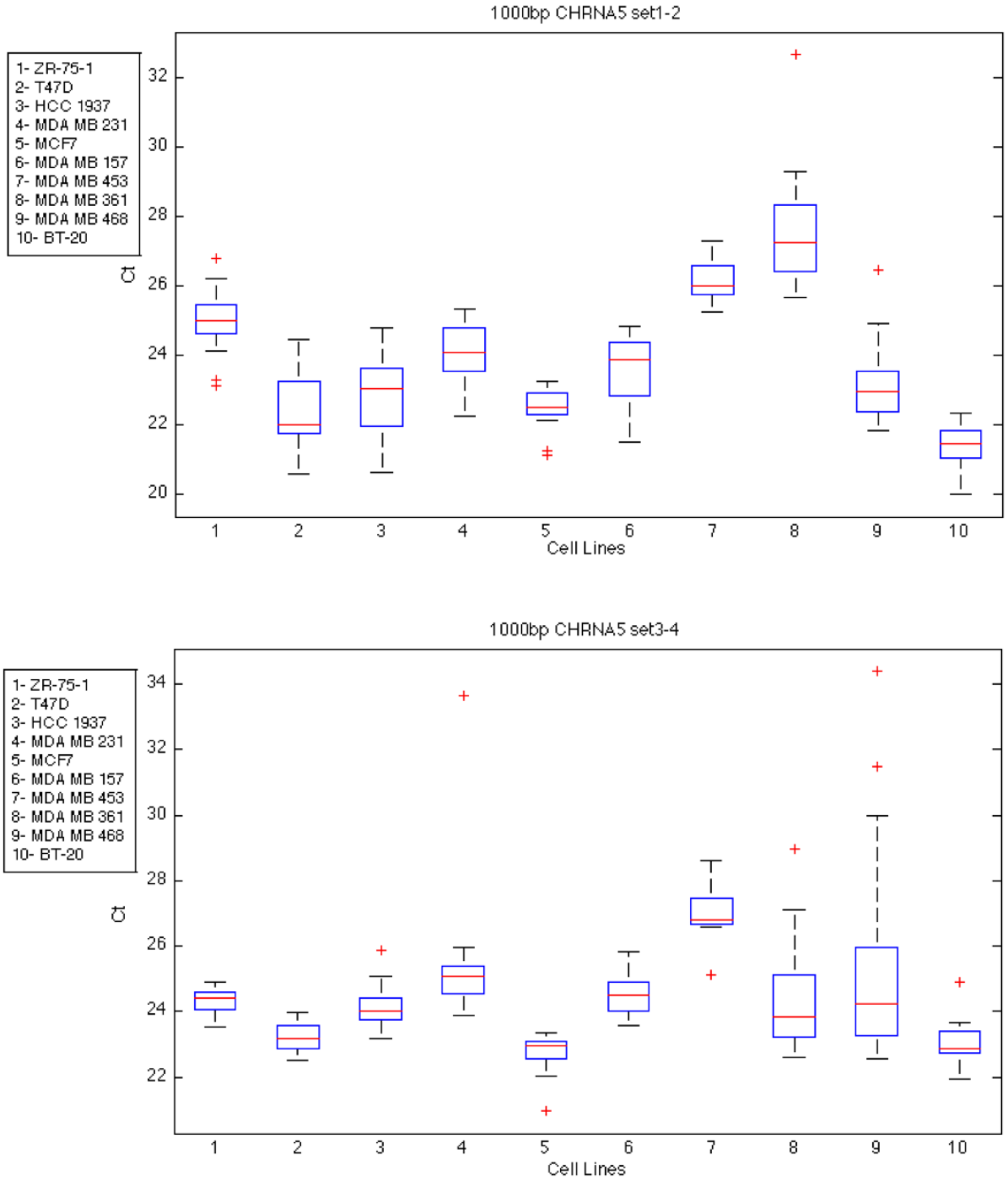

Figure 4.16: Outlier analysis for 1000bp CHRNA5.

4.2.2.2 CHRNA5 variant expression in Cell Lines

Expression of 200bp and 1000bp CHRNA5 variants were compared in 10% and 0.1% FBS treated cell lines by drawing scatter plots using their respective ΔCt values. Figures 4.17 and 4.18 show the comparisons. Since we are using ΔCt values as $targetCt - referenceCt$, higher ΔCt values correspond to lower mRNA expression.

In both 10% and 0.1% FBS treated cells, 200bp variant of CHRNA5 and 1000bp variant of CHRNA5 were correlated. 10% treated cells have an r value (r; Pearson correlation coefficient) of 0.9221 and a p-value of 0 and the 0.1 % treated cells have an r value of 0.8859 and a p-value of 0. There is a grouping of cell lines according to expressions of CHRNA5 variants and this correlates with the molecular subtypes of cell lines. Based on ΔCt values, cell lines belonging to the HER2+ subtype, MDA MB 453 and MDA MB 361, have the lowest expression (highest ΔCt) of CHRNA5 variants, while luminal cell lines MCF7, T47D and ZR-75-1 cell lines, together with post-EMT basal cell lines MDA MB 231 and MDA MB 157, are grouped in the middle. Basal type cell lines BT-20 and MDA MB 468 have the highest expression of CHRNA5 variants, when considering expression of both isoforms simultaneously. Figures 4.17 and 4.18 also indicate that there is considerable batch effect, particularly in 0.1% FBS treatment, e.g., MDA MB 468, MDA MB 361, T47D.

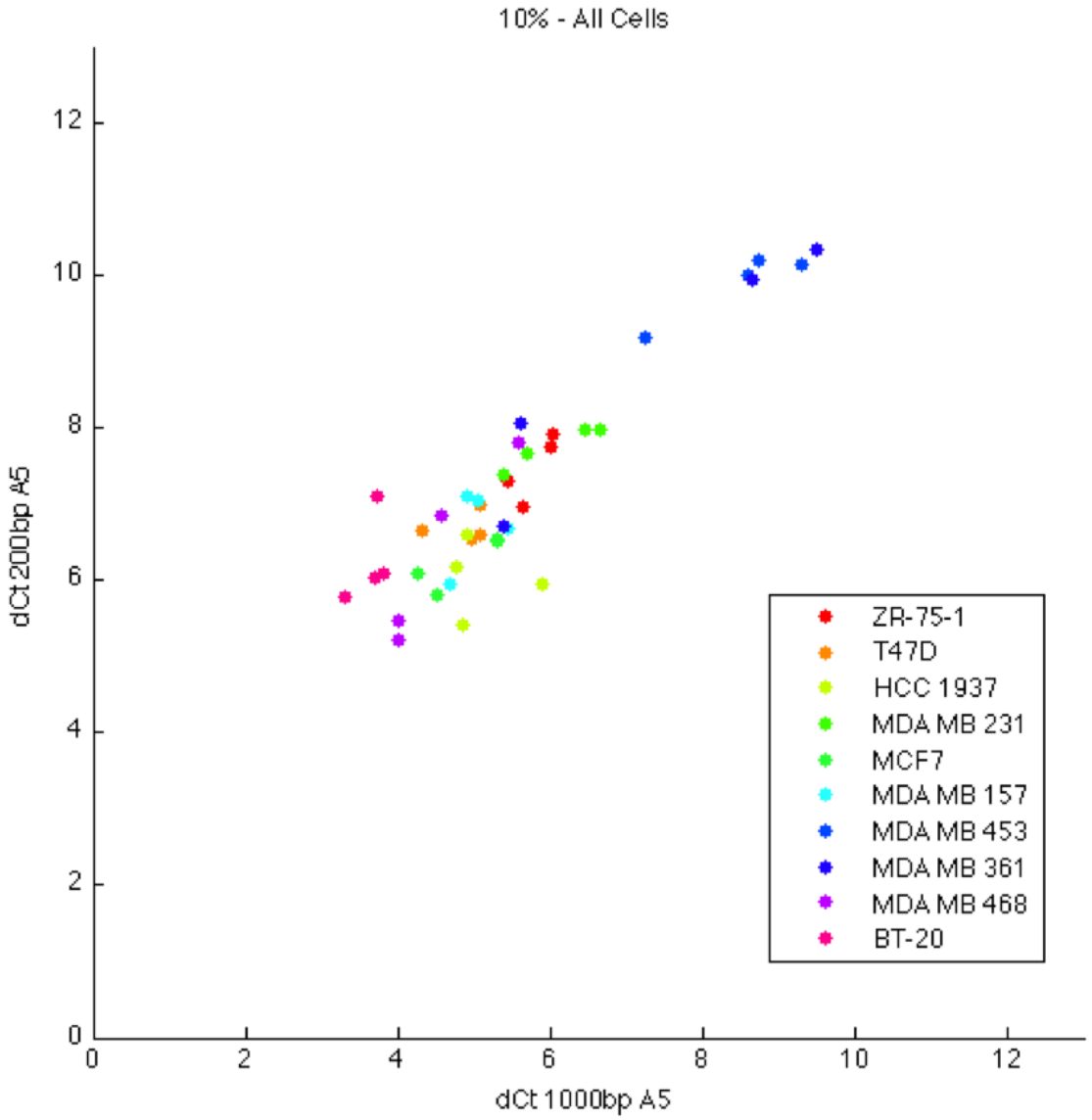

Figure 4.17: 200bp and 1000bp CHRNA5 expression across 10% FBS treated cell lines.

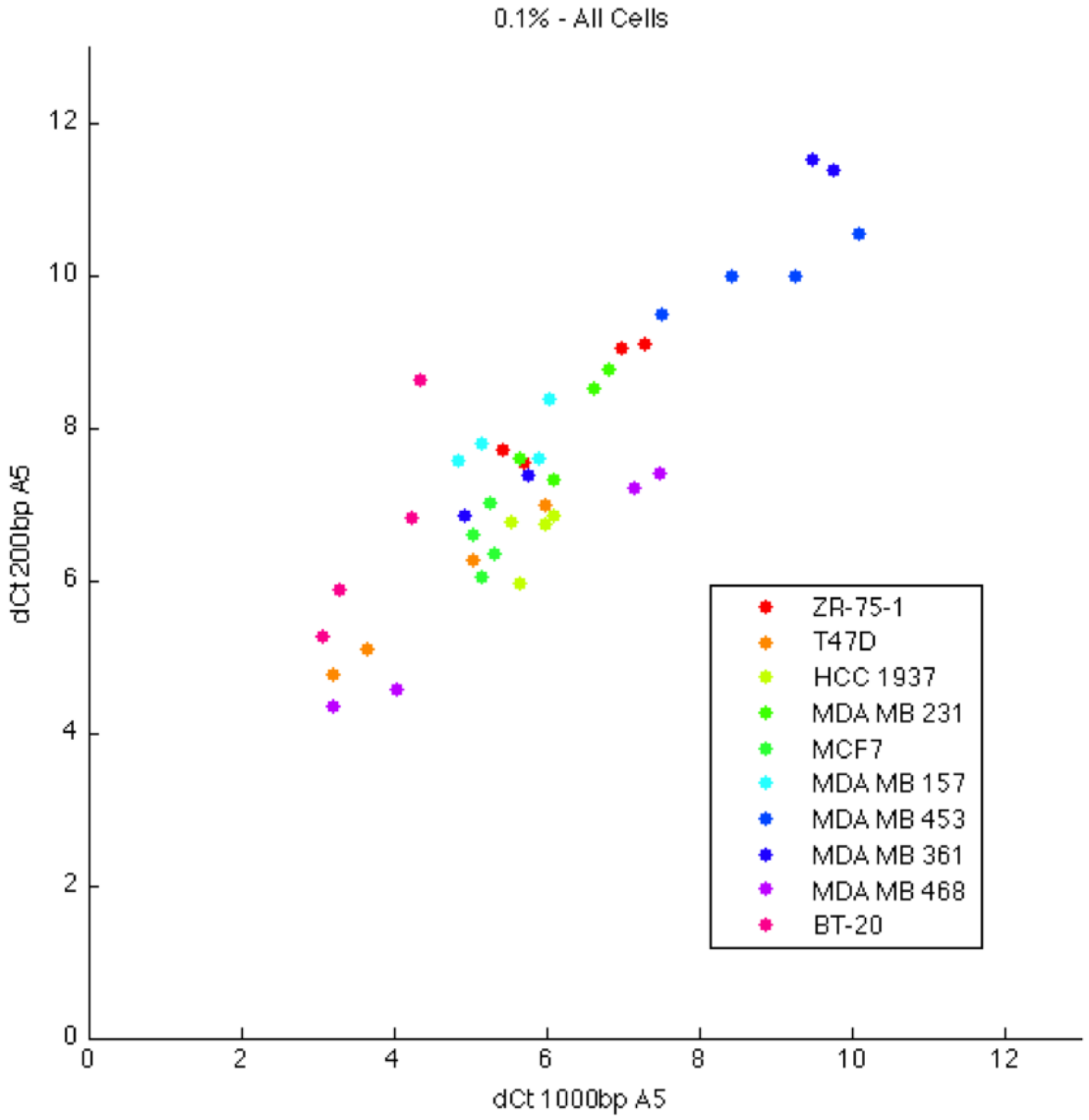

Figure 4.18: 200bp and 1000bp CHRNA5 expression across 0.1% FBS treated cell lines.

ANCOVA was done to investigate the statistical significance of the correlation between 200bp and 1000bp CHRNA5 variants in 10% and 0.1% FBS treated cells. Figure 4.19 shows the comparison.

ANCOVA shows that expressions of 200bp and 1000bp CHRNA5 variants do not differ significantly across all cell lines, both in 10% and 0.1% FBS treated cells.

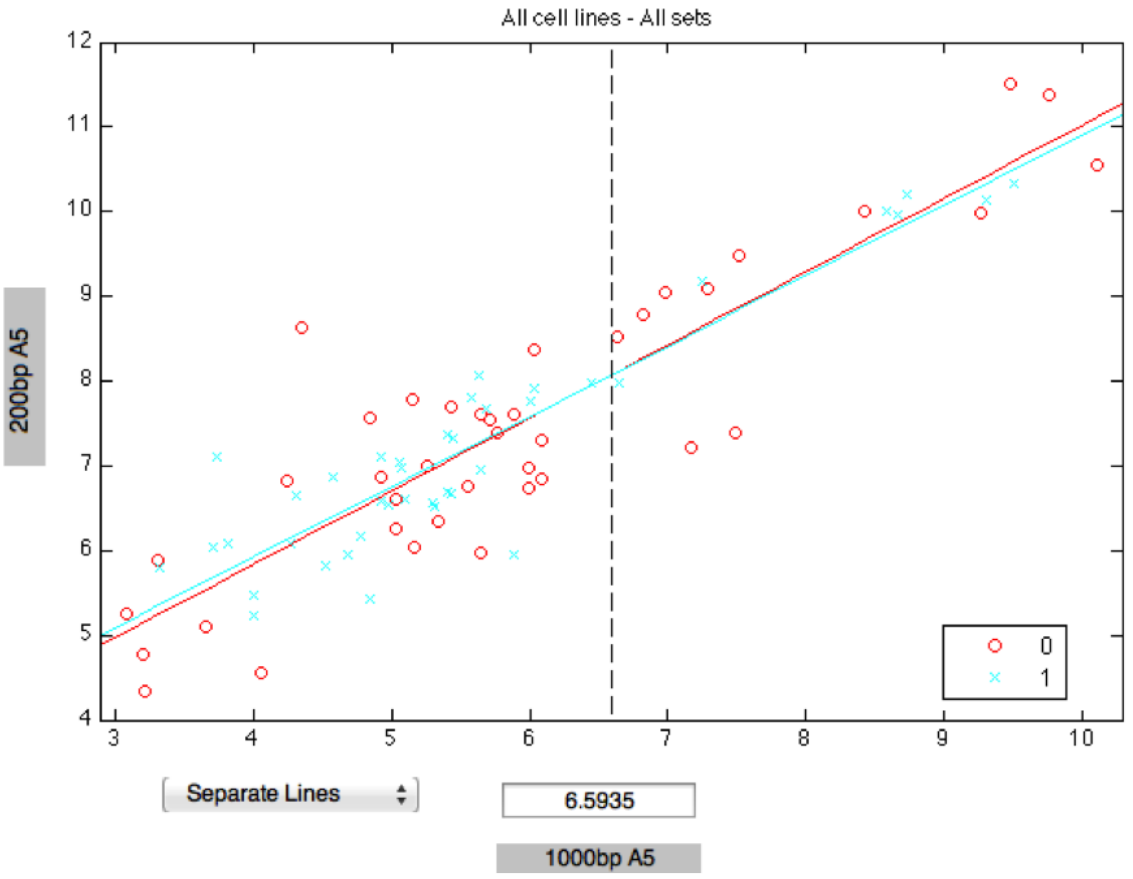

Coefficient Estimates

Term	Estimate	Std. Err.	T	Prob>|T|
Intercept	2.4849	0.28302	8.78	0
0	-0.1056	0.28302	-0.37	0.71
1	0.1056	0.28302	0.37	0.71
Slope	0.8477	0.04763	17.8	0
0	0.0163	0.04763	0.34	0.7333
1	-0.0163	0.04763	-0.34	0.7333

ANOVA Table

Source	d.f.	Sum Sq	Mean Sq	F	Prob>F
grp	1	0.013	0.013	0.03	0.872
eh	1	155.934	155.934	324.97	0
grp*eh	1	0.056	0.056	0.12	0.7333
Error	76	36.467	0.48		

Figure 4.19: ANCOVA of 200bp and 1000bp CHRNA5 variants in 10% and 0.1% FBS treated cell lines. grp, serum treatment effect; eh, slope for isoform comparison across expression. 0 (red) refers to 0.1% FBS and 1 (blue) refers to 10% FBS treatment, respectively.

4.2.2.3 Comparison of CHRNA5 Variant Expression Between Cell Lines

The panel of 10 breast cancer cell lines were compared with respect to their expression of the 1000bp variant and the 200bp variant under different serum supplement regimes. ANCOVA was used to obtain an estimate of relative expression for each line associated with a specific p-value (Table 4.3. ANCOVA was performed assuming parellel lines, i.e., all cell lines were related with reference genes with a similar slope).

The higher the value, the lower the expression, since we used Ct values in comparison. ANCOVA takes the reference gene expression (i.e. geometric mean of TPT1 and SDHA) as a covariate and tests the mean differences among cell lines. Parallel lines were assumed, considering the reference genes will behave similarly for each cell line. ANCOVA produces two p-values, one for the treatment effect and the other for the correlation of reference gene expression with that of the target genes (i.e., 1000bp and 200bp CHRNA5 isoforms). A p-value of less than 0.05 was considered significant.

Figures 4.20 to 4.27 compare the expression values between cell lines. Both in 10% FBS treated cells and 0.1% FBS treated cells, MDA MB 453 and MDA MB 361 cells (HER2 positive subtype) have the lowest expression of both variants.

The order of expression in the controls from the lowest to the highest for 200bp CHRNA5 is as follows: MDA MB 453; MDA MB 361; MDA MB 231; ZR-75-1; MDA MB 157; T47D; MDA MB 468; BT-20; MCF7; HCC 1937.

The order of expression in the controls from the lowest to the highest for 1000bp CHRNA5 is as follows: MDA MB 453; MDA MB 361; MDA MB 231; ZR-75-1; MDA MB 157; HCC 1937; MCF7; T47D; MDA MB 468; BT-20. Table 4.3 shows the p-values for each cell line.

Table 4.3: p-values of ANCOVA for all cell lines, pertaining to Figures 4.20-4.27.

	200bp CHRNA5		**1000bp CHRNA5**	
Cell Line	**10%**	**0.1%**	**10%**	**0.1%**
ZR-75-1	0.253	0.0449	0.4528	0.2224
T47D	0.0789	0.0102	0.0764	0.0482
HCC 1973	0.002	0.0054	0.2363	0.1502
MDA MB 231	0.1252	0.3445	0.2208	0.6094
MCF7	0.0066	0.0018	0.0704	0.0029
MDA MB 157	0.3727	0.1153	0.3169	0.9453
MDA MB 453	0	0	0	0
MDA MB 361	0.0002	0.0007	0.0002	0.002
MDA MB 468	0.0476	0.0294	0.0263	0.5945
BT-20	0.0185	0.1185	0.0001	0

ANCOVA also gives intercept values for each cell line that indicates where the cell line expressions are located along the expression gradient of the target gene. Each intercept has a p-value reflecting whether that cell line is statistically distinguishable from the others. The tables associated with each gene under a given serum treatment show the sources of variation (cell line, slope of the reference gene; and also the intercepts) (Figures 4.20 to 4.26).

Figure 4.20 shows the comparison for the expression of 200bp CHRNA5 variant in 10% FBS treated cell lines. 200bp CHRNA5 expression highly significantly varies between cell lines, with Ct values ranging between 23 and 29, while the reference genes' expression stays relatively unchanged, with Ct values ranging from 17 to 19.5. The slope of the reference gene is also significant, suggesting that there might be an RNA quantification bias or a mild variability of the reference genes among cell lines, due to individual sample variability or batch effect.

Figure 4.22 shows the comparison for the expression of 200bp CHRNA5 variant in 0.1% FBS treated cell lines. 200bp expression has Ct values between 23 and 29, while reference Ct values are between 17 and 19.5. In 0.1% FBS

treated cells, the correlation between 200bp CHRNA5 and reference genes seem to disappear.

Figure 4.24 shows the comparison for the expression of 1000bp CHRNA5 variant in 10% FBS treared cell lines. 1000bp CHRNA5 expression varies between cell lines, with Ct values ranging from 21 to 28, while the reference genes' expression stays relatively unchanged, with Ct values between 17 and 19.5. The slope of the reference gene is also significant here, suggesting that there might, again, be an RNA quantification bias or a mild variability of the reference genes among cell lines, due to individual sample variability or batch effect.

Figure 4.26 shows the comparison for the expression of 1000bp CHRNA5 variant in 0.1% treated cell lines. 1000bp expression has Ct values between 21 and 28, while reference Ct values are between 17 and 19.5. Again, the correlation between the 1000bp CHRNA5 variant and reference genes disappears in 0.1% FBS treated cells.

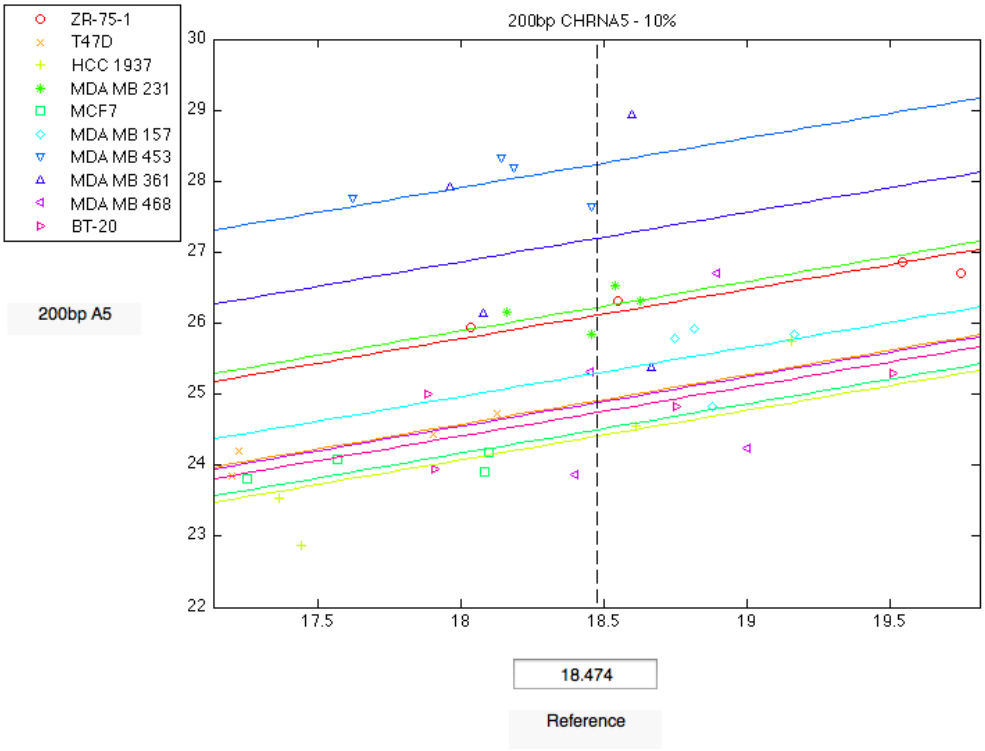

Figure 4.20: Comparison of 200bp CHRNA5 expression among brest cancer cell lines grown with 10% FBS.

ANOVA Table

Source	d.f.	Sum Sq	Mean Sq	F	Prob>F
g	9	58.0858	6.45397	11.11	0
ref	1	4.1458	4.14584	7.14	0.0123
Error	29	16.8445	0.58085		

Coefficient Estimates

Term	Estimate	Std. Err.	T	Prob>|T|
Intercept	12.7842	4.7836	2.67	0.0122
1	0.4622	0.39625	1.17	0.253
2	-0.7441	0.4086	-1.82	0.0789
3	-1.2426	0.36533	-3.4	0.002
4	0.5723	0.36247	1.58	0.1252
5	-1.1512	0.39338	-2.93	0.0066
6	-0.3527	0.38957	-0.91	0.3727
7	2.5893	0.367	7.06	0
8	1.5453	0.36154	4.27	0.0002
9	-0.77	0.37223	-2.07	0.0476
10	-0.9085	0.36416	-2.49	0.0185
Slope	0.6964	0.26066	2.67	0.0123

Figure 4.21: Probability values of 200bp CHRNA5 expression of breast cancer cell lines grown in 10% FBS.

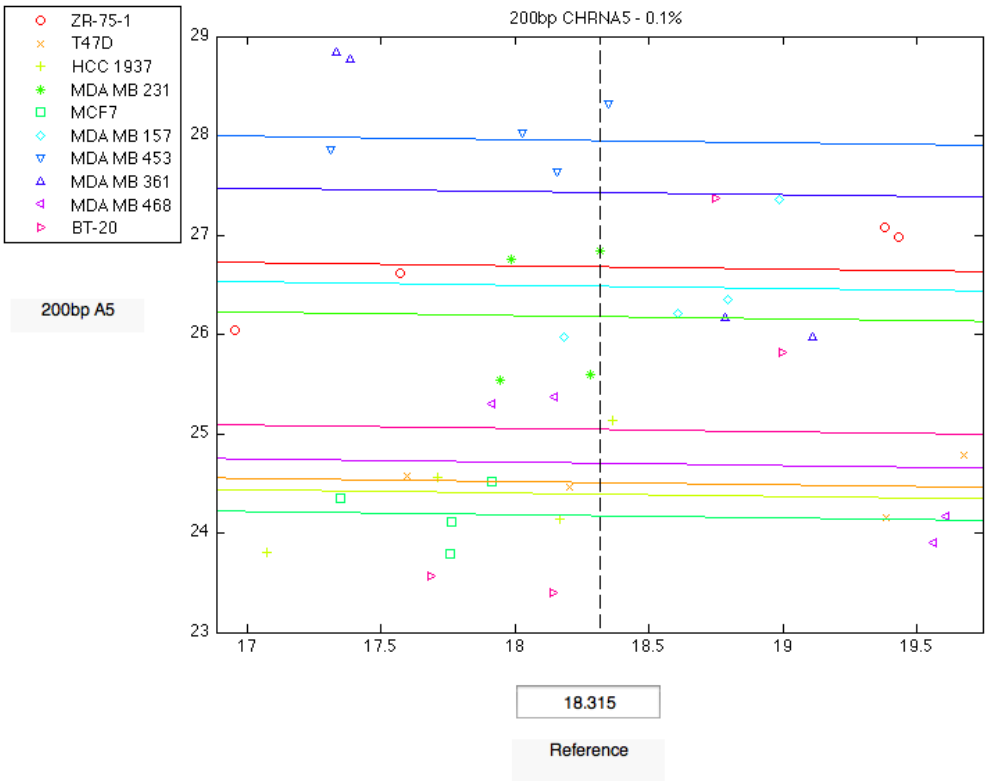

Figure 4.22: Comparison of 200bp CHRNA5 expression among brest cancer cell lines grown with 0.1% FBS.

ANOVA Table

Source	d.f.	Sum Sq	Mean Sq	F	Prob>F
g	9	66.8097	7.4233	8.57	0
ref	1	0.0174	0.01741	0.02	0.8882
Error	29	25.1217	0.86627		

Coefficient Estimates

Term	Estimate	Std. Err.	T	Prob>|T|
Intercept	26.3582	4.25436	6.2	0
1	0.926	0.44177	2.1	0.0449
2	-1.2466	0.45373	-2.75	0.0102
3	-1.3624	0.453	-3.01	0.0054
4	0.4253	0.4426	0.96	0.3445
5	-1.5798	0.46104	-3.43	0.0018
6	0.7307	0.45007	1.62	0.1153
7	2.1967	0.44716	4.91	0
8	1.674	0.44227	3.79	0.0007
9	-1.0521	0.45912	-2.29	0.0294
10	-0.7119	0.44244	-1.61	0.1185
Slope	-0.033	0.23277	-0.14	0.8882

Figure 4.23: Probability values of 200bp CHRNA5 expression of breast cancer cell lines grown in 0.1% FBS.

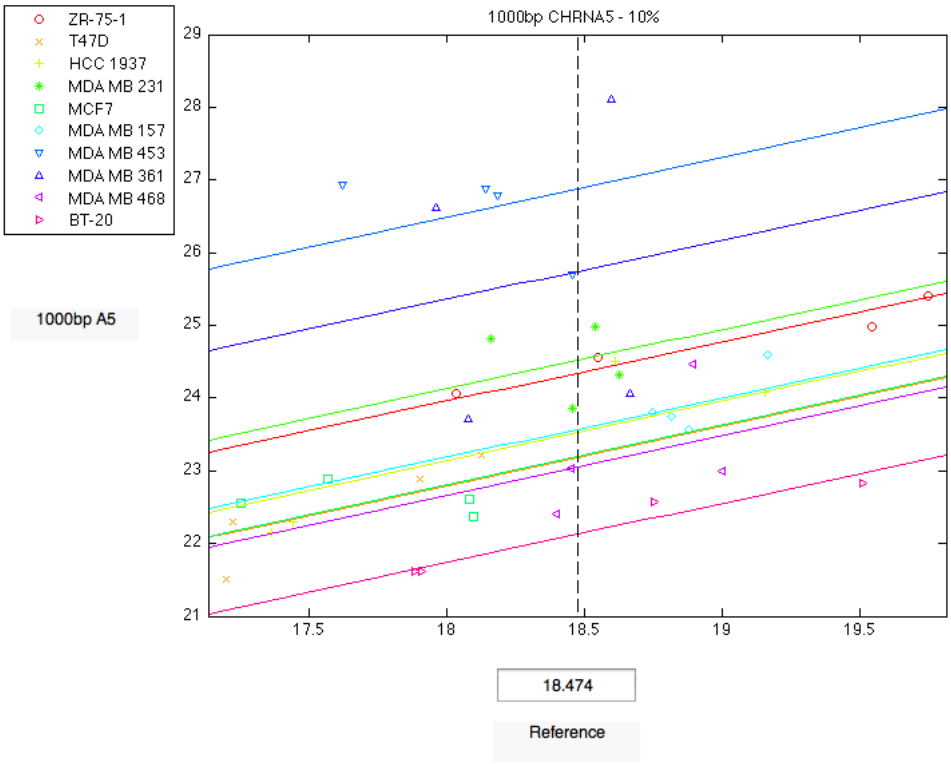

Figure 4.24: Comparison of 1000bp CHRNA5 expression among brest cancer cell lines grown with 10% FBS.

ANOVA Table

Source	d.f.	Sum Sq	Mean Sq	F	Prob>F
g	9	71.326	7.92511	11.15	0
ref	1	5.7616	5.76159	8.11	0.008
Error	29	20.6032	0.71046		

Coefficient Estimates

Term	Estimate	Std. Err.	T	Prob>|T|
Intercept	8.8462	5.29045	1.67	0.1053
1	0.3335	0.43824	0.76	0.4528
2	-0.8303	0.45189	-1.84	0.0764
3	-0.4887	0.40404	-1.21	0.2363
4	0.5016	0.40087	1.25	0.2208
5	-0.8173	0.43506	-1.88	0.0704
6	-0.4388	0.43085	-1.02	0.3169
7	2.8616	0.40588	7.05	0
8	1.7317	0.39985	4.33	0.0002
9	-0.9638	0.41167	-2.34	0.0263
10	-1.8896	0.40275	-4.69	0.0001
Slope	0.821	0.28828	2.85	0.008

Figure 4.25: Probability values of 1000bp CHRNA5 expression of breast cancer cell lines grown in 10% FBS.

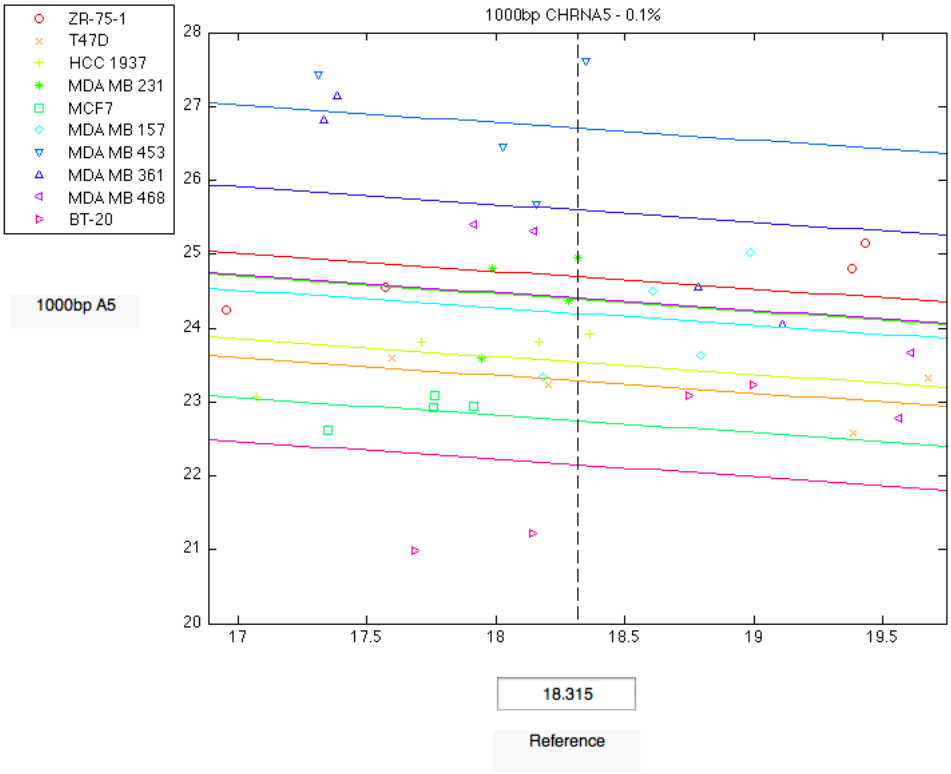

Figure 4.26: Comparison of 1000bp CHRNA5 expression among brest cancer cell lines grown with 0.1% FBS.

ANOVA Table

Source	d.f.	Sum Sq	Mean Sq	F	Prob>F
g	9	64.4653	7.16281	9.19	0
ref	1	0.9078	0.90783	1.16	0.2895
Error	29	22.6132	0.77977		

Coefficient Estimates

Term	Estimate	Std. Err.	T	Prob>|T|
Intercept	28.5334	4.03637	7.07	0
1	0.5226	0.41913	1.25	0.2224
2	-0.8878	0.43048	-2.06	0.0482
3	-0.6351	0.42979	-1.48	0.1502
4	0.2169	0.41992	0.52	0.6094
5	-1.4243	0.43741	-3.26	0.0029
6	0.0295	0.42701	0.07	0.9453
7	2.5361	0.42424	5.98	0
8	1.4267	0.41961	3.4	0.002
9	0.2345	0.43559	0.54	0.5945
10	-2.019	0.41977	-4.81	0
Slope	-0.2383	0.22084	-1.08	0.2895

Figure 4.27: Probability values of 1000bp CHRNA5 expression of breast cancer cell lines grown in 0.1% FBS.

4.2.2.4 Comparison of CHRNA5 Variant Expression in Response to Serum Starvation Treatment

ANCOVA was done in order to assess the effects of serum starvation treatment in each cell line. ANCOVA gives a p-value for the significance of the treatment, and a p-value for the slope of the correlation graph, which shows whether there is a significant correlation between the target gene (either 200bp or 1000bp CHRNA5) and reference genes that might be due to individual variability, experimental error and/or batch effect. Table 4.4 shows the p-values of treatment, slope and intercept of each cell line for the expression of the 200bp variant of CHRNA5. A p-value below 0.05 is considered significant. According to this cutoff, expression of 200bp CHRNA5 is significantly altered in ZR-75-1 and MDA MB 157 cells with serum starvarion treatment.

Table 4.4: ANCOVA results of each cell line for 200bp CHRNA5.

Cell Line	**p-value**	**Slope(p)**	**Intercept(p)**
ZR-75-1	0.0132	0.0018	0
T47D	0.8867	0.5047	0.001
HCC 1937	0.1391	0.006	0.5296
MDA MB 231	0.7916	0.666	0.4971
MCF7	0.3319	0.698	0.0136
MDA MB 157	0.0314	0.163	0.8314
MDA MB 453	0.9816	0.6345	0.0092
MDA MB 361	0.9399	0.1006	0.0106
MDA MB 468	0.7359	0.3949	0.0303
BT-20	0.6386	0.1326	0.9266

Table 4.5 shows the p-values of treatment, slope and intercept of each cell line for the expression of the 1000bp variant of CHRNA5. A p-value below 0.05 is considered significant. According to this cutoff, there seems to be no significant change in the expression of 1000bp CHRNA5.

Table 4.5: ANCOVA results of each cell line for 1000bp CHRNA5.

Cell Line	**p-value**	**Slope(p)**	**Intercept(p)**
ZR-75-1	0.3723	0.0101	0.0003
T47D	0.3422	0.8694	0.0197
HCC 1937	0.0757	0.0075	0.3917
MDA MB 231	0.8936	0.7298	0.5129
MCF7	0.1276	0.9197	0.0059
MDA MB 157	0.1313	0.0465	0.4994
MDA MB 453	0.852	0.3404	0.03
MDA MB 361	0.8602	0.2299	0.0399
MDA MB 468	0.132	0.1247	0.0094
BT-20	0.7394	0.0094	0.9602

Figures 4.28 to 4.47 show ANCOVA graphs with p-values of treatment and slope of each cell line, separately for 200bp isoform of CHRNA5 and 1000bp isoform of CHRNA5.

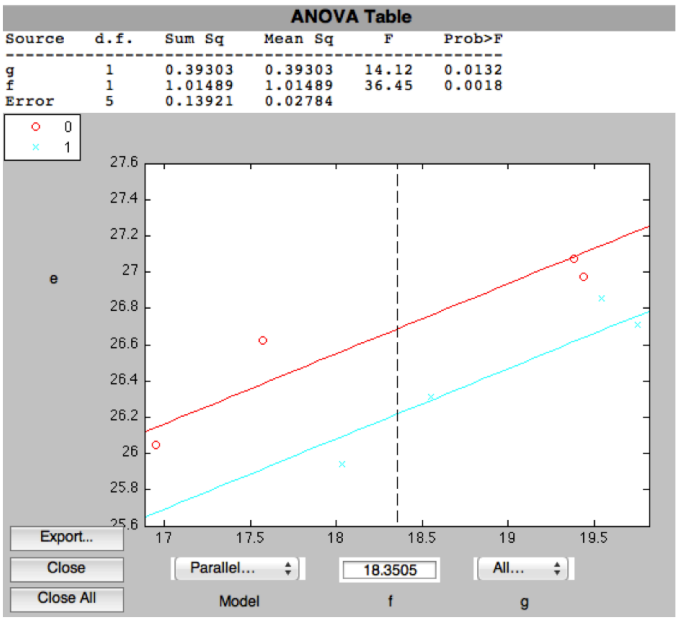

Figure 4.28: ANCOVA for 200bp CHRNA5 expression in ZR-75-1 cell line. 0 (red) refers to 0.1% FBS and 1 (blue) refers to 10% FBS treatment, respectively. sources of variation: g, treatment group; f, covariate.

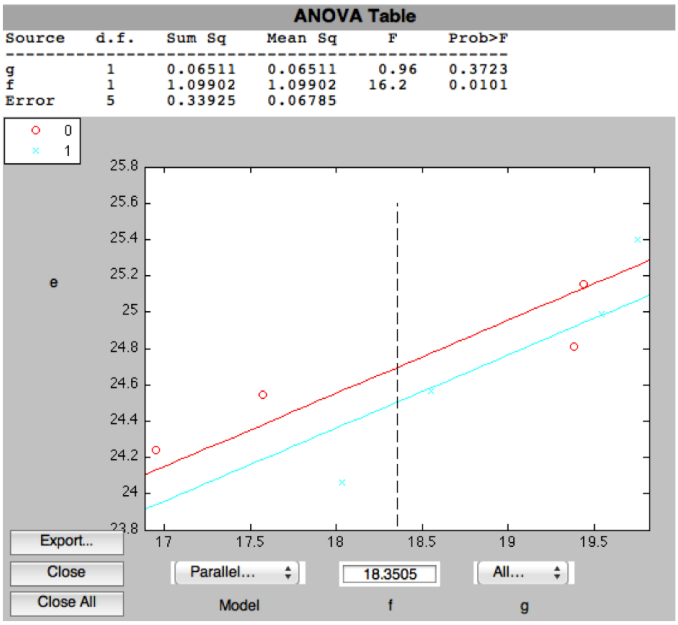

Figure 4.29: ANCOVA for 1000bp CHRNA5 expression in ZR-75-1 cell line. 0 (red) refers to 0.1% FBS and 1 (blue) refers to 10% FBS treatment, respectively. sources of variation: g, treatment group; f, covariate.

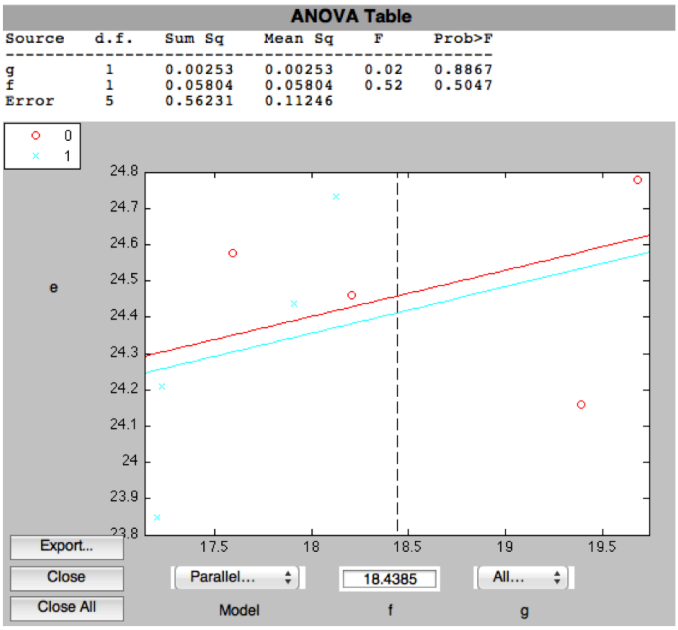

Figure 4.30: ANCOVA for 200bp CHRNA5 expression in T47D cell line. 0 (red) refers to 0.1% FBS and 1 (blue) refers to 10% FBS treatment, respectively. sources of variation: g, treatment group; f, covariate.

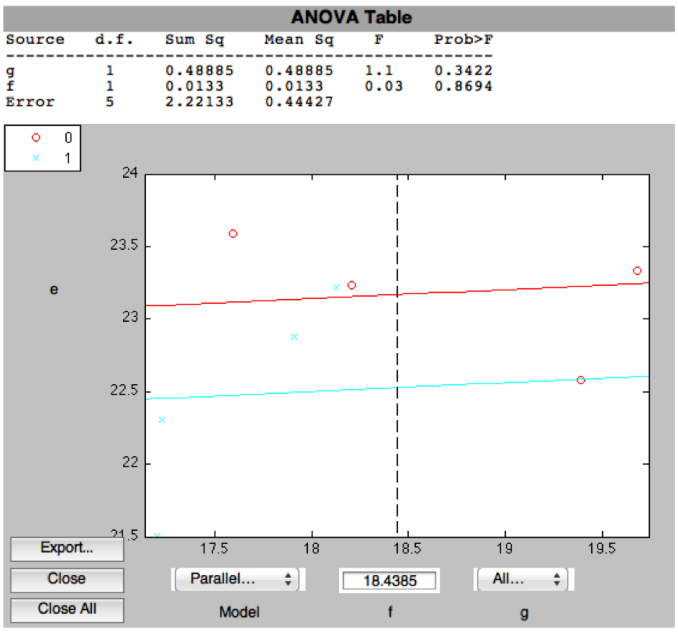

Figure 4.31: ANCOVA for 1000bp CHRNA5 expression in T47D cell line. 0 (red) refers to 0.1% FBS and 1 (blue) refers to 10% FBS treatment, respectively. sources of variation: g, treatment group; f, covariate.

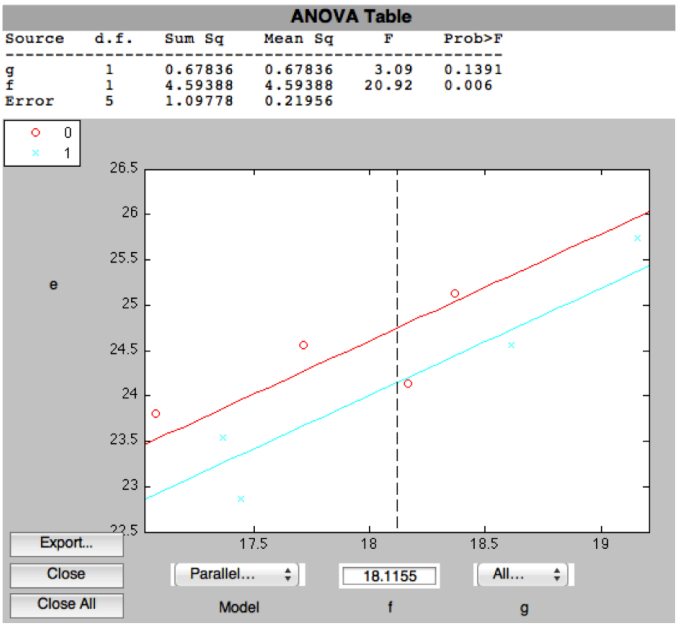

Figure 4.32: ANCOVA for 200bp CHRNA5 expression in HCC 1937 cell line. 0 (red) refers to 0.1% FBS and 1 (blue) refers to 10% FBS treatment, respectively. sources of variation: g, treatment group; f, covariate.

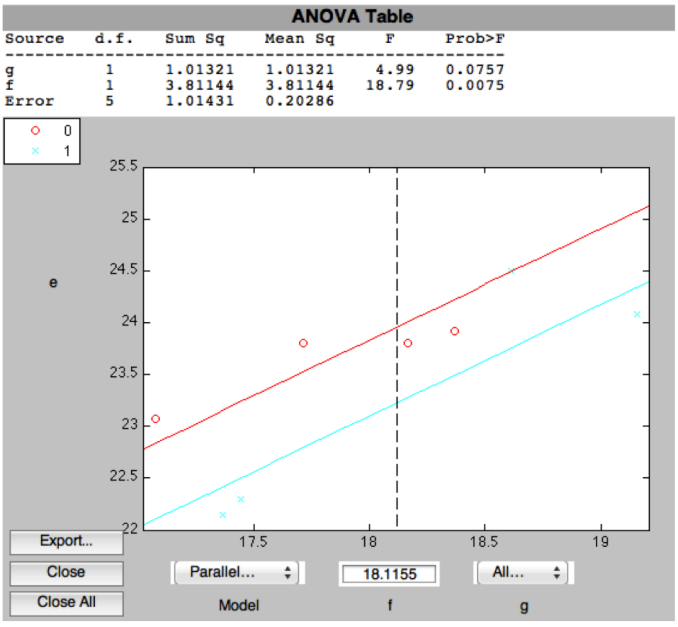

Figure 4.33: ANCOVA for 1000bp CHRNA5 expression in HCC 1937 cell line. 0 (red) refers to 0.1% FBS and 1 (blue) refers to 10% FBS treatment, respectively. sources of variation: g, treatment group; f, covariate.

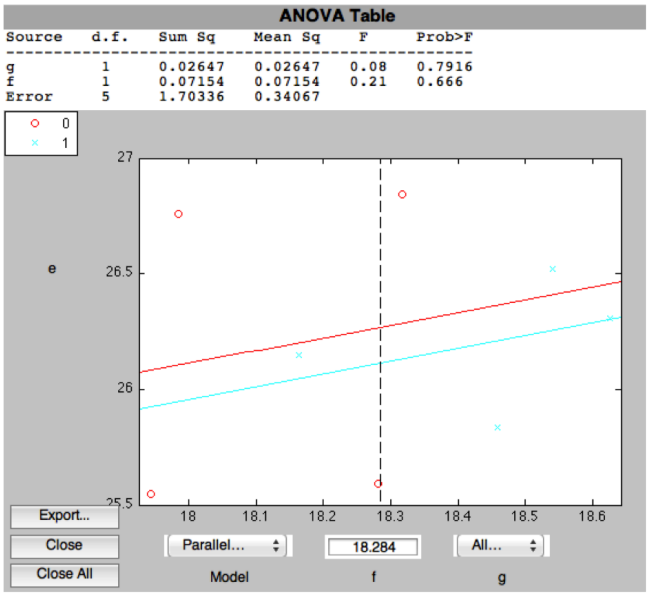

Figure 4.34: ANCOVA for 200bp CHRNA5 expression in MDA MB 231 cell line. 0 (red) refers to 0.1% FBS and 1 (blue) refers to 10% FBS treatment, respectively. sources of variation: g, treatment group; f, covariate.

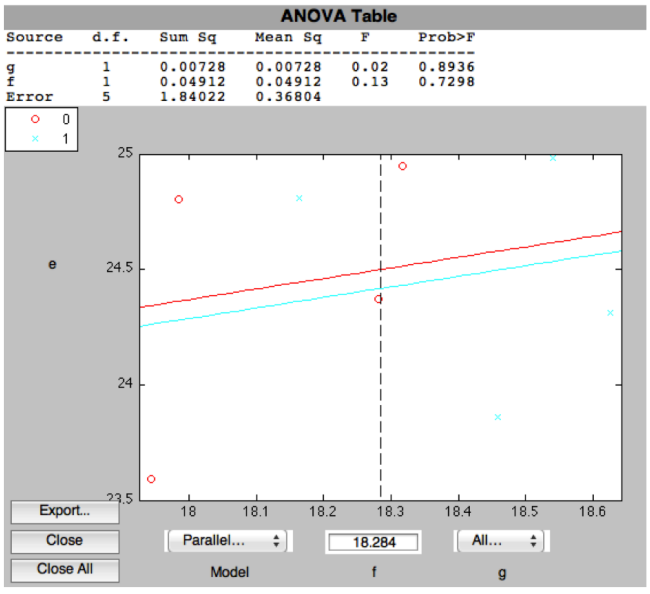

Figure 4.35: ANCOVA for 1000bp CHRNA5 expression in MDA MB 231 cell line. 0 (red) refers to 0.1% FBS and 1 (blue) refers to 10% FBS treatment, respectively. sources of variation: g, treatment group; f, covariate.

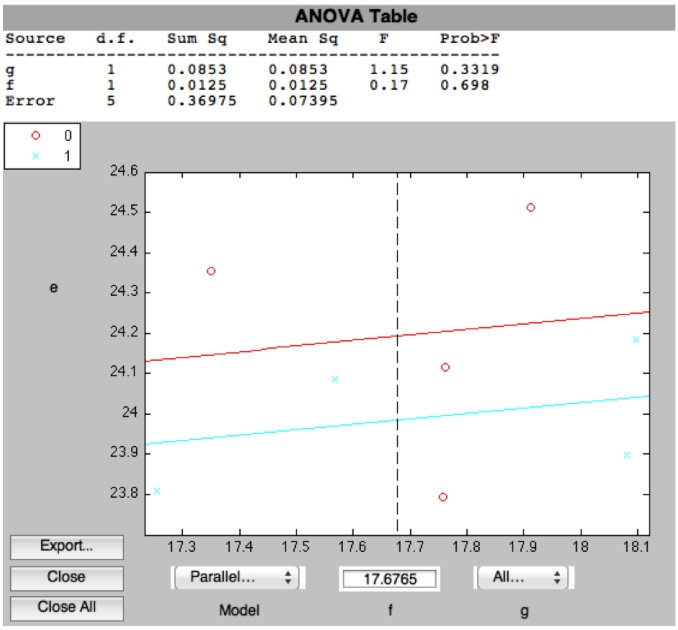

Figure 4.36: ANCOVA for 200bp CHRNA5 expression in MCF7 cell line. 0 (red) refers to 0.1% FBS and 1 (blue) refers to 10% FBS treatment, respectively. sources of variation: g, treatment group; f, covariate.

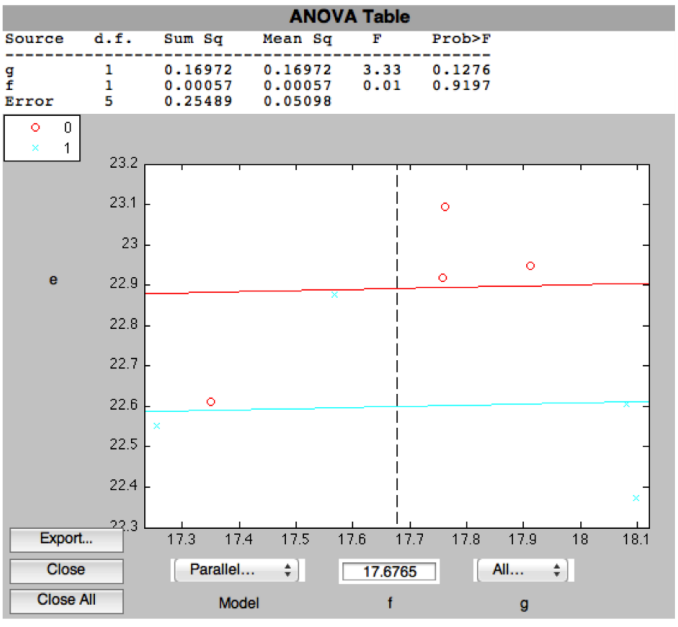

Figure 4.37: ANCOVA for 1000bp CHRNA5 expression in MCF7 cell line. 0 (red) refers to 0.1% FBS and 1 (blue) refers to 10% FBS treatment, respectively. sources of variation: g, treatment group; f, covariate.

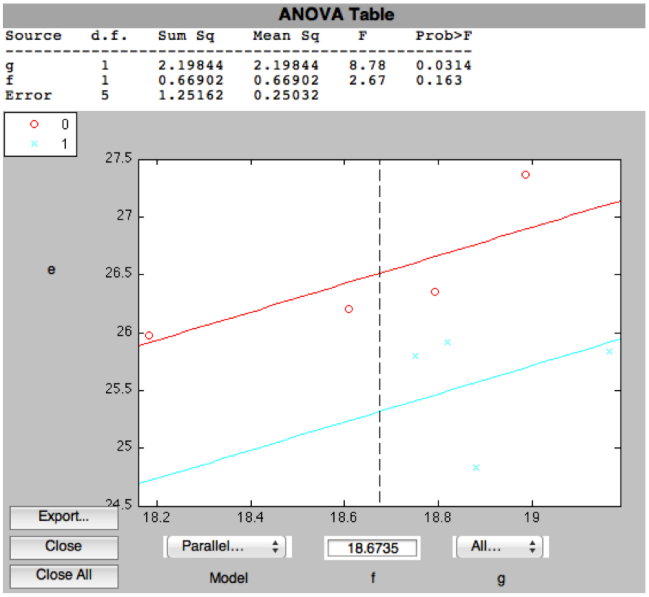

Figure 4.38: ANCOVA for 200bp CHRNA5 expression in MDA MB 157 cell line. 0 (red) refers to 0.1% FBS and 1 (blue) refers to 10% FBS treatment, respectively. sources of variation: g, treatment group; f, covariate.

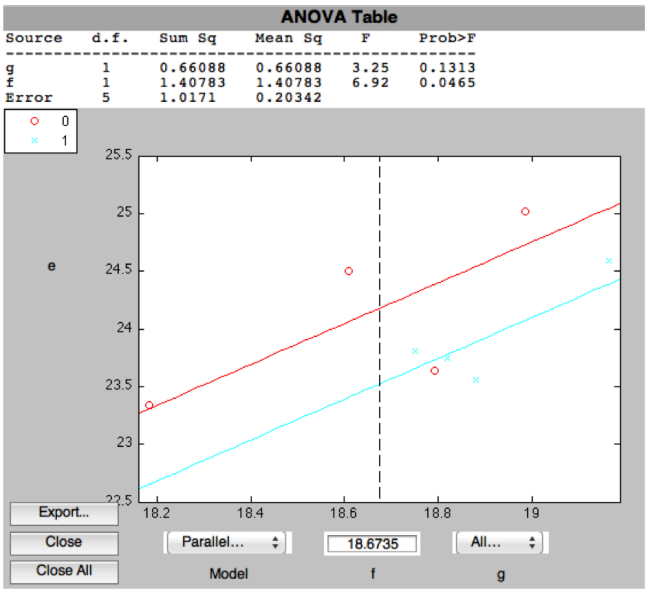

Figure 4.39: ANCOVA for 1000bp CHRNA5 expression in MDA MB 157 cell line. 0 (red) refers to 0.1% FBS and 1 (blue) refers to 10% FBS treatment, respectively. sources of variation: g, treatment group; f, covariate.

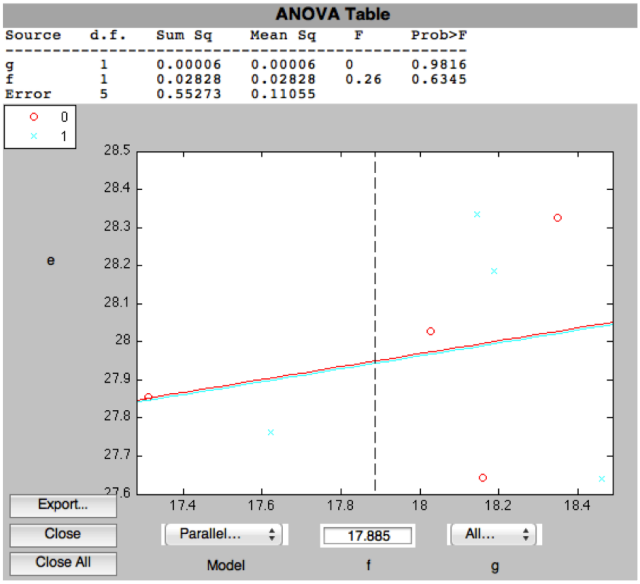

Figure 4.40: ANCOVA for 200bp CHRNA5 expression in MDA MB 453 cell line. 0 (red) refers to 0.1% FBS and 1 (blue) refers to 10% FBS treatment, respectively. sources of variation: g, treatment group; f, covariate.

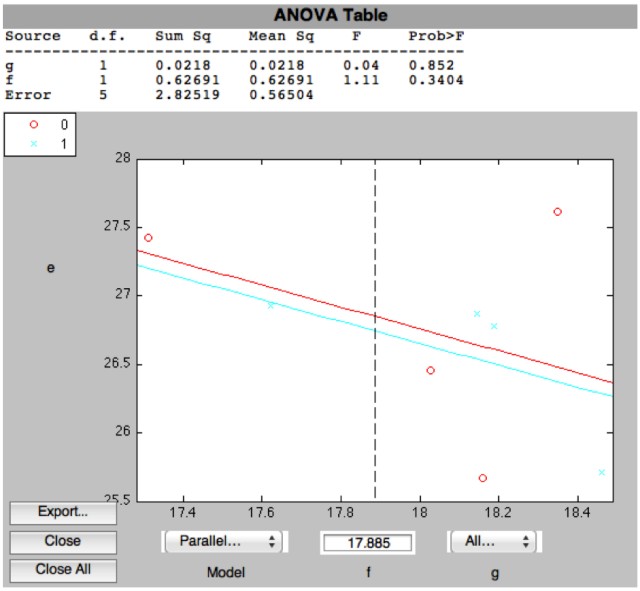

Figure 4.41: ANCOVA for 1000bp CHRNA5 expression in MDA MB 453 cell line. 0 (red) refers to 0.1% FBS and 1 (blue) refers to 10% FBS treatment, respectively. sources of variation: g, treatment group; f, covariate.

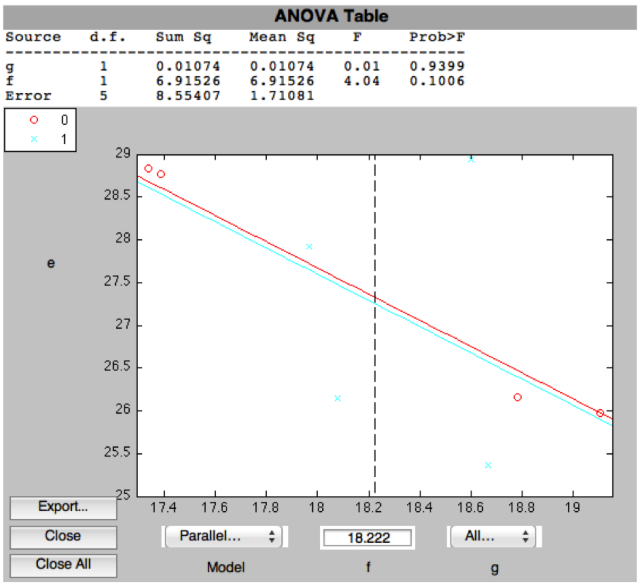

Figure 4.42: ANCOVA for 200bp CHRNA5 expression in MDA MB 361 cell line. 0 (red) refers to 0.1% FBS and 1 (blue) refers to 10% FBS treatment, respectively. sources of variation: g, treatment group; f, covariate.

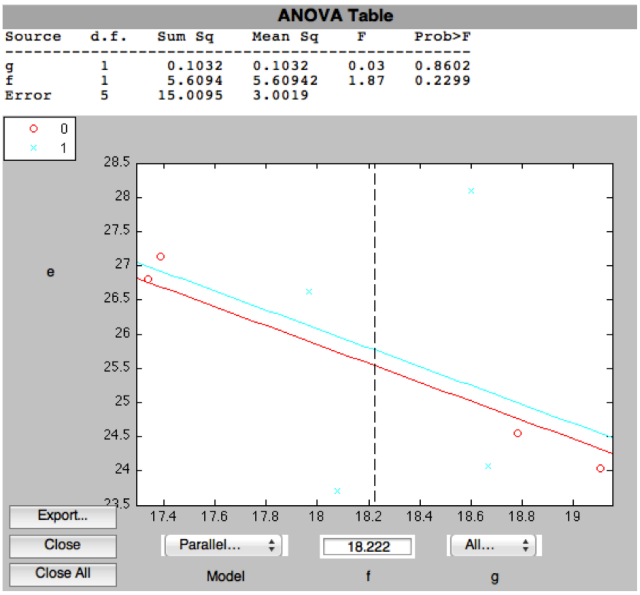

Figure 4.43: ANCOVA for 1000bp CHRNA5 expression in MDA MB 361 cell line. 0 (red) refers to 0.1% FBS and 1 (blue) refers to 10% FBS treatment, respectively. sources of variation: g, treatment group; f, covariate.

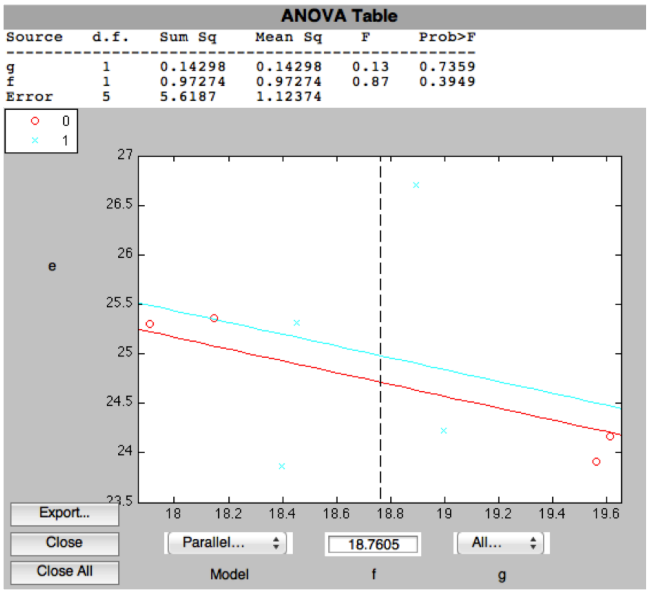

Figure 4.44: ANCOVA for 200bp CHRNA5 expression in MDA MB 468 cell line. 0 (red) refers to 0.1% FBS and 1 (blue) refers to 10% FBS treatment, respectively. sources of variation: g, treatment group; f, covariate.

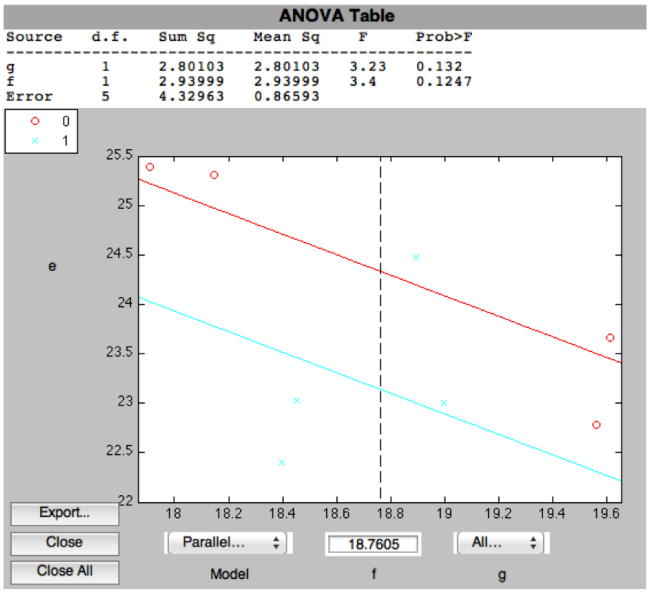

Figure 4.45: ANCOVA for 1000bp CHRNA5 expression in MDA MB 468 cell line. 0 (red) refers to 0.1% FBS and 1 (blue) refers to 10% FBS treatment, respectively. sources of variation: g, treatment group; f, covariate.

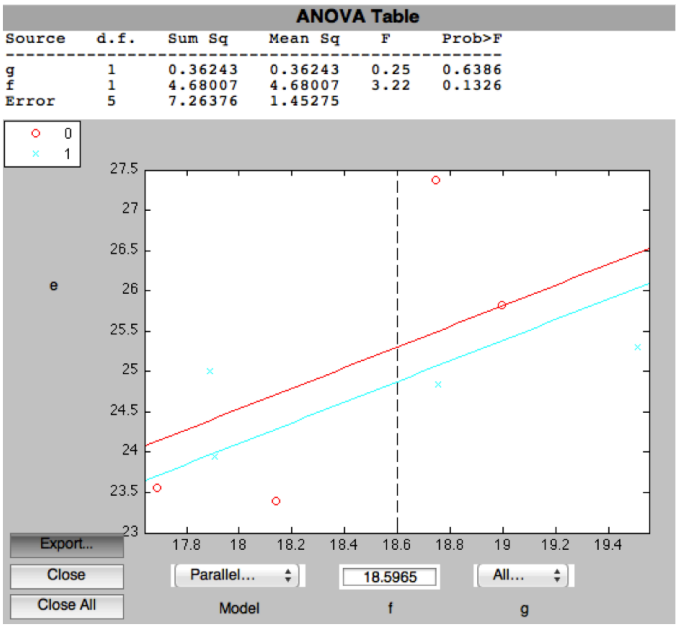

Figure 4.46: ANCOVA for 200bp CHRNA5 expression in BT-20 cell line. 0 (red) refers to 0.1% FBS and 1 (blue) refers to 10% FBS treatment, respectively. sources of variation: g, treatment group; f, covariate.

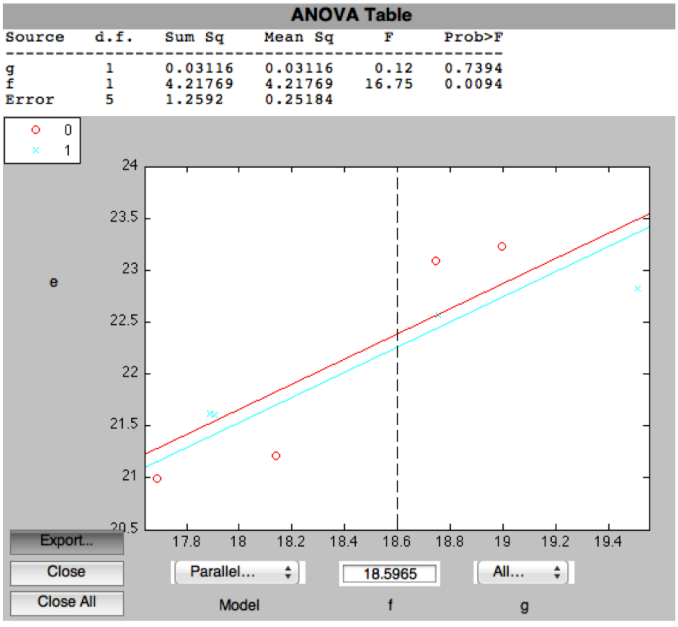

Figure 4.47: ANCOVA for 1000bp CHRNA5 expression in BT-20 cell line. 0 (red) refers to 0.1% FBS and 1 (blue) refers to 10% FBS treatment, respectively. sources of variation: g, treatment group; f, covariate.

4.3 Effects of E2 treatment

4.3.1 Two-way Anova According to Dose and Time

In order to assess the effects of E2 treatment, two-way ANOVA was used in R, taking the log fold change between the target gene and geometric mean of TPT1 and SDHA (ΔCt) as input. Figures 4.48 to 4.54 show ANOVA tables and boxplots for the seven genes/primers investigated.

Estrogen may act directly or indirectly to induce or repress expression of its target genes. Previous microarray experiments have shown that in the presence of cycloheximide, where new protein synthesis is inhibited, most of the E2 responsive genes are primary targets and this includes pS2 gene.[19,74,84] A secondary target of E2 is anilin (ANLN), whose expression is negatively correlated with survival.[84]

Tables 4.6 and 4.7 shows fold changes in PS2 expression in response to E2 treatment in MCF7 cells and their significance values according to dose, time and dose:time. Results indicate that PS2 expression significantly increases in response to E2 treatment in time and dose:time ($p<0.01$) tests. Figure 4.48 shows the boxplot of the results.

Table 4.6: Log2-fold changes of PS2 in response to E2 treatment.

	ps2	group	dose	time
1	-1.9213997	0nm12	0	12
2	1.9213997	0nm12	0	12
3	-2.5747162	100nm12	100	12
4	-6.7655195	100nm12	100	12
5	-0.5830048	0nm24	0	24
6	0.5830048	0nm24	0	24
7	9.5587232	100nm24	100	24
8	10.0925052	100nm24	100	24

Table 4.7: Significance values of change in PS2 expression in response to E2 treatment. **=p<0.01.

Response:	ps2					
	Df	Sum Sq	Mean Sq	F value	Pr(>F)	
dose	1	13.290	13.29	3.1293	0.151619	
time	1	105.063	105.063	24.7393	0.007631	**
dose:time	1	105.063	105.063	24.7393	0.007631	**
Residuals	4	16.987	4.247			

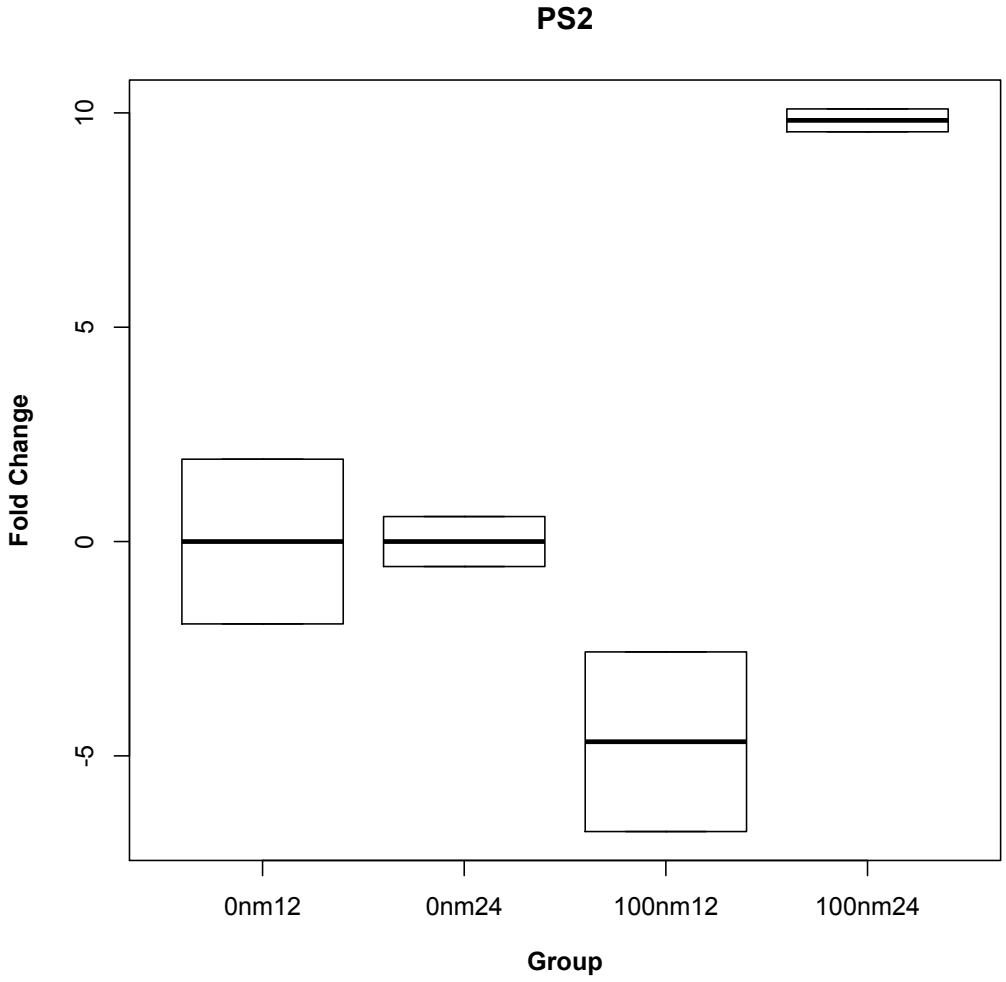

Figure 4.48: Boxplot for PS2 in E2 treated cells.

Table 4.8 and 4.9 shows fold changes in ANLN expression in response to E2 treatment in MCF7 cells and their significance values according to dose, time and dose:time. ANLN expression significantly increases in response to E2 treatment in time and dose:time ($p<0.05$) tests. Figure 4.49 shows the boxplot of the results. Since the interaction component is significant, the response to E2 in time differs such that it is greater at a later time point (i.e., 24 hr vs. 12h).

Table 4.8: Log2-fold changes of ANLN in response to E2 treatment.

	ANLN	**group**	**dose**	**time**
1	0.3636003	0nm12	0	12
2	-0.3636003	0nm12	0	12
3	-0.9847162	100nm12	100	12
4	-0.2755195	100nm12	100	12
5	-0.6605048	0nm24	0	24
6	0.6605048	0nm24	0	24
7	2.9312232	100nm24	100	24
8	2.0400052	100nm24	100	24

Table 4.9: Significance values of change in ANLN expression in response to E2 treatment. *=$p<0.05$.

Response:	Anln				
	Df	Sum Sq	Mean Sq	F value	Pr(>F)	
dose	1	1.7214	1.7214	3.8563	0.121	
time	1	4.8539	4.8539	10.8737	0.03	*
dose:time	1	4.8539	4.8539	10.8737	0.03	*
Residuals	4	1.7856	0.4464			

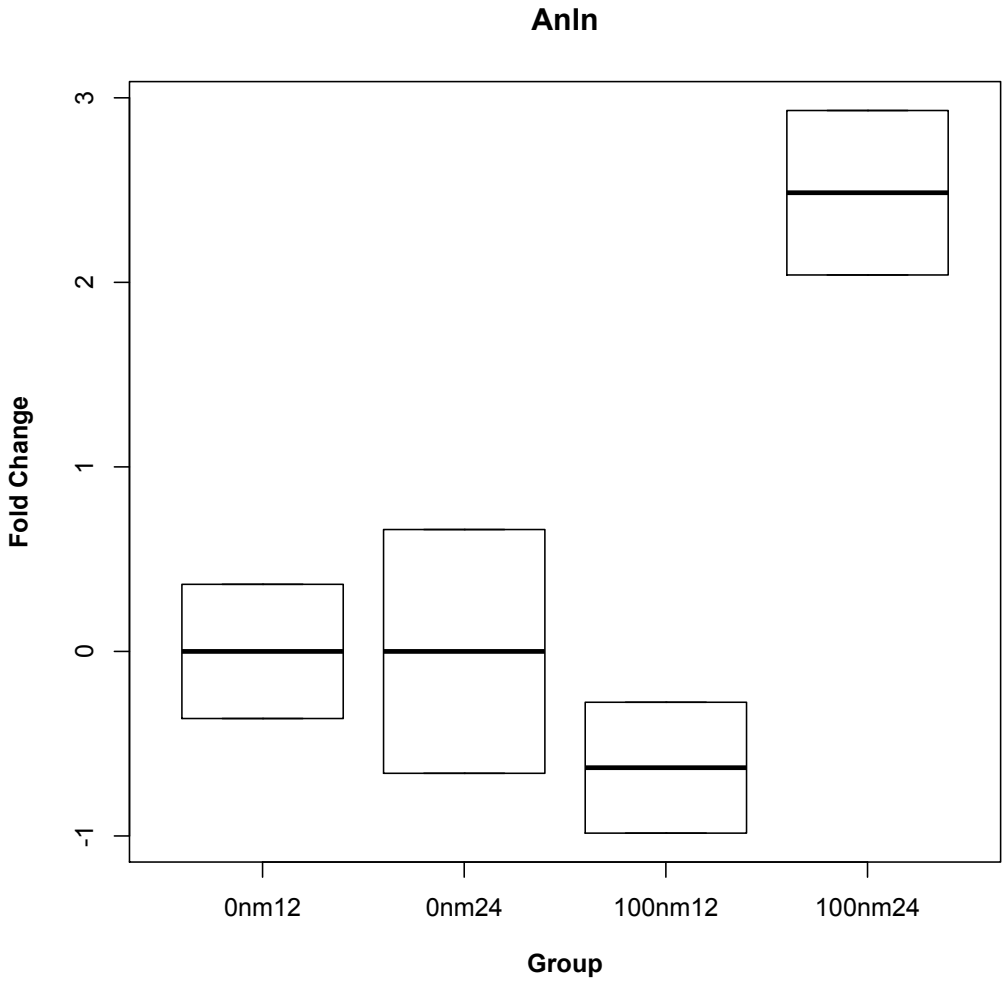

Figure 4.49: Boxplot for ANLN in E2 treated cells.

Table 4.10 and 4.11 shows fold changes in total CHRNA5 expression in response to E2 treatment in MCF7 cells and their significance values according to dose, time and dose:time. They show that total CHRNA5 expression significantly increases in response to E2 treatment in time dose:time test ($p<0.05$). Figure 4.50 shows the boxplot of the results. This findings is similar to that about ANLN; again CHRNA5 expression is different across time points since the effect of E2 is more prominent at 24h.

Table 4.10: Log2-fold changes of total CHRNA5 in response to E2 treatment.

	A5.all	**group**	**dose**	**time**
1	0.2811003	0nm12	0	12
2	-0.2811003	0nm12	0	12
3	-0.1922162	100nm12	100	12
4	-2.2830195	100nm12	100	12
5	-0.4230048	0nm24	0	24
6	0.4230048	0nm24	0	24
7	2.6237232	100nm24	100	24
8	2.7025052	100nm24	100	24

Table 4.11: Significance values of change in total CHRNA5 expression in response to E2 treatment. *=p<0.05.

Response:	A5.all				
	Df	Sum Sq	Mean Sq	F value	Pr(>F)	
dose	1	1.0160	1.016	1.5026	0.28751	
time	1	7.6078	7.6078	11.2513	0.02846	*
dose:time	1	7.6078	7.6078	11.2513	0.02846	*
Residuals	4	2.7047	0.6762			

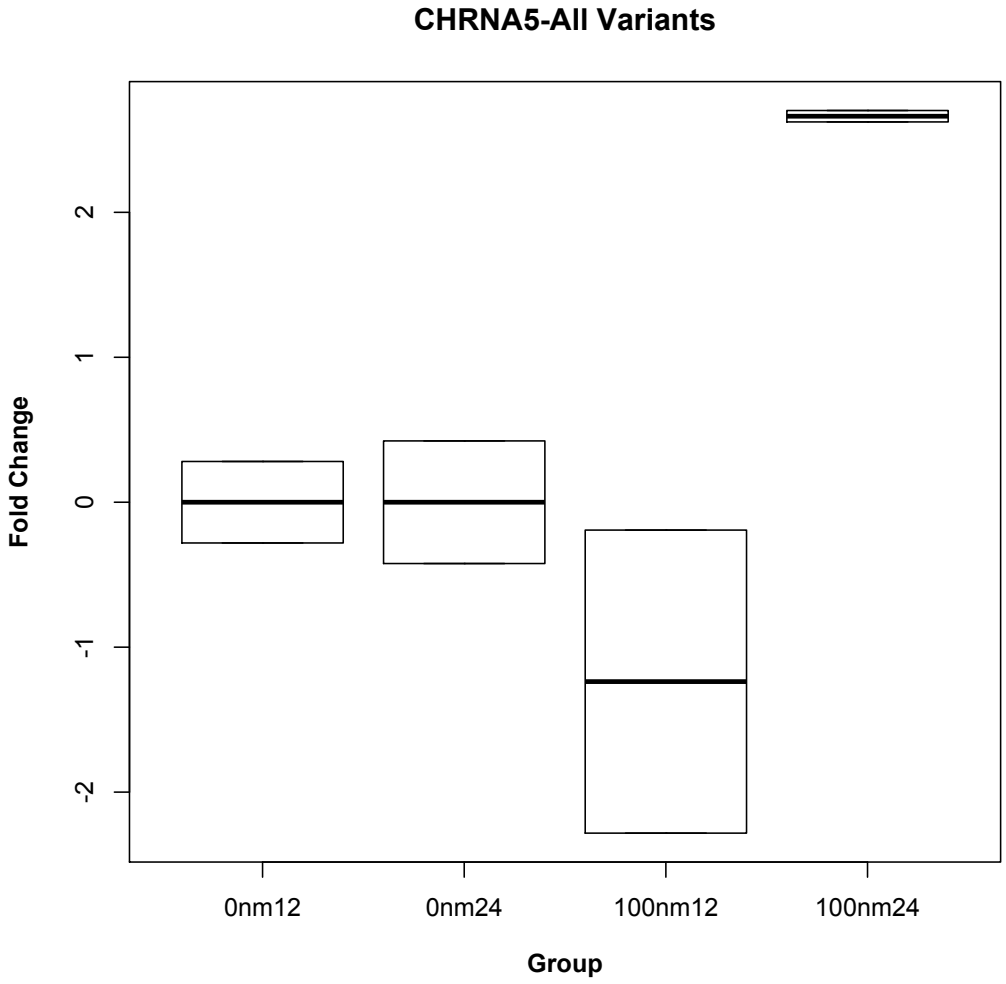

Figure 4.50: Boxplot for all variants of CHRNA5 in E2 treated cells.

Table 4.12 and 4.13 shows fold changes in 1000bp CHRNA5 expression in response to E2 treatment in MCF7 cells and their significance values according to dose, time and dose:time. They show that 1000bp CHRNA5 expression significantly increases in response to E2 treatment in dose test ($p<0.01$). Figure 4.51 shows the boxplot of the results. Interestingly, 1000bp isoform of CHRNA5 behaves differently than all forms in the sense that E2 exhibits effect at 12h although to a lesser degree than 24h.

Table 4.12: Log2-fold changes of 1000bp variant of CHRNA5 in response to E2 treatment.

	1000bpA5	**group**	**dose**	**time**
1	-0.3338997	0nm12	0	12
2	0.3338997	0nm12	0	12
3	0.8077838	100nm12	100	12
4	1.7169805	100nm12	100	12
5	0.1469952	0nm24	0	24
6	-0.1469952	0nm24	0	24
7	2.0287232	100nm24	100	24
8	1.6275052	100nm24	100	24

Table 4.13: Significance values of change in 1000bp CHRNA5 expression in response to E2 treatment. **=p<0.01.

Response:	1000bp					
	Df	Sum Sq	Mean Sq	F value	Pr(>F)	
dose	1	4.7756	4.7756	25.1346	0.00742	**
time	1	0.1600	0.16	0.8422	0.41069	
dose:time	1	0.1600	0.16	0.8422	0.41069	
Residuals	4	0.7600	0.19			

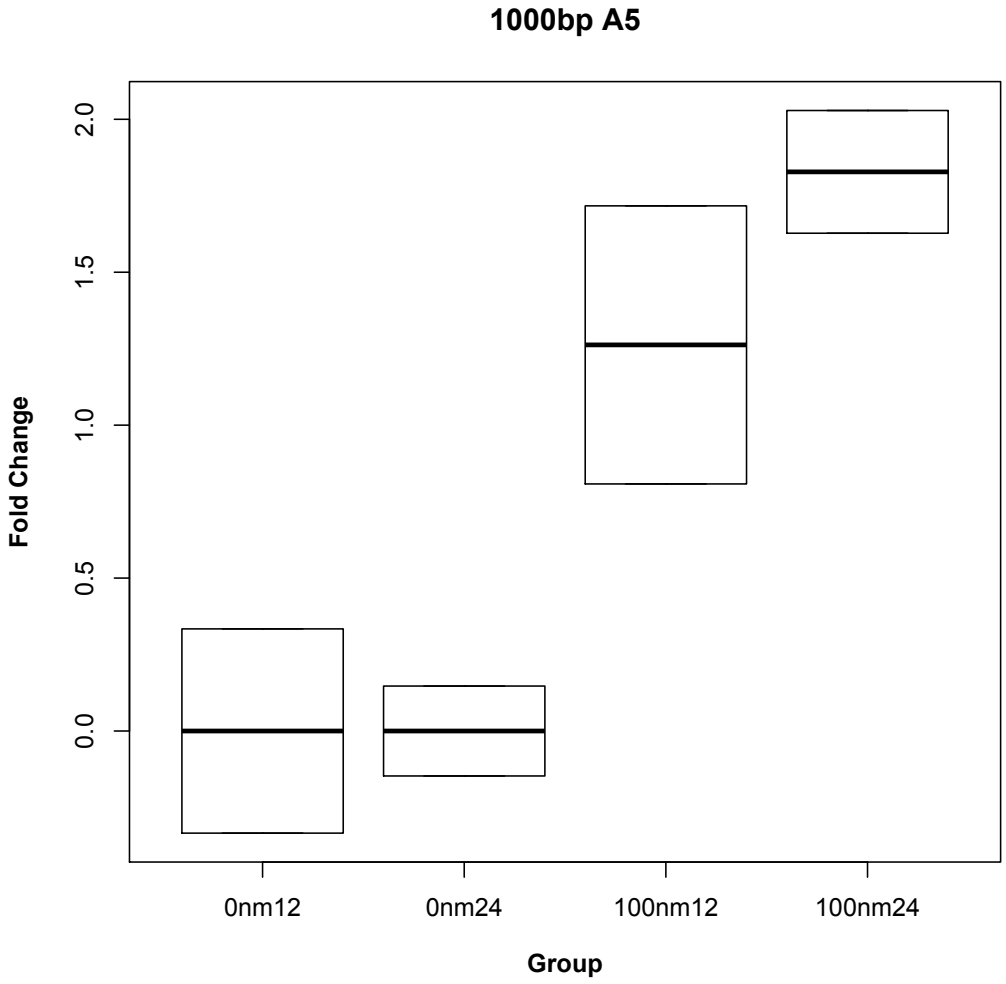

Figure 4.51: Boxplot for 1000bp variant of CHRNA5 in E2 treated cells.

Table 4.14 and 4.15 shows fold changes in 200bp CHRNA5 expression in response to E2 treatment in MCF7 cells and their significance values according to dose, time and dose:time. They show that 200bp CHRNA5 expression has an approaching significance in response to E2 treatment in dose test ($p<0.1$). Figure 4.52 shows the boxplot of the results. E2 is equally effective at 12h and 24h for 200bp variant of CHRNA5 since no significance is seen in time and the interaction component of ANOVA table is also insignificant, emphasizing that there is no differential effect of dose at different times.

Table 4.14: Log2-fold changes of 200bp variant of CHRNA5 in response to E2 treatment.

	200bp	**group**	**dose**	**time**
1	0.5261003	0nm12	0	12
2	-0.5261003	0nm12	0	12
3	3.2477838	100nm12	100	12
4	0.1719805	100nm12	100	12
5	-0.9580048	0nm24	0	24
6	0.9580048	0nm24	0	24
7	2.8437232	100nm24	100	24
8	3.2675052	100nm24	100	24

Table 4.15: Significance values of change in 200bp CHRNA5 expression in response to E2 treatment. .=p<0.1.

Response:	200bp				
	Df	Sum Sq	Mean Sq	F value	Pr(>F)	
dose	1	11.3549	11.3549	6.3002	0.06606	.
time	1	0.9055	0.9055	0.5024	0.51757	
dose:time	1	0.9055	0.9055	0.5024	0.51757	
Residuals	4	7.2092	1.8023			

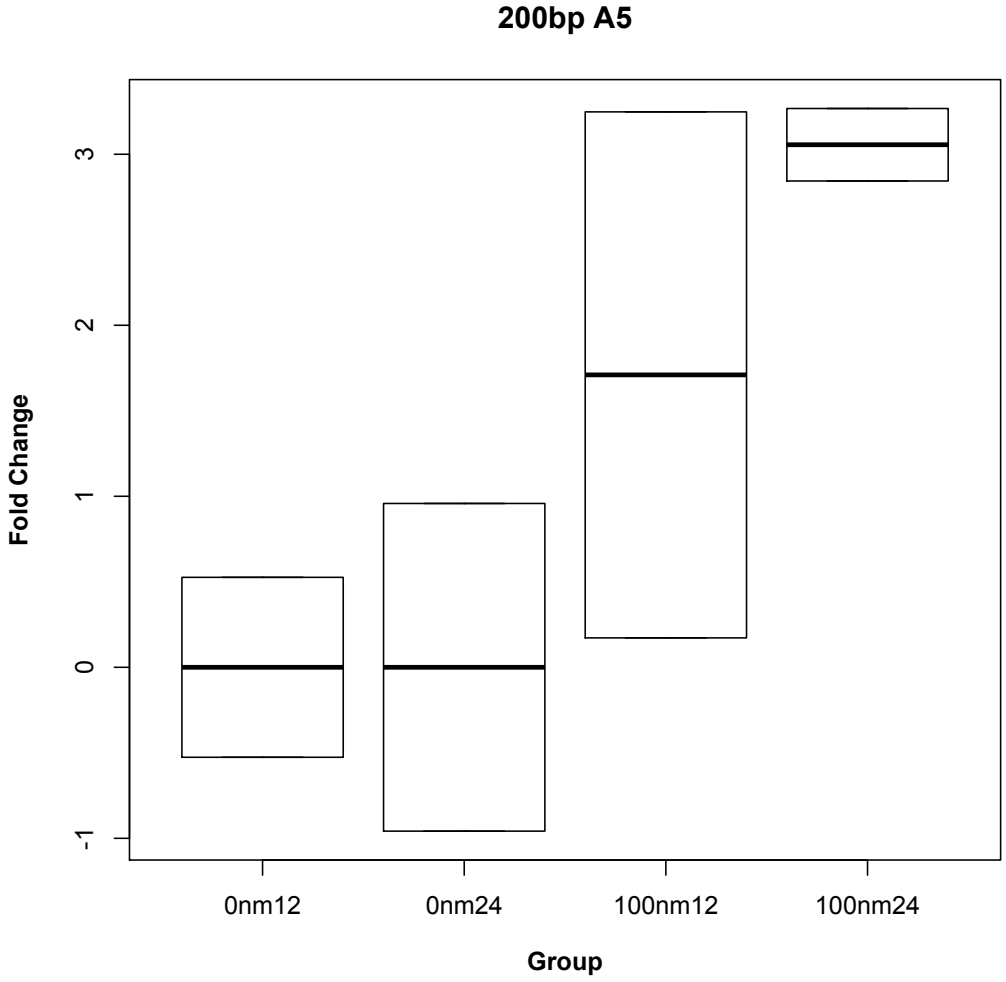

Figure 4.52: Boxplot for 200bp variant of CHRNA5 in E2 treated cells.

Table 4.16 and 4.17 shows fold changes in isoform2 CHRNA5 expression in response to E2 treatment in MCF7 cells and their significance values according to dose, time and dose:time. There is a dose effect such that 100nM of E2 is effective on expression of isoform2 of CHRNA5 while this effect is time dependent ($p<0.05$) and the interaction is also significant, supporting this. Figure 4.53 shows the boxplot of the results.

Table 4.16: Log2-fold changes of isoform2 of CHRNA5 in response to E2 treatment.

	iso2	**group**	**dose**	**time**
1	-0.05889974	0nm12	0	12
2	0.05889974	0nm12	0	12
3	1.63278379	100nm12	100	12
4	1.34198051	100nm12	100	12
5	-0.21050476	0nm24	0	24
6	0.21050476	0nm24	0	24
7	2.69622324	100nm24	100	24
8	3.34500519	100nm24	100	24

Table 4.17: Significance values of change in isoform2 CHRNA5 expression in response to E2 treatment. ***=p<0.001, *=p<0.5.

Response:	iso2					
	Df	Sum Sq	Mean Sq	F value	Pr(>F)	
dose	1	10.1610	10.161	116.689	0.0004166	***
time	1	1.1754	1.1754	13.498	0.0213175	*
dose:time	1	1.1754	1.1754	13.498	0.0213175	*
Residuals	4	0.3483	0.0871			

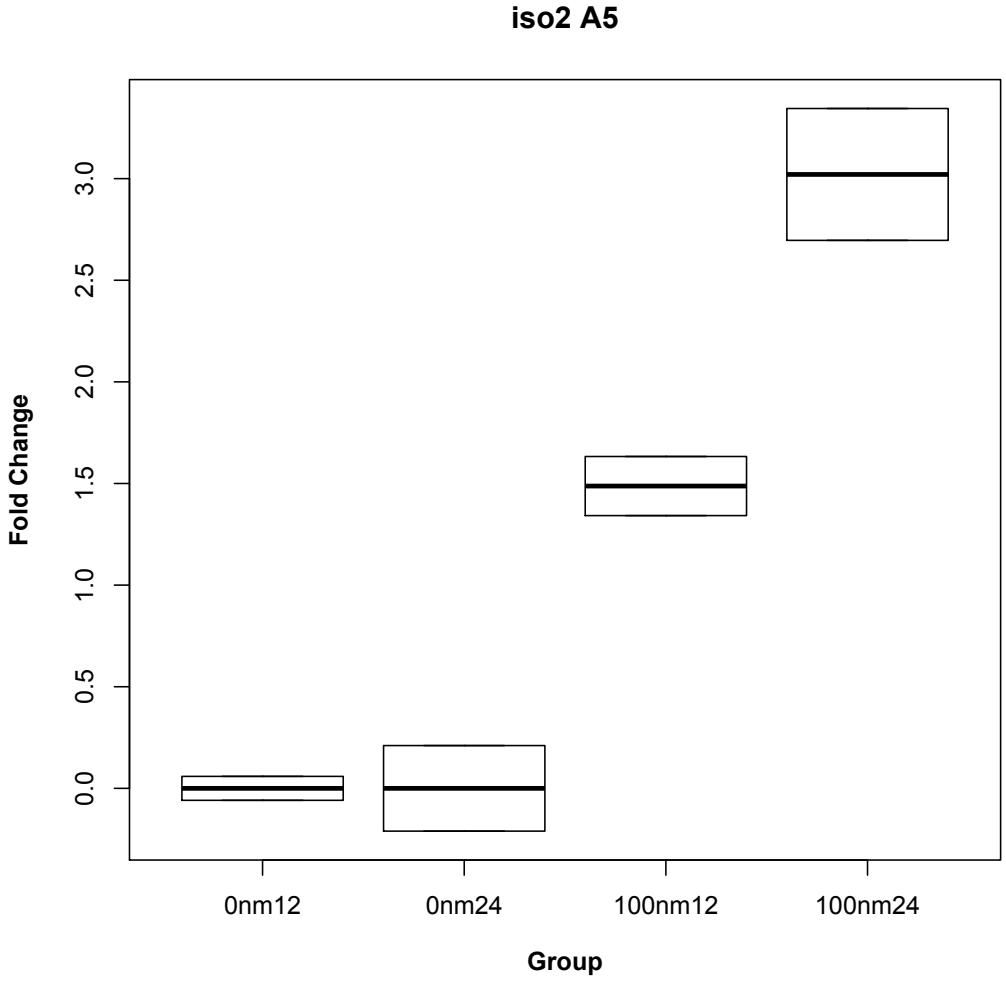

Figure 4.53: Boxplot for isoform 2 of CHRNA5 in E2 treated cells.

Table 4.18 and 4.19 shows fold changes in isoform3 CHRNA5 expression in response to E2 treatment in MCF7 cells and their significance values according to dose, time and dose:time. They show that isoform3 CHRNA5 expression significantly increases in response to E2 treatment in dose test ($p<0.05$), independent of time. Figure 4.54 shows the boxplot of the results.

Table 4.18: Log2-fold changes of isoform3 of CHRNA5 in response to E2 treatment.

	iso3	**group**	**dose**	**time**
1	0.1536003	0nm12	0	12
2	-0.1536003	0nm12	0	12
3	2.0352838	100nm12	100	12
4	0.4294805	100nm12	100	12
5	-0.9830048	0nm24	0	24
6	0.9830048	0nm24	0	24
7	3.3487232	100nm24	100	24
8	3.1325052	100nm24	100	24

Table 4.19: Significance values of change in isoform3 CHRNA5 expression in response to E2 treatment. *=p<0.05.

Response:	iso3					
	Df	Sum Sq	Mean Sq	F value	Pr(>F)	
dose	1	10.0038	10.0038	12.1536	0.02521	*
time	1	2.0165	2.0165	2.4498	0.19259	
dose:time	1	2.0165	2.0165	2.4498	0.19259	
Residuals	4	3.2925	0.8231			

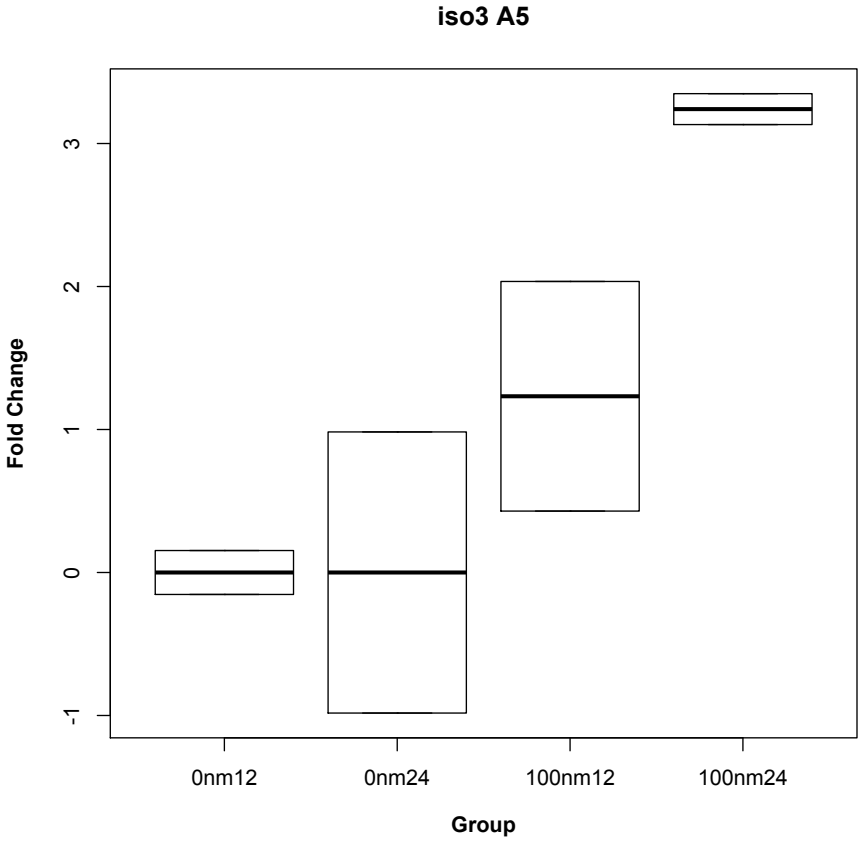

Figure 4.54: Boxplot for isoform 3 of CHRNA5 in E2 treated cells.

The summary of the data in Tables 4.6 to 4.19 can be seen in Table 4.20

Table 4.20: 2-way ANOVA results for all genes.

Genes	dose	time	dose:time
PS2	0.151619	0.007631	0.007631
ANLN	0.121	0.03	0.03
CHRNA5_All	0.28751	0.02846	0.02846
1000bp CHRNA5	0.00742	0.41069	0.41069
200bp CHRNA5	0.06606	0.51757	0.51757
iso2 CHRNA5	0.0004166	0.0213175	0.0213175
iso3 CHRNA5	0.02521	0.19259	0.19259

4.3.2 ANCOVA of CHRNA5 expression

ANCOVA was done in Matlab in order to see if there is a difference in the trends of response to E2 between 12h and 24h. Figures 4.55 to 4.59 show ANCOVA graphs and tables for each of the 5 CHRNA5 primers. A significant p-value for the slope indicates that there is a dose effect of E2, while a significant p-value between groups indicates that there is a time effect for CHRNA5 and the expression levels of the target genes differ between 12h and 24h.

In ANCOVA, separate lines were assumed since each time point has its own controls and these respective controls were used in $\Delta\Delta Ct$ calculations for 12h and 24h.

Total CHRNA5 expression is not significantly altered with 100nM E2 treatment, but the significant p-value ($p<0.05$) shows that total CHRNA5 expression significantly differs between 12h and 24h E2 treatment.

The expression of 1000bp CHRNA5 variant is highly significantly altered with 100nM E2 treatment ($p<0.01$), but this effect seems to be time-independent.

The expression of 200bp CHRNA5 variant is altered with a trend toward significance ($p=0.0661$) with 100nM E2 treatment, but this trend seem to be time-independent.

The expression of isoform2 of CHRNA5 variant is highly significantly altered with 100nM E2 treatment ($p<0.001$), and this effect seems to be time-dependent, since the p-value ($p<0.05$) indicates that the expression is significantly different between 12h and 24h of treatment.

The expression of isoform3 of CHRNA5 variant is significantly altered with 100nM E2 treatment ($p<0.05$), but this effects seem to be time-independent.

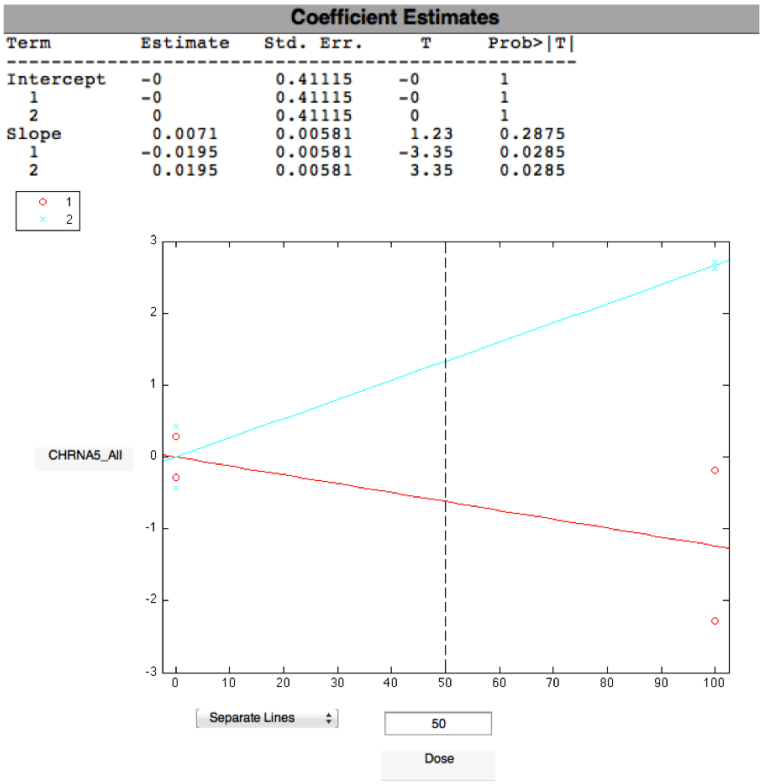

Figure 4.55: ANCOVA of CHRNA5_All in response to E2 treatment. 1 (red) refers to 12h of treatment and 2 (blue) refers to 24h of treatment, respectively.

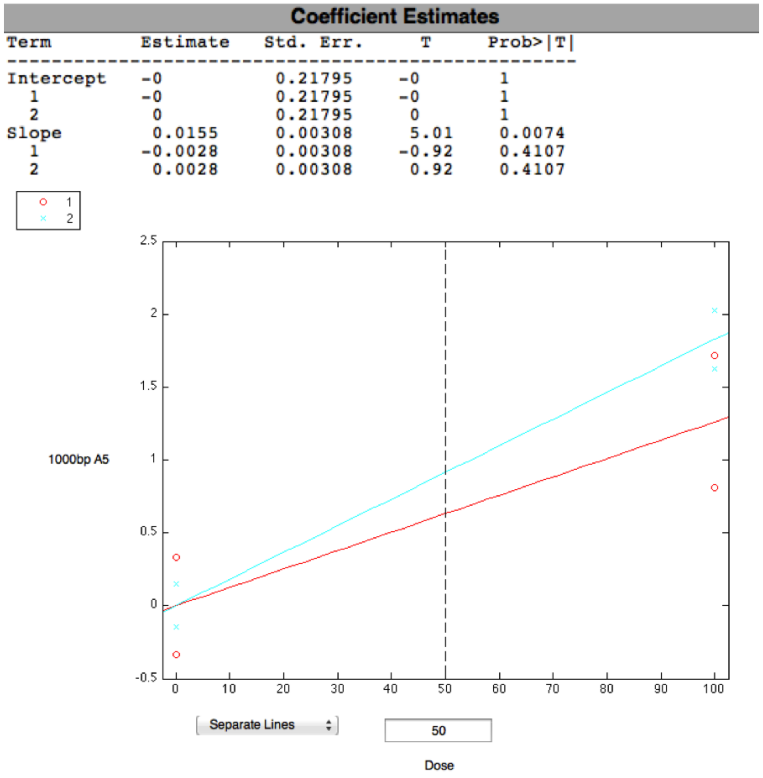

Figure 4.56: ANCOVA of 1000bp CHRNA5 in response to E2 treatment. 1 (red) refers to 12h of treatment and 2 (blue) refers to 24h of treatment, respectively.

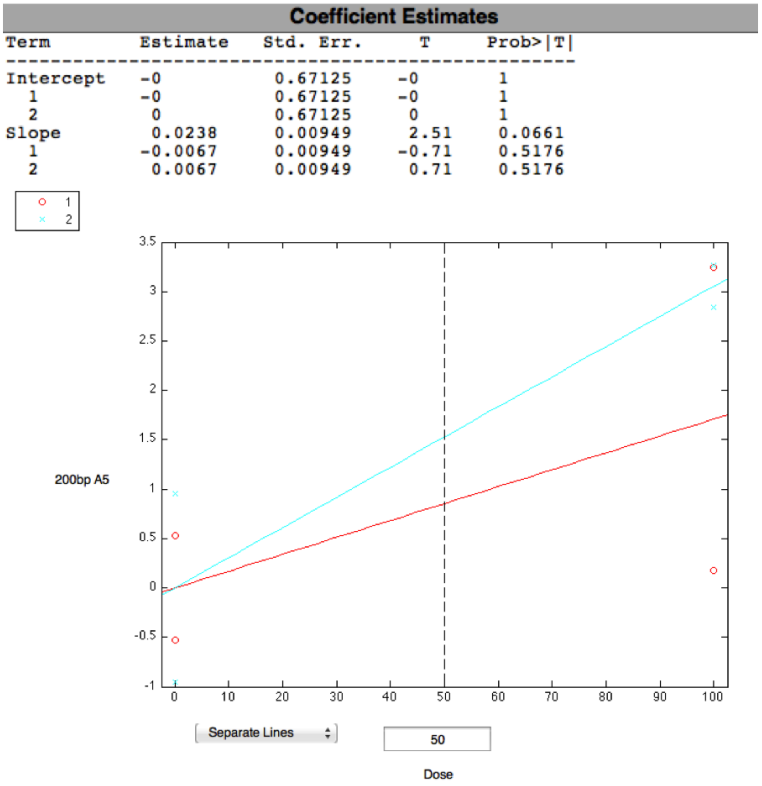

Figure 4.57: ANCOVA of 200bp CHRNA5 in response to E2 treatment. 1 (red) refers to 12h of treatment and 2 (blue) refers to 24h of treatment, respectively.

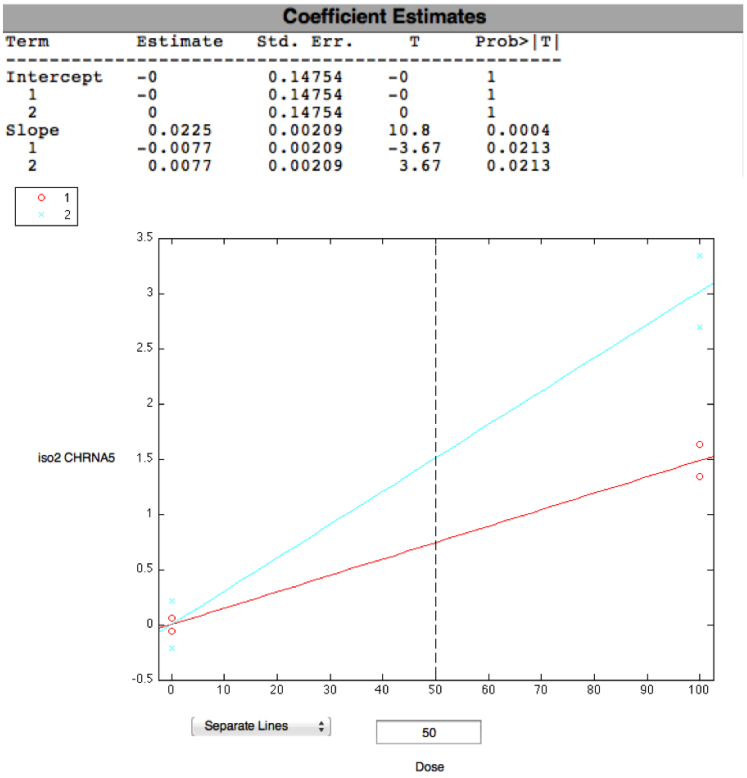

Figure 4.58: ANCOVA of iso2 CHRNA5 in response to E2 treatment. 1 (red) refers to 12h of treatment and 2 (blue) refers to 24h of treatment, respectively.

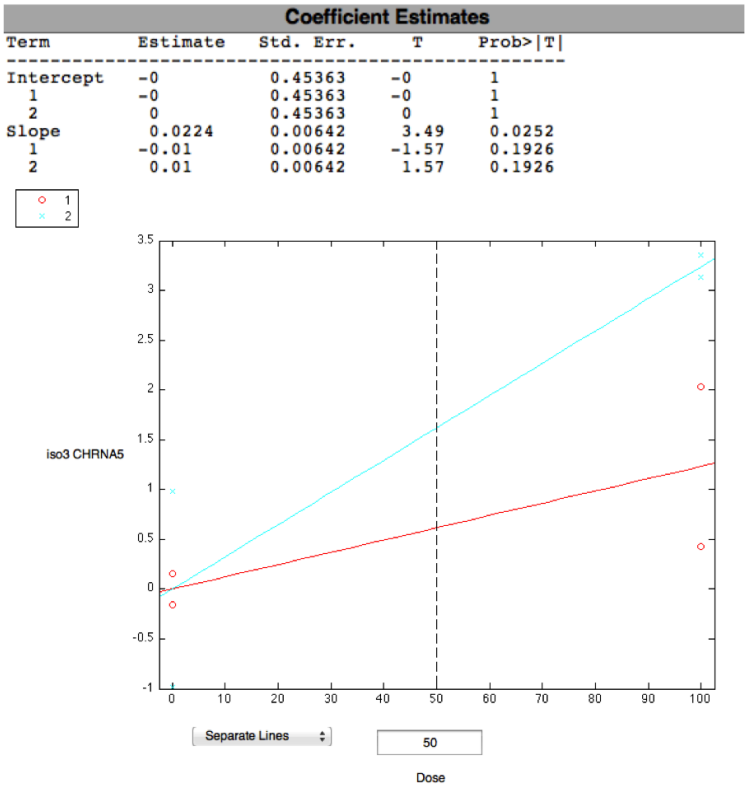

Figure 4.59: ANCOVA of iso3 CHRNA5 in response to E2 treatment. 1 (red) refers to 12h of treatment and 2 (blue) refers to 24h of treatment, respectively.

4.3.2.1 Saturation Points of E2 Treatment

In order to determine whether 100nM is the saturation point of expressions of the genes of interest or a lower concentration is sufficient, we added 30nM E2-treated samples to our analysis. Although the 30nM E2-treated samples lack their own control, they will give us an idea about how to proceed in our future studies with E2.

Figures 4.60 to 4.64 shows the graphs of the analysis. These results indicate that effects of E2 treatment on gene expression is always more prominent at 24h. There is a decrease in expression of the total CHRNA5 amount at 12h, but apart from that both 12h and 24h of E2 treatment increased expression of CHRNA5 variants. Results indicate that gene expression levels are saturated

before the concentration is increased to 100nM.

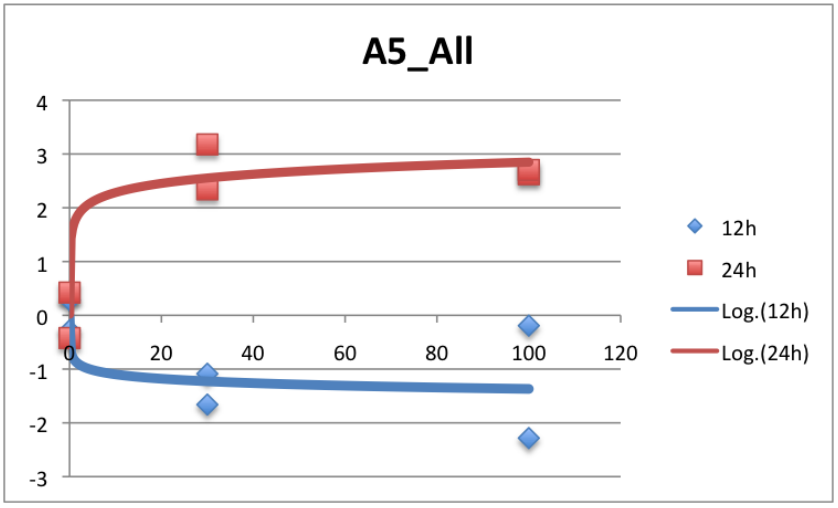

Figure 4.60: Expression levels of all isoforms of CHRNA5 in response to E2 treatment

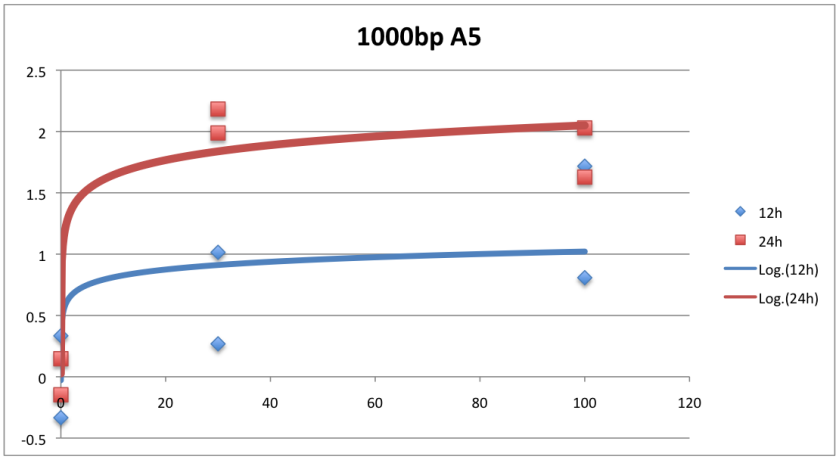

Figure 4.61: Expression levels of 1000bp isoform of CHRNA5 in response to E2 treatment

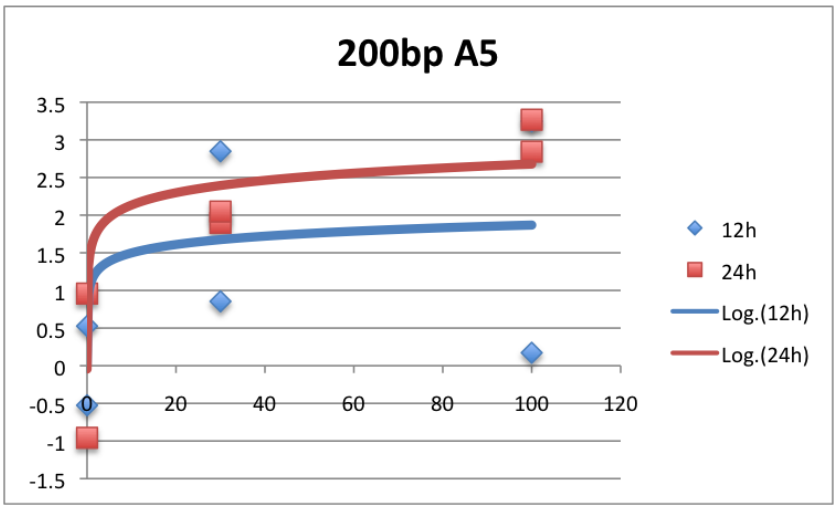

Figure 4.62: Expression levels of 200bp isoform of CHRNA5 in response to E2 treatment

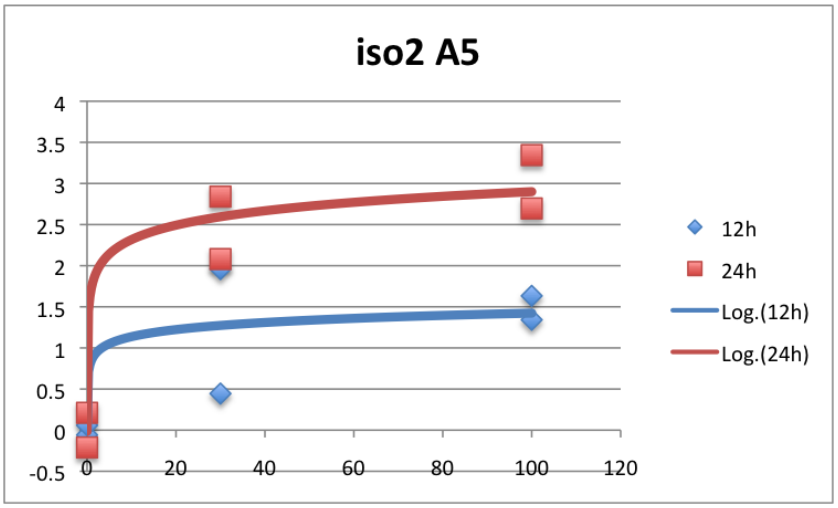

Figure 4.63: Expression levels of isoform 2 of CHRNA5 in response to E2 treatment

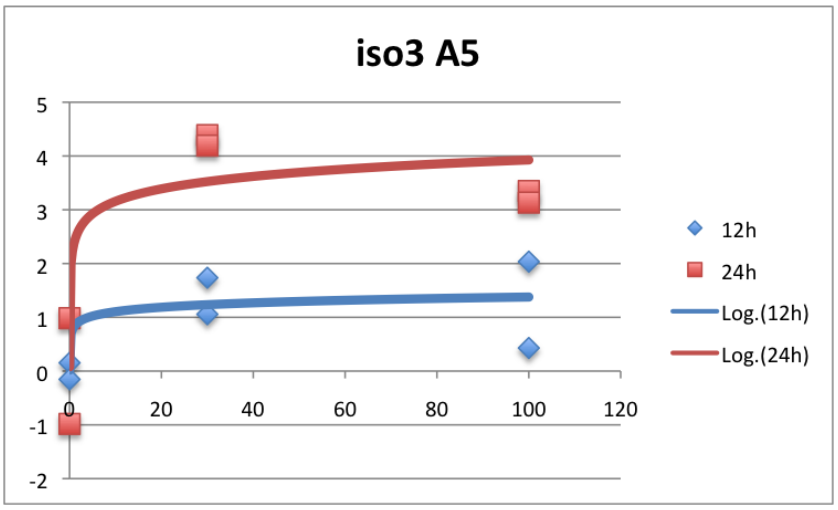

Figure 4.64: Expression levels of isoform 3 of CHRNA5 in response to E2 treatment

Chapter 5

CONCLUSION AND DISCUSSION

Abnormal or aberrant alternative splicing was previously associated with a variety of diseases, including cancer. Abnormal splicing of pre-mRNAs can lead to malignancy by the production of 'unnatural' variants that are not normally present in a tissue type, or by changing the normal ratio between natural variants in a specific tissue.[46,47]

CHRNA5 is a subtype of cholinergic nicotinic alpha receptors, that has been implicated in smoking behavior, cognitive performance, and more recently in lung cancer.[36–39] CHRNA5 was also found to be alternatively spliced in cell lines, normal lung tissue and lung adenocarcinoma.[43,73] The expression levels of CHRNA5 isoforms were shown to be increased in lung cancer.[43] In light of these findings, we investigated alternative splicing patterns of CHRNA5 as well as the response of some of these splicing variants to serum starvation and β-estradiol treatment.

To this end, we choose 10 different breast cancer cell lines belonging to 3 different molecular subtypes HER2+, Luminal and Basal.[22,24,25]

Serum starvation treatment has been used for a long time in experimental setups to obtain synchronized cells. It has also been used in studies dealing with gene expression regulation, apoptosis and stress response of cells.[62] We investigated the effects of serum starvation of cell viability using MTT assay. Our results showed that all of the cell lines, except MCF7 and T47D, responded to serum starvation with a decrease in cell viability. It is interesting

that both of the cell lines that did not respond have very similar characteristics (Table 3.1) and belonged to the same molecular subtype (Table 1.3). This might be due to a specific response of the molecular subtype, or a possible resistance to starvation that these cell lines obtained in culture conditions.

We then decided to investigate how the two variants of CHRNA5 responded to serum starvation in breast cancer cell lines. For our serum starvation experiments, we used 2 different sets for each cell line, including 2 biological replicates each for 10% FBS treatment and 0.1% FBS treatment. This allowed us to have two batches from each cell line, with 4 samples each.

First, using regular PCR, we identified the splice variants of CHRNA5 among these cell lines using primers that can amplify all of the variants separately. This implicated that there was a difference in expression of different CHRNA5 isoforms between breast cancer cell lines. However when we tried to see these differences using variant-specific primers with regular PCR, we were not able to visualize the changes. To overcome this, we decided to proceed to qPCR in order to quantify the differences. We chose two of the variants (200bp variant and 1000bp variant) for qPCR analysis.

We designed our qPCR experiments so that a single batch was run on a single plate. 4 samples from each cell line (2 controls and 2 treatment samples) were run in duplicates on the same plate, resulting in 80 data points. 2 qPCR runs were done for each gene, bringing the number of data points to 160 per batch. Having a bigger sample size with technical and biological replicates enables us to estimate the statistical significance of the results with a higher confidence level.[63–65] Since the sample size is relatively big, qPCR experiments are prone to sample-to-sample or run-to-run variations that can be due to biological variation of samples or technical errors in experimental steps.[63,67,68] The presence of this variability calls for a normalization so that the effects of a particular treatment can be assessed correctly.

Due to the nature of qPCR (high number of experimental steps, variables and sample size) there might be some data points that do not represent the

normal distribution of the data. Identification and exclusion of these data points is important to obtain statistically meaningful results.[66] Since we have multiple runs as well as technical and biological replicates, our data qualified for outlier detection and exclusion.[70] Several outlier detection methods were proposed. In our study we used a method that was similar to that of Burns et. al, (2005), in which we used boxplots to identify data points that fell outside around 99% range of the data. Among a total of 1280 data points analyzed, 45 data points were identified as potential outliers, and 41 of them were replaced. This corresponds to an error rate of 3.2% for the whole serum starvation data. It is important to note that these potential outliers were detected with the default parameters in IQR of Matlab. To identify the probable outlier values with a statistical significance, a more stringent test may be employed. To this end, Grubb's test was suggested in order to identify the data points that differ from the rest of that data set with significance.[66]

For normalization we chose two genes (TPT1 and SDHA) as reference, and took the geometric means of the expression values of these two genes, as previously suggested.[63,64]

Scatter plots and ANCOVA of 200bp and 1000bp CHRNA5 variants showed that expression of these variants were correlated in breast cancer cell lines, both in 10% and 0.1% FBS treated cells. This suggests that 200bp and 1000bp variants of CHRNA5 are co-regulated or regulated similarly in breast cancer cells. The expression levels of the 2 isoforms groups the breast cancer cell lines and this grouping correlates with the molecular subtypes of breast cancer cell lines. HER2 positive cell lines MDA MB 361 and MDA MB 468 seem to have the lowest CHRNA5 expression, while cell lines belonging to the basal type, MDA MB 468 and BT-20 have the highest CHRNA5 expression, especially for the 1000bp variant. The cell lines in the luminal subtype and basal cell lines MDA MB 231 and MDA MB 157 have expression values between the two.

We have expression data from two different batches of the same cell lines. Our sample size enables us to assess and get rid of the batch effect. For

this we used ANCOVA. This method takes the reference gene expression, which is the geometric mean of TPT1 and SDHA, as a covariate and tests the differences in response to treatment among cell lines. We assumed that the reference genes would behave similarly among cell lines, hence we used parallel lines to assess the covariance. The outcome of the ANCOVA is two p-values, one for the significance of the treatment and the other for the correlation of reference gene with the target gene. The second p-value is given as the p-value of the slope. In some of our data, p-values of the slopes are significant ($p<0.05$), which implies that reference gene expression varies between cell lines. This suggests that TPT1 and SDHA may vary only a limited degree between samples since the Ct values for reference genes are around 17 and 19.5 and those for the target transcripts are between 21 and 29. Thus, geometric average of TPT1 and SDHA is a reasonable estimate of RNA amount used in the tests.

When we analyzed the starvation response separately for each cell line, we considered a p value below 0.05 significant and a p value below 0.15 to have a trend. In 200bp CHRNA5 variant, only ZR-75-1 and MDA MB 157 cells showed a significant alteration in response to starvation and only HCC-1937 cells seemed to have trend toward a change. In 1000bp CHRNA5 variant none of the cell lines showed a significant alteration but 4 cell lines had trends toward a change. This might be due to the batch effect, or due to inappropriate choice of reference genes. Another possibility is that CHRNA5 may not be highly responsive to serum starvation so that we are not able to detect these small changes in expression. Serum starvation treatment may be repeated for the cell lines that showed promising results, that is those with a trend toward change, with a p value below 0.15, using a higher number of samples within a batch in order to increase statistical power.

While we tried a variety of other statistical analyses such as t-test (data not shown), we decided that ANCOVA was the one that was the most appropriate for the nature of our data set. But other analysis methods, such as two-way ANOVA can also be used to analyse this data.

Estrogen has previously been associated with both the initiation and the progression of breast carcinogenesis.[13–15] Estrogens were also shown to regulate the expression of a variety of genes, having primary and secondary targets.[16,19,84] To this end, we wanted to see if CHRNA5 expression was E2-responsive and used ER+, estrogen-responsive MCF7 cell line. To see if E2 treatment was effective, we used PS2 and ANLN which were shown to be primary target and secondary targets of E2, respectively.[19,74] Among the 5 variants of CHRNA5 that were tested (total CHRNA5, 200bp CHRNA5, 1000bp CHRNA5, CHRNA5 isoform2 and CHRNA5 isofrom3), all of the variants, except total CHRNA5, showed a significant difference in expression with 100nM E2 with ANCOVA while total CHRNA5 expression was shown to be significantly different between 12h and 24h time points. Whereas 2-way ANOVA results showed a significant difference in 1000bp CHRNA5, isoform2 CHRNA5 and isoform3 CHRNA5 with 100nM E2 treatment. Interestingly, total CHRNA5 expression seems to have a delayed response, and no increase in expression can be seen at 12h, which is not the case for any of the other variants (although at a lower level, they show increased expression at 12h also)

We also have 30nM E2-treated samples. Even though they lack their own controls, we decided to add the data from those samples to our analysis to estimate the saturation concentration for E2 (i.e. the E2 concentration that is sufficient to generate the highest response for a given gene). This analysis showed us that saturation can be reached with a lower concentration than 100nM, so in order to assess the effects of E2 on CHRNA5 expression more precisely, a dose curve consisting of 0nM, 1nM, 10nM, 30nM and 100nM can be used in future experiments.

Our data shows that 200bp and 1000bp variants of CHRNA5 are regulated similarly in breast cancer cell lines. The two variants respond differently to serum starvation treatments in different cell lines. A larger sample size may be required to assess the changes in expression of different CHRNA5 variants in breast cancer cell lines with different molecular subtypes.

Chapter 6

FUTURE PERSPECTIVES

In order to get a dataset that is more statistically significant, additional treatments on cell lines from the same batch can be done. This will increase the sample size and allow us to have statistical data with more confidence.

In order to determine whether the potential outliers that we identified using boxplot function of Matlab are true outliers, Grubb's test, modified for multiple outliers, can be used to identify the data points among these potential outliers that significantly differ from the rest of the data set.

Changes in proliferation that were recorded with MTT assay might be checked to see if they correlate with changes in CHRNA5 expression in response to serum starvation.

There are additional variants of CHRNA5, other than the ones that we chose to focus on this study. Primers that are specific to these other CHRNA5 isoforms should be tested in order to get a more complete and accurate understanding of alternative splicing of CHRNA5 in breast cancer cell lines.

Adding normal breast cell lines to our panel would show us if the expression ratios of different CHRNA5 variants change in breast cancer, compared to that of normal breast.

To get a broader idea of the regulation of CHRNA5 in humans, expression in normal human tissues, especially breast tissue should be investigated. cDNA panels can be used for this purpose. To see if the results obtained from our

cell line and cDNA panel studies are compatible in a clinical level, samples from normal breast tissue and patient tumor samples should be investigated for CHRNA5 variant expression.

E2-treatment is a promising aspect that affects CHRNA5 expression. In order to solidify these results further we should be able to repeat them with a cell line that is similar to MCF7 (e.g: T47D). E2 response of the cell lines that are ER-, like MDA MB 231, should also be investigated.

A dose curve for E2 treatment will give us a better idea of the E2 level necessary to induce and increase in CHRNA5 expression. Co-treatment of E2 with its competitors, such as tamoxifen can be done in order to see if CHRNA5 will respond differently. In addition, E2 treatment can be tried in CHRNA5-silenced and -overexpressing cells to investigate how the responses differ from that of controls.

Bibliography

[1] Jemal, A., Siegel, R., Xu, J. & Ward, E. Cancer Statistics , 2010. *CA: A Cancer Journal for Clinicians* **60**, 277–300 (2010).

[2] Wooster, R. & Weber, B. L. Breast and ovarian cancer. *The New England journal of medicine* **348**, 2339–47 (2003).

[3] Kenemans, P., Verstraeten, R. a. & Verheijen, R. H. M. Oncogenic pathways in hereditary and sporadic breast cancer. *Maturitas* **49**, 34–43 (2004).

[4] Margolese, R., Fisher, B., Hortobagyi, G. & Al., E. Neoplasms of the Breast. In et al. Bast RC Jr, Kufe DW, Pollock RE (ed.) *Holland-Frei Cancer Medicine.*, chap. 118 (BC Decker, 2000), 5th editio edn.

[5] Weigelt, B., Geyer, F. C. & Reis-Filho, J. S. Histological types of breast cancer: how special are they? *Molecular oncology* **4**, 192–208 (2010).

[6] Elston, C. W. & Ellis, I. O. Pathological prognostic factors in breast cancer. I. The value of histological grade in breast cancer: experience from a large study with long-term follow-up. *Histopathology* **19**, 403–10 (1991).

[7] Benson, J. R. The TNM staging system and breast cancer. *The Lancet Oncology* **4**, 56–57 (2003).

[8] Singletary, S. E. Revision of the American Joint Committee on Cancer Staging System for Breast Cancer. *Journal of Clinical Oncology* **20**, 3628–3636 (2002).

[9] Perou, C. M. *et al.* Molecular portraits of human breast tumours. *Nature* **406**, 747–52 (2000).

[10] Sø rlie, T. *et al.* Gene expression patterns of breast carcinomas distinguish tumor subclasses with clinical implications. *Proceedings of the National Academy of Sciences of the United States of America* **98**, 10869–74 (2001).

[11] Sorlie, T. *et al.* Repeated observation of breast tumor subtypes in independent gene expression data sets. *Proceedings of the National Academy of Sciences of the United States of America* **100**, 8418–23 (2003).

[12] Hu, Z. *et al.* The molecular portraits of breast tumors are conserved across microarray platforms. *BMC genomics* **7**, 96 (2006).

[13] Henderson, B. E., Ross, R. & Bernstein, L. Estrogens as a Cause of Human Cancer : The Richard and Hinda Rosenthal Foundation Award Lecture. *Cancer Research* **48**, 246–253 (1988).

[14] Clemons, M. & Goss, P. Estrogen and the Risk of Breast Cancer. *N engl J med* **344**, 276–285 (2001).

[15] Yager, J. & Davidson, N. Estrogen carcinogenesis in breast cancer. *New England Journal of Medicine* **354**, 270–282 (2006).

[16] Frasor, J. *et al.* Profiling of estrogen up- and down-regulated gene expression in human breast cancer cells: insights into gene networks and

pathways underlying estrogenic control of proliferation and cell phenotype. *Endocrinology* **144**, 4562–74 (2003).

[17] Cunliffe, H. E. *et al.* The Gene Expression Response of Breast Cancer to Growth Regulators: Patterns and Correlation with Tumor Expression Profiles. *Cancer Res.* **63**, 7158–7166 (2003).

[18] Coser, K. R. *et al.* Global analysis of ligand sensitivity of estrogen inducible and suppressible genes in MCF7/BUS breast cancer cells by DNA microarray. *Proceedings of the National Academy of Sciences of the United States of America* **100**, 13994–9 (2003).

[19] Bourdeau, V. *et al.* Mechanisms of primary and secondary estrogen target gene regulation in breast cancer cells. *Nucleic acids research* **36**, 76–93 (2008).

[20] Wang, D.-Y., Fulthorpe, R., Liss, S. N. & Edwards, E. a. Identification of estrogen-responsive genes by complementary deoxyribonucleic acid microarray and characterization of a novel early estrogen-induced gene: EEIG1. *Molecular endocrinology (Baltimore, Md.)* **18**, 402–11 (2004).

[21] Lin, C.-Y. *et al.* Discovery of estrogen receptor alpha target genes and response elements in breast tumor cells. *Genome biology* **5**, R66 (2004).

[22] Neve, R. M. *et al.* A collection of breast cancer cell lines for the study of functionally distinct cancer subtypes. *Cancer cell* **10**, 515–27 (2006).

[23] Holliday, D. L. & Speirs, V. Choosing the right cell line for breast cancer research. *Breast cancer research : BCR* **13**, 215 (2011).

[24] Kao, J. *et al.* Molecular profiling of breast cancer cell lines defines relevant tumor models and provides a resource for cancer gene discovery. *PloS one* **4**, e6146 (2009).

[25] Riaz, M. *et al.* miRNA expression profiling of 51 human breast cancer cell lines reveals subtype and driver mutation-specific miRNAs. *Breast cancer research : BCR* **15**, R33 (2013).

[26] Weiland, S., Bertrand, D. & Leonard, S. Neuronal nicotinic acetylcholine receptors: from the gene to the disease. *Behavioural brain research* **113**, 43–56 (2000).

[27] Itier, V. & Bertrand, D. Neuronal nicotinic receptors: from protein structure to function. *FEBS Letters* **504**, 118–125 (2001).

[28] Paterson, D. & Nordberg, A. Neuronal nicotinic receptors in the human brain. *Progress in neurobiology* **61**, 75–111 (2000).

[29] Boulter, J. *et al.* Alpha 3, alpha 5, and beta 4: three members of the rat neuronal nicotinic acetylcholine receptor-related gene family form a gene cluster. *The Journal of biological chemistry* **265**, 4472–82 (1990).

[30] Couturier, S., Erkman, L. & Valera, S. Alpha 5, alpha 3, and non-alpha 3. Three clustered avian genes encoding neuronal nicotinic acetylcholine receptor-related subunits. *Journal of Biological ...* **265**, 17560–67 (1990).

[31] Eng, C. M., Kozak, C. A., Beaudet, A. L. & Zoghbi, H. Y. Mapping of multiple subunits of the neuronal nicotinic acetylcholine receptor to chromosome 15 in man and chromosome 9 in mouse. *Genomics* **9**, 278–282 (1991).

[32] Gerzanich, V. Assembly of Human Neuronal Nicotinic Receptor alpha 5 Subunits with alpha 3, beta 2, and beta 4 Subunits. *Journal of Biological Chemistry* **271**, 17656–17665 (1996).

[33] Gerzanich, V., Wang, F., Kuryatov, A. & Lindstrom, J. alpha 5 Subunit alters desensitization, pharmacology, Ca++ permeability and Ca++ modulation of human neuronal alpha 3 nicotinic receptors. *The Journal of pharmacology and experimental therapeutics* **286**, 311–20 (1998).

[34] Soldà, G. *et al.* In vivo RNA-RNA duplexes from human alpha3 and alpha5 nicotinic receptor subunit mRNAs. *Gene* **345**, 155–64 (2005).

[35] Greenbaum, L. *et al.* Why do young women smoke? I. Direct and interactive effects of environment, psychological characteristics and nicotinic cholinergic receptor genes. *Molecular psychiatry* **11**, 312–22, 223 (2006).

[36] Berrettini, W. *et al.* Alpha-5/alpha-3 nicotinic receptor subunit alleles increase risk for heavy smoking. *Molecular psychiatry* **13**, 368–73 (2008).

[37] Improgo, M. R. D., Scofield, M. D., Tapper, A. R. & Gardner, P. D. The nicotinic acetylcholine receptor CHRNA5/A3/B4 gene cluster: dual role in nicotine addiction and lung cancer. *Progress in neurobiology* **92**, 212–26 (2010).

[38] Winterer, G. *et al.* Risk gene variants for nicotine dependence in the CHRNA5-CHRNA3-CHRNB4 cluster are associated with cognitive performance. *American journal of medical genetics. Part B, Neuropsychiatric genetics : the official publication of the International Society of Psychiatric Genetics* **153B**, 1448–58 (2010).

[39] Rigbi, a. *et al.* Why do young women smoke? V. Role of direct and interactive effects of nicotinic cholinergic receptor gene variation on neurocognitive function. *Genes, brain, and behavior* **7**, 164–72 (2008).

[40] Thorgeirsson, T. E. *et al.* A variant associated with nicotine dependence, lung cancer and peripheral arterial disease. *Nature* **452**, 638–42 (2008).

[41] Hung, R. J. *et al.* A susceptibility locus for lung cancer maps to nicotinic acetylcholine receptor subunit genes on 15q25. *Nature* **452**, 633–7 (2008).

[42] Amos, C. I. *et al.* Genome-wide association scan of tag SNPs identifies a susceptibility locus for lung cancer at 15q25.1. *Nature genetics* **40**, 616–22 (2008).

[43] Falvella, F. S. *et al.* Multiple isoforms and differential allelic expression of CHRNA5 in lung tissue and lung adenocarcinoma. *Carcinogenesis* **34**, 1281–5 (2013).

[44] Lee, C.-H. *et al.* Overexpression and activation of the alpha9-nicotinic receptor during tumorigenesis in human breast epithelial cells. *Journal of the National Cancer Institute* **102**, 1322–35 (2010).

[45] Matlin, A. J., Clark, F. & Smith, C. W. J. Understanding alternative splicing: towards a cellular code. *Nature reviews. Molecular cell biology* **6**, 386–98 (2005).

[46] Pajares, M. J. *et al.* Alternative splicing: an emerging topic in molecular and clinical oncology. *The lancet oncology* **8**, 349–57 (2007).

[47] Kalnina, Z., Zayakin, P., Silina, K. & LinÄŞ, A. Alterations of pre-mRNA splicing in cancer. *Genes, chromosomes & cancer* **42**, 342–57 (2005).

[48] Venables, J. P. Unbalanced alternative splicing and its significance in cancer. *BioEssays : news and reviews in molecular, cellular and developmental biology* **28**, 378–86 (2006).

[49] Black, D. L. Mechanisms of alternative pre-messenger RNA splicing. *Annual review of biochemistry* **72**, 291–336 (2003).

[50] Ladomery, M. R., Harper, S. J. & Bates, D. O. Alternative splicing in angiogenesis: the vascular endothelial growth factor paradigm. *Cancer letters* **249**, 133–42 (2007).

[51] Sammeth, M., Foissac, S. & Guigó, R. A general definition and nomenclature for alternative splicing events. *PLoS computational biology* **4**, e1000147 (2008).

[52] David, C. J. & Manley, J. L. Alternative pre-mRNA splicing regulation in cancer: pathways and programs unhinged. *Genes & development* **24**, 2343–64 (2010).

[53] Venables, J. Aberrant and alternative splicing in cancer. *Cancer research* 7647–7654 (2004).

[54] Cooper, S. Reappraisal of serum starvation, the restriction point, G0, and G1 phase arrest points. *FASEB journal : official publication of the Federation of American Societies for Experimental Biology* **17**, 333–40 (2003).

[55] Cooper, S. & Gonzalez-Hernandez, M. Experimental reconsideration of the utility of serum starvation as a method for synchronizing mammalian cells. *Cell biology international* **33**, 71–7 (2009).

[56] Demidenko, Z. N. & Blagosklonny, M. V. Growth stimulation leads to cellular senescence when the cell cycle is blocked. *Cell cycle (Georgetown, Tex.)* **7**, 3355–61 (2008).

[57] Kim, M. J. *et al.* Mitochondrial ribosomal protein L41 mediates serum starvation-induced cell-cycle arrest through an increase of p21(WAF1/CIP1). *Biochemical and biophysical research communications* **338**, 1179–84 (2005).

[58] Hasan, N. M., Adams, G. E. & Joiner, M. C. Effect of serum starvation on expression and phosphorylation of PKC-alpha and p53 in V79 cells: implications for cell death. *International journal of cancer. Journal international du cancer* **80**, 400–5 (1999).

[59] Ming, L. *et al.* Sp1 and p73 activate PUMA following serum starvation. *Carcinogenesis* **29**, 1878–84 (2008).

[60] Haviv, R., Lindenboim, L., Yuan, J. & Stein, R. Need for caspase-2 in apoptosis of growth-factor-deprived PC12 cells. *Journal of neuroscience research* **52**, 491–7 (1998).

[61] Schamberger, C. J., Gerner, C. & Cerni, C. Caspase-9 plays a marginal role in serum starvation-induced apoptosis. *Experimental cell research* **302**, 115–28 (2005).

[62] Pirkmajer, S. & Chibalin, A. Serum starvation: caveat emptor. *American Journal of Physiology- ...* 272–279 (2011).

[63] Derveaux, S., Vandesompele, J. & Hellemans, J. How to do successful gene expression analysis using real-time PCR. *Methods (San Diego, Calif.)* **50**, 227–30 (2010).

[64] Bollmann, F., Casper, I., Henke, J. & Pautz, A. qRT-PCR: a method and its difficulties. *Naunyn-Schmiedeberg's archives of pharmacology* **385**, 949–51 (2012).

[65] Bustin, S. a. Why the need for qPCR publication guidelines?–The case for MIQE. *Methods (San Diego, Calif.)* **50**, 217–26 (2010).

[66] Burns, M. J., Nixon, G. J., Foy, C. a. & Harris, N. Standardisation of data from real-time quantitative PCR methods - evaluation of outliers and comparison of calibration curves. *BMC biotechnology* **5**, 31 (2005).

[67] Cankar, K., Stebih, D., Dreo, T., Zel, J. & Gruden, K. Critical points of DNA quantification by real-time PCR–effects of DNA extraction method and sample matrix on quantification of genetically modified organisms. *BMC biotechnology* **6**, 37 (2006).

[68] Ling, D., Pike, C. J. & Salvaterra, P. M. Deconvolution of the confounding variations for reverse transcription quantitative real-time polymerase chain reaction by separate analysis of biological replicate data. *Analytical biochemistry* **427**, 21–5 (2012).

[69] Wong, M. L. & Medrano, J. F. Real-time PCR for mRNA quantitation. *BioTechniques* **39**, 75–85 (2005).

[70] Goni, R., García, P. & Foissac, S. The qPCR data statistical analysis. *Integromics white paper: ...* 1–9 (2009).

[71] Siegel, R. Cancer statistics, 2013. *CA: A Cancer Journal for Clinicians* **63**, 11–30 (2013).

[72] Biyik, R. *Nicotone-Modulated Gene Expression Profiles in MCF7 Breast Cancer Cell Line and Involvement of Estrogen in CHRNA5 Expression.* Ph.D. thesis, Bilkent University (2009).

[73] Warzecha, C. C., Shen, S., Xing, Y. & Carstens, R. P. The epithelial splicing factors ESRP1 and ESRP2 positively and negatively regulate diverse types of alternative splicing events. *RNA Biology* **6**, 546–562 (2009).

[74] Alotaibi, H., Yaman, E. C., Demirpençe, E. & Tazebay, U. H. Unliganded estrogen receptor-alpha activates transcription of the mammary gland Na+/I- symporter gene. *Biochemical and biophysical research communications* **345**, 1487–96 (2006).

[75] Gur-Dedeoglu, B. *et al.* Identification of endogenous reference genes for qRT-PCR analysis in normal matched breast tumor tissues. *Oncology research* **17**, 353–65 (2009). URL `http://www.ncbi.nlm.nih.gov/pubmed/19544972`.

[76] Konu, O. *et al.* Application of a customized pathway-focused microarray for gene expression profiling of cellular homeostasis upon exposure to nicotine in PC12 cells. *Brain research. Molecular brain research* **121**, 102–13 (2004).

[77] Tichopad, A. *et al.* Quality control for quantitative PCR based on amplification compatibility test. *Methods (San Diego, Calif.)* **50**, 308–12 (2010).

[78] Bar, T. Kinetic Outlier Detection (KOD) in real-time PCR. *Nucleic Acids Research* **31**, 105e–105 (2003).

[79] Ling, D. & Salvaterra, P. M. Robust RT-qPCR data normalization: validation and selection of internal reference genes during post-experimental data analysis. *PloS one* **6**, e17762 (2011).

[80] Hellemans, J., Mortier, G., De Paepe, A., Speleman, F. & Vandesompele, J. qBase relative quantification framework and software for management and automated analysis of real-time quantitative PCR data. *Genome biology* **8**, R19 (2007).

[81] Grubbs, F. Procedures for detecting outlying observations in samples. *Technometrics* **11**, 1–21 (1969).

[82] Pfaffl, M. W. A new mathematical model for relative quantification in real-time RT-PCR. *Nucleic acids research* **29**, e45 (2001).

[83] Yuan, J. S., Reed, A., Chen, F. & Stewart, C. N. Statistical analysis of real-time PCR data. *BMC bioinformatics* **7**, 85 (2006).

[84] O Leary, P. C. *et al.* Systematic antibody generation and validation via tissue microarray technology leading to identification of a novel protein prognostic panel in breast cancer. *BMC cancer* **13**, 175 (2013).

Chapter 7

APPENDICES

Appendix A

Matlab Codes Used For Analyses

Matlab codes that were used in this study are for:

- Outlier detection and exclusion
- taking arithmetic and geometric means of references
- ANCOVA for all cell lines
- ANCOVA for separate cell lines

Table 7.1: Matlab code for outlier detection and exclusion

```
function [data1]=outlier(data)
data=xlsread('200bp set3-4 run1-2') %input:data; a 80x2 matrix that contains the
the qPCR measurements from a cell line, for a total of 10 cell lines.  Each cell
line has 2 groups and each group has two biological replicates and 2 technical
replicates
j=1
data1=[]; % creates a vector
boxdata=zeros(16,10); % creates an array of all zeroes (16 by 10)
for i=1:10
boxdata
data1
a=[data(j:j+7,1);data(j:j+7,2)] % collects the data for each cell line from 2
separate runs
j=j+8
figure()
boxplot(a) % draws a boxplot for each cell line, showing the outliers
boxdata(:,i)=a;
h = findobj(gcf,'tag','Outliers'); % gets the handles of the boxplots for
'Outliers'
yc= get(h,'YData'); % gets the index of the outliers
d=find(a(:,1)==yc(1,:)); % finds the index of the ouliers in our data
d
a(d)=NaN % replaces the outliers with 'NaN'
data1=[data1;[a(1:8) a(9:16)]]
data1
data1
boxdata
end
data1
boxdata
boxplot(boxdata)
```

Table 7.2: Matlab code for arithmetic mean and geometric mean of references

```
function[]=geomeans(temp);
temp=xlsread('covdesc.xls');
ref1=uigetfile('*.csv','ref1');
ref1=csvread(ref1);
ref2=uigetfile('*.csv','ref2');
ref2=csvread(ref2);
i1=find(temp(:,4)==1);
i2=find(temp(:,4)==2);
ref1m=nanmean(ref1,2);
ref2m=nanmean(ref2,2);
ref1_means=[ref1m(i1,:),ref1m(i2,:)];
ref2_means=[ref2m(i1,:),ref2m(i2,:)];
m=nanmean(ref1_means,2);
n=nanmean(ref2_means,2);
a=[m,n]
b=geomean(a,2)
xlswrite('Refset12', b)
```

Table 7.3: Matlab code for ANCOVA of all cell lines

```
function[]=aoccl(trg,ref);
trg=uigetfile('*.csv','trg');
trg=csvread(trg);
ref=csvread('Ref01.csv');
g=repmat(1:10,[4 1]);
g=g(:)';
[h,a,c,s]=aoctool(ref,trg,g,'',...
'','','','','parallel lines')
```

Table 7.4: Matlab code for ANCOVA of separate cell lines

```
function[]=aoc(temp,data);
temp2=xlsread('temp2.xls');
ref12=uigetfile('*.csv','ref12');
ref12=csvread(ref12);
trg12=uigetfile('*.csv', 'trg12');
trg12=csvread(trg12);
ref34=uigetfile('*.csv','ref34');
ref34=csvread(ref34);
trg34=uigetfile('*.csv', 'trg34');
trg34=csvread(trg34);
for i=1:10
i3=find(temp2(:,1)==i)
a=trg12(i3)
b=trg34(i3)
c=ref12(i3)
d=ref34(i3)
e=[a;b]
f=[c;d]
g=[1 1 0 0 1 1 0 0 ]';
[h,a,c,s]=aoctool(f,e,g,",...
",",",",'parallel lines')
end
```

Appendix B

Expression values of TPT1 and SDHA probesets in analyzed GSE datasets

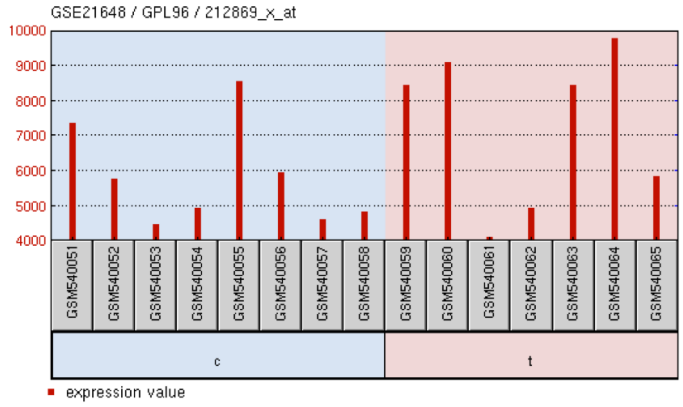

Figure 7.1: Expression values of TPT1 probeset in GSE21648 dataset in control and starvation groups

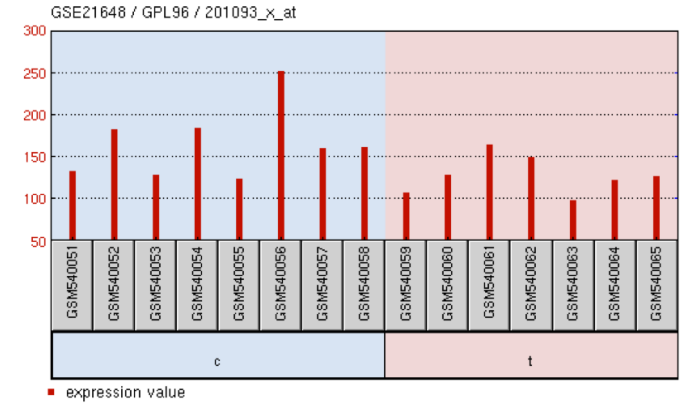

Figure 7.2: Expression values of SDHA probeset in GSE21648 dataset in control and starvation groups

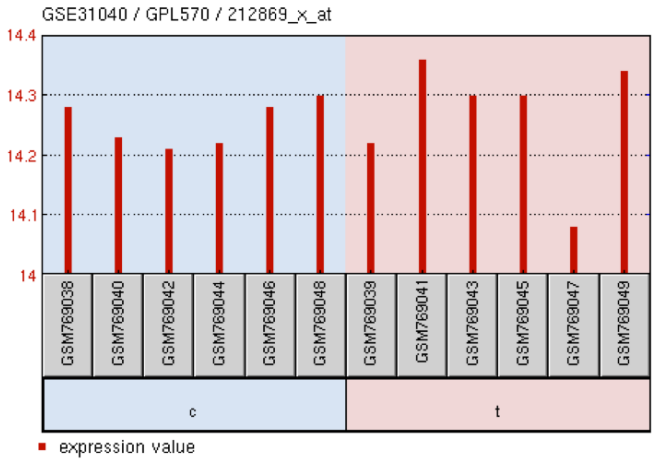

Figure 7.3: Expression values of TPT1 probeset in GSE31040 dataset in control and starvation groups

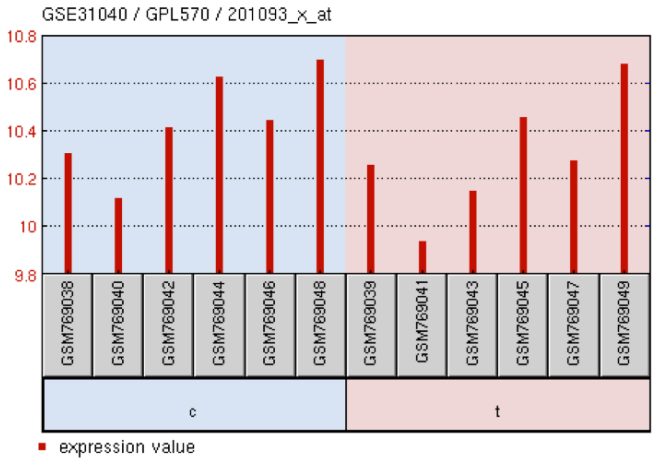

Figure 7.4: Expression values of SDHA probeset in GSE31040 dataset in control and starvation groups

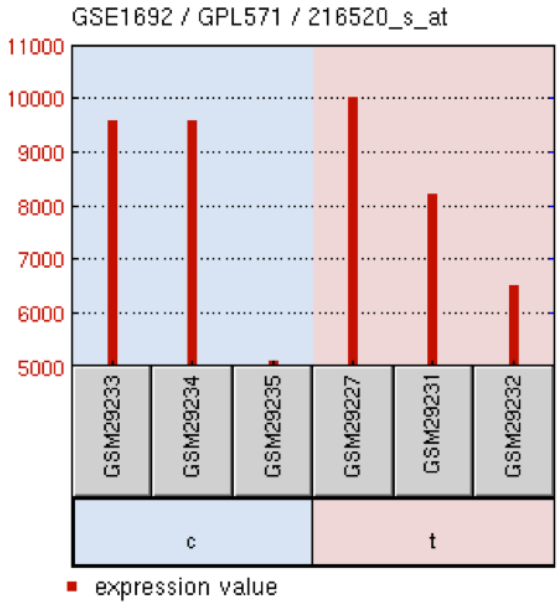

Figure 7.5: Expression values of TPT1 probeset in GSE1692 dataset in control and starvation groups

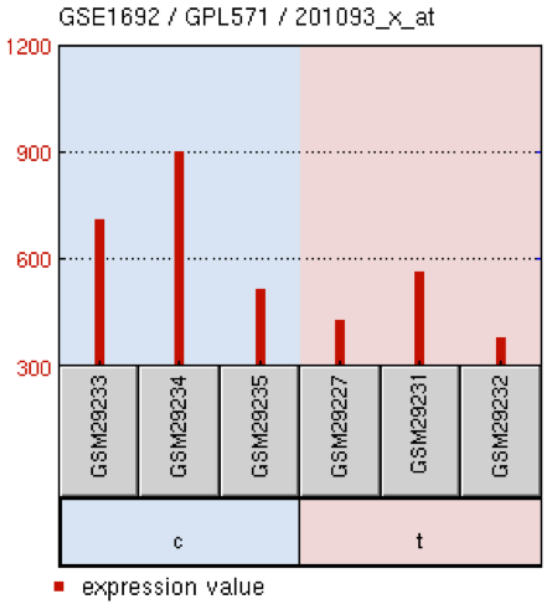

Figure 7.6: Expression values of SDHA probeset in GSE1692 dataset in control and starvation groups

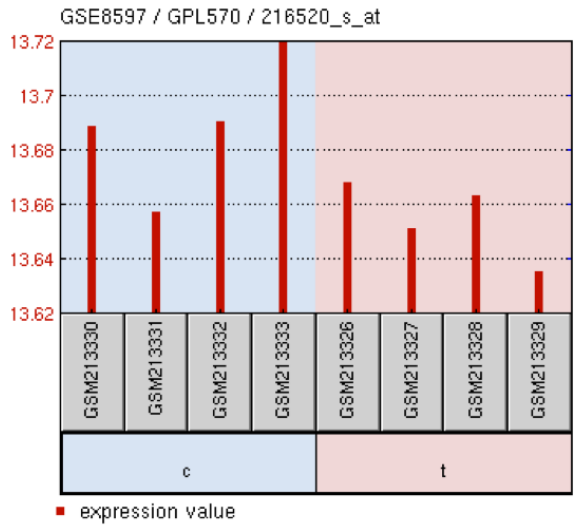

Figure 7.7: Expression values of TPT1 probeset in GSE8597 dataset in control and estradiol treatment groups

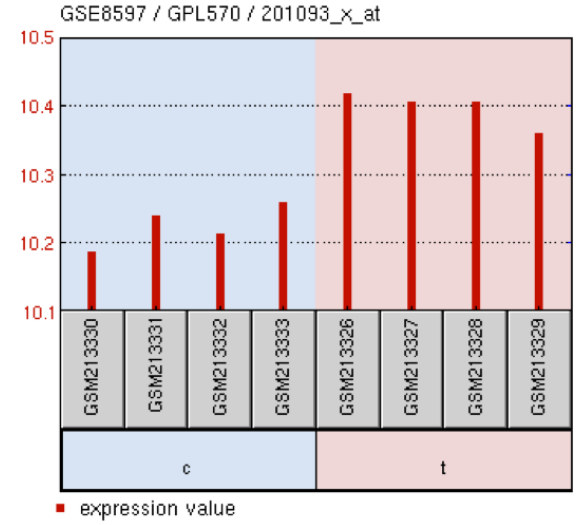

Figure 7.8: Expression values of SDHA probeset in GSE8597 dataset in control and estradiol treatment groups

Permissions for the Copyrighted Materials

My Orders > Orders > All Orders

License Details

This is a License Agreement between Azer Acikgoz ("You") and Elsevier ("Elsevier"). The license consists of your order details, the terms and conditions provided by Elsevier, and the payment terms and conditions.

Get the printable license.

License Number	3200320896731
License date	Aug 01, 2013
Licensed content publisher	Elsevier
Licensed content publication	Progress in Neurobiology
Licensed content title	The nicotinic acetylcholine receptor CHRNA5/A3/B4 gene cluster: Dual role in nicotine addiction and lung cancer
Licensed content author	Ma. Reina D. Improgo,Michael D. Scofield,Andrew R. Tapper,Paul D. Gardner
Licensed content date	October 2010
Licensed content volume number	92
Licensed content issue number	2
Number of pages	15
Type of Use	reuse in a thesis/dissertation
Portion	figures/tables/illustrations
Number of figures/tables/illustrations	1
Format	both print and electronic
Are you the author of this Elsevier article?	No
Will you be translating?	No
Order reference number	None
Title of your thesis/dissertation	Analysis of CHRNA5 Expression in Breast Cancer Cell Lines in Response to Serum Starvation and Estrogen Treatment
Expected completion date	Aug 2013
Elsevier VAT number	GB 494 6272 12
Permissions price	0.00 USD
VAT/Local Sales Tax	0.00 USD / 0.00 GBP
Total	**0.00 USD**

My Orders > Orders > All Orders

License Details

This is a License Agreement between Azer Acikgoz ("You") and Elsevier ("Elsevier"). The license consists of your order details, the terms and conditions provided by Elsevier, and the payment terms and conditions.

Get the printable license.

License Number	3200110498088
License date	Aug 01, 2013
Licensed content publisher	Elsevier
Licensed content publication	FEBS Letters
Licensed content title	Neuronal nicotinic receptors: from protein structure to function
Licensed content author	Valérie Itier,Daniel Bertrand
Licensed content date	31 August 2001
Licensed content volume number	504
Licensed content issue number	3
Number of pages	8
Type of Use	reuse in a thesis/dissertation
Portion	figures/tables/illustrations
Number of figures/tables/illustrations	1
Format	both print and electronic
Are you the author of this Elsevier article?	No
Will you be translating?	No
Order reference number	None
Title of your thesis/dissertation	Analysis of CHRNA5 Expression in Breast Cancer Cell Lines in Response to Serum Starvation and Estrogen Treatment
Expected completion date	Aug 2013
Elsevier VAT number	GB 494 6272 12
Permissions price	0.00 USD
VAT/Local Sales Tax	0.00 USD / 0.00 GBP
Total	**0.00 USD**

My Orders > Orders > All Orders

License Details

This is a License Agreement between Azer Acikgoz ("You") and Elsevier ("Elsevier"). The license consists of your order details, the terms and conditions provided by Elsevier, and the payment terms and conditions.

Get the printable license.

License Number	3200320896731
License date	Aug 01, 2013
Licensed content publisher	Elsevier
Licensed content publication	Progress in Neurobiology
Licensed content title	The nicotinic acetylcholine receptor CHRNA5/A3/B4 gene cluster: Dual role in nicotine addiction and lung cancer
Licensed content author	Ma. Reina D. Improgo,Michael D. Scofield,Andrew R. Tapper,Paul D. Gardner
Licensed content date	October 2010
Licensed content volume number	92
Licensed content issue number	2
Number of pages	15
Type of Use	reuse in a thesis/dissertation
Portion	figures/tables/illustrations
Number of figures/tables/illustrations	1
Format	both print and electronic
Are you the author of this Elsevier article?	No
Will you be translating?	No
Order reference number	None
Title of your thesis/dissertation	Analysis of CHRNA5 Expression in Breast Cancer Cell Lines in Response to Serum Starvation and Estrogen Treatment
Expected completion date	Aug 2013
Elsevier VAT number	GB 494 6272 12
Permissions price	0.00 USD
VAT/Local Sales Tax	0.00 USD / 0.00 GBP
Total	**0.00 USD**

My Orders > Orders > All Orders

License Details

This is a License Agreement between Azer Acikgoz ("You") and Oxford University Press ("Oxford University Press"). The license consists of your order details, the terms and conditions provided by Oxford University Press, and the payment terms and conditions.

Get the printable license.

License Number	3211321321392
License date	Aug 17, 2013
Licensed content publisher	Oxford University Press
Licensed content publication	Carcinogenesis
Licensed content title	Multiple isoforms and differential allelic expression of CHRNA5 in lung tissue and lung adenocarcinoma:
Licensed content author	Felicia S. Falvella, Tiziana Alberio, Sara Noci, Luigi Santambrogio, Mario Nosotti, Matteo Incarbone, Ugo Pastorino, Mauro Fasano, Tommaso A. Dragani
Licensed content date	06/01/2013
Volume number	34
Issue number	6
Type of Use	Thesis/Dissertation
Requestor type	Academic/Educational institute
Format	Print and electronic
Portion	Figure/table
Number of figures/tables	1
Will you be translating?	No
Author of this OUP article	No
Order reference number	None
Title of your thesis / dissertation	Analysis of CHRNA5 Expression in Breast Cancer Cell Lines in Response to Serum Starvation and Estrogen Treatment
Expected completion date	Aug 2013
Estimated size(pages)	100
Publisher VAT ID	GB 125 5067 30
Total	**0.00 USD**

My Orders > Orders > All Orders

License Details

This is a License Agreement between Azer Acikgoz ("You") and Elsevier ("Elsevier"). The license consists of your order details, the terms and conditions provided by Elsevier, and the payment terms and conditions.

Get the printable license.

License Number	3202620689465
License date	Aug 05, 2013
Licensed content publisher	Elsevier
Licensed content publication	Cancer Letters
Licensed content title	Alternative splicing in angiogenesis: The vascular endothelial growth factor paradigm
Licensed content author	Michael R. Ladomery,Steven J. Harper,David O. Bates
Licensed content date	8 May 2007
Licensed content volume number	249
Licensed content issue number	2
Number of pages	10
Type of Use	reuse in a thesis/dissertation
Portion	figures/tables/illustrations
Number of figures/tables/illustrations	1
Format	both print and electronic
Are you the author of this Elsevier article?	No
Will you be translating?	No
Order reference number	None
Title of your thesis/dissertation	Analysis of CHRNA5 Expression in Breast Cancer Cell Lines in Response to Serum Starvation and Estrogen Treatment
Expected completion date	Aug 2013
Estimated size (number of pages)	100
Elsevier VAT number	GB 494 6272 12
Permissions price	0.00 USD
VAT/Local Sales Tax	0.00 USD / 0.00 GBP
Total	**0.00 USD**

My Orders > Orders > All Orders

License Details

This is a License Agreement between Azer Acikgoz ("You") and Elsevier ("Elsevier"). The license consists of your order details, the terms and conditions provided by Elsevier, and the payment terms and conditions.

Get the printable license.

License Number	3203700275104
License date	Aug 07, 2013
Licensed content publisher	Elsevier
Licensed content publication	The Lancet Oncology
Licensed content title	Alternative splicing: an emerging topic in molecular and clinical oncology
Licensed content author	María J Pajares,Teresa Ezponda,Raúl Catena,Alfonso Calvo,Ruben Pio,Luis M Montuenga
Licensed content date	April 2007
Licensed content volume number	8
Licensed content issue number	4
Number of pages	9
Type of Use	reuse in a thesis/dissertation
Portion	figures/tables/illustrations
Number of figures/tables/illustrations	1
Format	both print and electronic
Are you the author of this Elsevier article?	No
Will you be translating?	No
Order reference number	None
Title of your thesis/dissertation	Analysis of CHRNA5 Expression in Breast Cancer Cell Lines in Response to Serum Starvation and Estrogen Treatment
Expected completion date	Aug 2013
Estimated size (number of pages)	100
Elsevier VAT number	GB 494 6272 12
Permissions price	0.00 USD
VAT/Local Sales Tax	0.00 USD / 0.00 GBP
Total	**0.00 USD**